# UC San Diego

## UC San Diego Electronic Theses and Dissertations

**Title**

Novel roles of NMDA receptors in release and plasticity

**Permalink**

https://escholarship.org/uc/item/74z1h5z4

**Author**

Brasier, Daniel James

**Publication Date**

2007

Peer reviewed|Thesis/dissertation

eScholarship.org Powered by the California Digital Library
University of California

**UNIVERSITY OF CALIFORNIA, SAN DIEGO**

# Novel roles of NMDA receptors in release and plasticity

A dissertation submitted in partial satisfaction of the

requirements for the degree Doctor of Philosophy

in

Neurosciences

by

Daniel James Brasier

Committee in charge:

Professor Daniel E. Feldman, Chair
Professor Sascha du Lac
Professor Jeffry S. Isaacson
Professor Massimo Scanziani
Professor Nicholas C. Spitzer

2007

Copyright
Daniel James Brasier, 2007
All rights reserved.

The Dissertation of Daniel James Brasier is approved, and it is acceptable in quality and form for publication on microfilm:

---

---

---

---

---

Chair

University of California, San Diego

2007

This thesis is dedicated to my wife, Aryn Gittis

and her gifts of

unfailing support,

unequaled advice,

unimaginable joy,

unexpected laughter,

uncanny ability to know which I need,

and above all,

unending love.

# Table of Contents


Signature Page ..... iii

Dedication ..... iv

Table of Contents ..... v

List of Figures ..... vii

Acknowledgments ..... ix

Vita and Publications ..... xi

Abstract of the dissertation ..... xii

I. Introduction ..... 1

- Synaptic release ..... 1
- Synaptic plasticity ..... 1
- Synapse specificity ..... 5
- Modulation by presynaptic receptors ..... 7
- References ..... 10

II. Spike-timing dependent synaptic plasticity measured in vivo in primary somatosensory cortex ..... 20

- Abstract ..... 20
- Introduction ..... 21
- Methods ..... 23
- Results ..... 26
- Discussion ..... 30
- Acknowledgment ..... 34
- References ..... 35

III. Partial blockade of NMDA receptors is not sufficient to cause depression at synaptic inputs onto L2/3 pyramidal cells ..... 42

- Abstract ..... 42
- Introduction ..... 43
- Methods ..... 45
- Results ..... 47

Discussion..... 51
References ..... 54

IV. Synapse specific expression of functional presynaptic NMDA receptors in rat somatosensory cortex..... 62

Abstract..... 62
Introduction ..... 63
Methods ..... 65
Results ..... 72
Discussion..... 85
Acknowledgment..... 91
References ..... 92

V. Concluding remarks on functional heterogeneity and presynaptic NMDA receptor function ..... 108

Heterogeneity between cortical areas..... 108
Synaptic heterogeneity within a cortical area..... 110
Speculative model of PreNMDAR function ..... 111
References ..... 114

# List of Figures


Chapter 1:

| | | |
|---|---|---|
| Fig. 1.1 | Two models of postsynaptic calcium integration | 17 |
| Fig. 1.2 | Two types of synapse-specificity | 18 |
| Fig. 1.3 | Blockade of postsynaptic NMDA currents by internal MK-801 does not block t-LTD | 19 |

Chapter 2:

| | | |
|---|---|---|
| Fig. 2.1 | Experimental protocol for induction of STDP in vivo | 38 |
| Fig. 2.2 | Induction of tLTD in a representative neuron | 39 |
| Fig. 2.3 | Induction of tLTP in a representative neuron | 40 |
| Fig. 2.4 | Learning rule for STDP in L2/3 in vivo | 41 |

Chapter 3:

| | | |
|---|---|---|
| Fig. 3.1 | Effects of increasing concentration of D-APV on postsynaptic NMDA currents | 58 |
| Fig. 3.2 | 2 μM D-APV does not cause depression at the L4-L2/3 projection | 59 |
| Fig. 3.3 | Induction of tLTD at the L4-L2/3 projection | 60 |
| Fig. 3.4 | 2 μM D-APV does not cause depression at local inputs onto the proximal apical dendrite of L2/3 pyramidal cells | 61 |

Chapter 4:

| | | |
|---|---|---|
| Fig. 4.1 | Putatively presynaptic NMDARs regulate release at the L4-L2/3 projection elevated extracellular glutamate | 99 |
| Fig. 4.2 | Non-postsynaptic NMDARs modulate synaptic transmission at L4-L2/3 synapses in S1 | 100 |

Fig. 4.3 Activation of PreNMDARs increase the frequency of mEPSCs on L2/3 pyramidal neurons ..... 101

Fig. 4.4 PreNMDARs at the L4-L2/3 projection exist on L4 terminals located in L2/3 ..... 102

Fig. 4.5 PreNMDARs preferentially contain NR2B subunits ..... 103

Fig. 4.6 PreNMDARs are located on the L4-2/3 projection, but not on other cortical inputs to L2/3 ..... 104

Fig. 4.7 There are not PreNMDARs at local synapses between L4 excitatory cells ..... 105

Fig. 4.8 PreNMDARs regulate transmission at synaptically-coupled L4-2/3 pairs ..... 106

Fig. 4.9 PreNMDARs are tonically active at physiological temperatures ..... 107

Chapter 5:

Fig. 5.1 Localization of PreNMDARs in the synaptic terminal ..... 118

## Acknowledgments

I have been extremely fortunate to have Dan Feldman as an advisor. Dan truly pours himself into the lab. He is deeply committed to the success of each person in his lab. No time was this more apparent than when my own career path forced me to spend less time in lab so I could gain some experience teaching. Dan's unfailing support made my professional growth possible, and for that I owe him a debt which I doubt I will ever be able to repay. Dan is also a uniquely gifted and motivated scientist. He is always asking what the next "key experiment" is and has a rare and infectious ability to see each mundane control as an exciting challenge. I've learned from him that science is an exciting process, and to embrace each obstacle.

Working in the Feldman lab is a daily treat. I can imagine no better support structure in which to do science: the readiness with which people in the lab come offer assistance is amazing. Special thanks go to: Tansu Celikel, whose patient assistance with my early *in vivo* experiments was vital, Kevin Bender, whose daily assistance on everything from electrophysiology to illustrations continues to this day, Renna Stevens without whose amazing technical help I wouldn't have finished by now.

I have been fortunate to have found many wonderful friends at UCSD. Since their departure, I find myself missing time spent with Kevin and Vanessa Bender. I've been lucky to know Monica Brown whose loyalty and dedication as a friend is nothing short of inspirational. Special thanks also go to Martha Bagnall and Lindsey Glickfeld, for the time spent in the Nerd Journal Club.

Most of all, I wish to thank my family. My friends and new in-laws the Gittis' continue to be supportive and welcoming. I cannot find the words to properly thank my wife, Aryn, to whom this thesis is dedicated. My brother, Tommy, is the brightest person I have ever known and at every step in his life I become more proud of all he has accomplished. Above all, I owe everything I have and everything I am to my parents. The unerring and unending sacrifices which they have made every day of my life have allowed me to pursue my dreams. Thanks has never been asked; indeed proper thanks is beyond my capacity.

Chapter 2 is a revised version of Jacob V, Brasier DJ, Erchova I, Feldman D, Shulz DE. Spike timing-dependent synaptic depression in the *in vivo* barrel cortex of the rat. J Neurosci. 2007 Feb 7; 27(6):1271-84. The data included in Chapter 2 only comprise those data for which the thesis author was primarily responsible. The portions present here are included with the permission of all the authors on the final publication. The co-authors on the final published paper are thanked for help in analysis for figures 2.1-2.3 and for substantial contribution to the text of Chapter 2.

Chapter 4 is original work submitted as Brasier DJ, Feldman DE. Synapse specific expression of functional presynaptic NMDA receptors in somatosensory cortex. J Neurosci. 2007, *submitted*. Chapter 4 has been reformatted and restructured to include data that was published in figure 8 of Bender VA, Bender KJ, Brasier DJ, Feldman DE. Two coincidence detectors for spike timing-dependent plasticity in somatosensory cortex. J Neurosci. 2006 Apr 19; 26(16):4166-77, for which the thesis author was primarily responsible and which has been incorporated into Chapter 4 as figure 4.1 with permission from all the paper's authors.

# Vita and Publications

2002 B.A., Biology & Philosophy, *cum laude*, Rice University, Houston, TX

2005 M.S., Neurosciences, University of California, San Diego

2007 Ph.D., Neurosciences, University of California, San Diego

## Publications

Peer reviewed competitive journals (published while at UCSD):

Brasier DJ, Feldman D (2007) Synapse specific modulation of synaptic transmission by presynaptic NMDA receptors. *Submitted*.

Jacob V, Brasier DJ, Erchova I, Feldman D, Shulz DE (2007) Spike timing-dependent synaptic depression in the in vivo barrel cortex of the rat. J Neurosci 27:1271-1284.

Bender VA, Bender KJ, Brasier DJ, Feldman DE (2006) Two coincidence detectors for STDP in somatosensory cortex. J Neurosci 26:4166-4177.

## Awards

| | |
|---|---|
| 2002-2007 | Howard Hughes Medical Institute Predoctoral Fellowship |
| 2006 | Ray Thomas Edwards Foundation Travel Award |
| 2003-2004 | Biology Dept. T.A. Excellence in Teaching Award, UCSD |
| 2002 | Outstanding Cell Biology Senior, Rice University |

# ABSTRACT OF THE DISSERTATION

Novel roles of NMDA receptors in release and plasticity

by

Daniel James Brasier

Doctor of Philosophy in Neurosciences

University of California, San Diego, 2007

Professor Daniel E. Feldman, Chair

Information transfer between neurons in the central nervous system occurs at specialized contacts, called synapses. Not all excitatory (glutamatergic) synapses in the brain are identical. Rather, different inputs to the same target can have markedly different properties, as can different targets of the same presynaptic cell. Excitatory synapses exhibit long-lasting changes in efficacy after experiencing brief patterns of coordinated activity, a characteristic which is thought to underlie learning and other forms of reorganization of the nervous system. The NMDA receptor (NMDAR) serves as an exquisitely sensitive coincidence detector in the postsynaptic density, and it is crucial for spike timing dependent synaptic plasticity. However, recently, it has been proposed that in addition to the classical role, the NMDAR functions to modulate synaptic release and plasticity in novel ways. In this thesis, I first tested whether spike timing dependent plasticity *in vivo* follows the same rules as it does *in vitro*. I found

evidence that the same basic rules are present (Chapter 2), but whether the phenomena studied *in vitro* and *in vivo* are the same remains to be fully confirmed. Next, I tested whether postsynaptic NMDARs exhibit calcium-dependent desensitization during coincident pre- and postsynaptic activity, as recently observed at one synapse on cortical layer 2/3 pyramidal cells. I found that this desensitization did not occur at a different input onto these neurons, suggesting that it is not a general property of NMDA receptor signaling. Finally, I investigated another novel role of NMDARs, to regulate release at presynaptic terminals. I confirmed that non-postysnaptic, likely presynaptic NMDARs regulate presynaptic release at some synapses in somatosensory cortex, but not at other synapses made by the same presynaptic cells, or made onto the same postsynaptic cells. Thus, presynaptic NMDAR function is highly target- and input-specific, indicating that presynaptic function of NMDARs underlies some of the functional heterogeneity at excitatory cortical synapses (Chapter 4). These results show that the classical view of NMDAR function is incomplete and that a full picture of synaptic release and of the diversity of excitatory synapses must include presynaptic NMDARs that govern release.

# I. Introduction

## Synaptic release

Sensory neurons in the nervous system encode information about the external world as a sequence of action potentials (spikes) which are transmitted along axons to synaptic terminals. When a spike invades the terminal, it activates voltage-sensitive calcium channels (VSCCs) which allow $Ca^{2+}$ into the terminal where it binds to synaptotagmin and transiently increases the probability that a vesicle will fuse with the synaptic membrane and release its neurotransmitter into the synaptic cleft (Sudhof, 2004; Martens et al., 2007). Neurotransmitter then binds to postsynaptic neurotransmitter receptors which in turn open to allow current to flow into the cell or trigger other biochemical processes. Thus, the information that a postsynaptic neuron has available to it about the external world is in the pattern with which neurotransmitter is released from its presynaptic partners. Therefore, in order to understand how information is received and processed in the brain, we need to understand the rules that govern neurotransmitter release after a single spike or a sequence of spikes.

## Synaptic plasticity

In addition to being crucial to information flow in the nervous system, synapses are highly plastic. Active synapses undergo long-term synaptic potentiation (LTP) and less active synapses are depressed (LTD; Hebb, 1949; Bliss and Lomo, 1973; Abbott and Nelson, 2000). Although there are many ways in which plasticity

can be induced, spike-timing dependent plasticity (STDP) is widely studied as a putative mechanism for cortical plasticity. Synapses undergo timing-dependent LTP (tLTP) when the presynaptic cell fires reliably up to roughly 20 ms before the postsynaptic cell, and tLTD when the postsynaptic cell fires up to about 20-50 ms before the presynaptic cell (Markram et al., 1997; Egger et al., 1999; Feldman, 2000; Holmgren and Zilberter, 2001; Sjöström et al., 2001; Bi and Poo; 2001; Froemke and Dan, 2002; Feldman and Brecht, 2005). STDP is Hebbian in nature, in that it serves to strengthen efficacious synapses and weaken those which are not effective in driving postsynaptic spikes (Abbott and Nelson, 2000; Dan and Poo, 2004). In contrast to rate-dependent mechanisms of inducing plasticity, STDP is especially relevant in neocortex where cells exhibit low spontaneous and stimulus-evoked firing rates *in vivo* (Zhu and Connors, 1999). Furthermore, *in vivo* sensory manipulations that are known to induce plasticity also alter the relative timing of presynaptic and postsynaptic firing, suggesting that STDP is used by the brain (Celikel et al., 2004).

Despite characterization at many synapses *in vitro*, whether STDP occurs in neocortex *in vivo* is not fully clear; before the work of this thesis, STDP had been demonstrated *in vivo* only for one cell class in visual cortex (V1; Meliza and Dan, 2006). The question of whether STDP can be induced in other cortical areas *in vivo* is taken up in Chapter 2. Results indicate that STDP can, in fact, be induced in intact brains *in vivo* for natural, sensory-evoked responses.

Additionally, the intracellular signaling mechanisms for STDP are not known in detail. It has long been theorized from *in vitro* work that small increases in postsynaptic calcium influx above baseline levels lead to LTD and larger increases

lead to LTP (Fig. 1.1A; Bienenstock et al., 1982; Bear et al., 1987; Lisman, 1989; Artola and Singer, 1993; Yang et al., 1999; Cormier et al., 2001). Synapses are exquisitely sensitive to the relative timing of presynaptic and postsynaptic spikes (Feldman, 2000; Celikel et al., 2005). It is well-established that pre- before postsynaptic coincidence is detected by the postsynaptic NMDAR. During normal baseline transmission the postsynaptic NMDAR is blocked by magnesium (Dingledine et al., 1999), although some of this block may be relieved by AMPA receptor-mediated depolarization of the postsynaptic spine (Sabatini et al., 2002; Ngo-Ahn et al., 2005). Supralinear increases in calcium above baseline levels resulting from coincident glutamate release and relief of magnesium block of the postsynaptic NMDAR leads to tLTP (Koester and Sakmann, 1998; Shouval et al., 2002; Johnston et al., 2003; Nevian and Sakmann, 2004), which would be predicted to cause LTP (Fig. 1.1A). However, the coincidence detector for tLTD has proven more elusive. It has been observed that post-leading-pre pairings cause a sublinear increase in postsynaptic calcium and it has therefore been hypothesized that the postsynaptic NMDAR may serve as a coincidence detector for LTD (Johnston et al., 2003), but this remains to be fully tested.

An assumption of this standard model for STDP is that the calcium concentration critical for LTP or LTD induction is dendritic or spine calcium pooled across many different classes of microdomains (Delmas et al., 2002; Bloodgood and Sabatini, 2007), including NMDA-dependent calcium flux, calcium flux from voltage-sensitive calcium channels, and calcium release from internal stores. If, instead, these different microdomains function independently to drive LTP, LTD, then important

aspects of coincidence detection may be misunderstood. Recently, the classical model for LTP and LTD induction (Fig. 1.1A) has been challenged by three different models which account for functional independence of different calcium sources. In the first, the postsynaptic NMDAR is the only coincidence detector for tLTP and tLTD. It departs from the classical view by excluding calcium from all other sources (e.g. internal stores or voltage-sensitive channels). According to this model, during baseline transmission, calcium influx through postsynaptic NMDARs is at the cross-over point between LTD and LTP (Fig. 1.1B), thus driving no net plasticity. Coincidence for tLTD is computed by calcium-dependent desensitization of postsynaptic NMDARs, triggered by the postsynaptic spike (Froemke, et al., 2005). Thus, in this model, the postsynaptic NMDAR is the sole coincidence detector for STDP, with pre-leading-post firing driving strong NMDAR-calcium accumulation, and post-leading pre driving substantially weaker NMDA-dependent calcium entry and LTD. This model was first proposed at inputs onto apical dendrites of layer (L) 2/3 pyramidal cells in V1; in Chapter 3 we test whether such a model can be applied to two different inputs onto L2/3 pyramidal cells in S1. We found that, unlike in V1, the L4-L2/3 projection in S1 shows no evidence of this type of integration by the postsynaptic NMDAR.

In a second model, pre-leading-post firing is detected by postsynaptic NMDARs, leading to tLTP, but post-leading-pre firing order for tLTD is detected by an entirely separate coincidence detector in the presynaptic terminal that compares the timing of retrograde endocannabinoid release and activation of presynaptic NMDARs (Sjostrom et al., 2003). In a third model, post-leading-pre firing is detected

postsynaptically by metabotropic glutamate receptors and voltage-sensitive calcium channels converging on the IP3 receptor is a well known molecular coincidence detector (Bezprozvanny et al. 1991). In this model, presynaptic NMDARs play a modulatory role; they are necessary for tLTD, but the precise role is undetermined (Bender et al., 2006; V. Bender and D. Feldman, unpublished observations). In both models, tLTD relies on presynaptic NMDARs, the remainder of this introduction and Chapter 4 take up the question of whether functional presynaptic NMDARs do actually exist at different synapses in S1. We found that presynaptic NMDARs do regulate release at the L4-L2/3 projection in S1. However, interestingly, this regulation exhibits precise synapse specificity.

**Synapse specificity**

A final issue addressed in this thesis is the role of presynaptic NMDA receptors in regulating normal release probability in a synapse-specific matter. Even before the induction of any long-term plasticity, the probability of vesicular release from a presynaptic terminal is not constant across excitatory synapses in the central nervous system (CNS), but varies widely. For example, synapses between layer (L) 4 and L2/3 (L4-L2/3) in primary somatosensory cortex (S1) as well as sensory afferents terminating in the olfactory bulb exhibit a high probability of release of a single vesicle when a spike invades the terminal (Silver et al., 2003; Murphy et al., 2004). By comparison, the excitatory connection between CA3 and CA1 in hippocampus shows a low probability of univesicular release (Bekkers et al., 1990; Stevens and Wang, 1995). Although uniquantal release still seems to be the norm, multivesicular

release has been identified at a few excitatory synapses in the CNS, most notably the climbing fiber to Purkinje cell synapse in cerebellum (Wadiche and Jahr, 2001) and the giant auditory synapse in the medial nucleus of the trapezoid body, the Calyx of Held (Schneggenburger et al., 2002).

Not only do synapses vary across brain regions, but even within a single area of the brain, excitatory synapses can vary widely in their properties. Excitatory contacts onto a single postsynaptic target that are of different origin can vary markedly in their properties (Fig. 1.2A): this "input-selective" difference is best illustrated in the cerebellum where glutamatergic inputs from the inferior olive evoke large, complex spikes and inputs from presynaptic granule cells evoke small excitatory postsynaptic currents (EPSCs; Schmolesky et al., 2002). In addition, axon collaterals from a single presynaptic excitatory cell can have markedly different release properties (Fig. 1.2B). This "target-selective" difference in probability of release has been observed at synapses made by excitatory afferents onto different types of inhibitory target cells in hippocampus (Murthy et al., 1997) and in neocortex (Reyes et al., 1998; Koester and Johnston, 2005).

However, two fundamental questions remain unanswered. First, it is not known whether target-selective differences in synaptic properties are unique to synapses onto different classes of interneurons or if different classes of excitatory targets might also exhibit systematic, target-selective properties in neocortex. (There does appear to be a bimodal distribution of release probability at CA3-CA1 synapses in hippocampus, but it is unknown whether this represents a systematic difference [L. Glickfeld & M. Scanziani, personal communication]). Second, it is incompletely

understood how different synaptic terminals achieve target-selective synaptic release properties; one contributing factor is likely to be targeted expression of presynaptic neurotransmitter receptors that regulate release (see next section).

**Modulation by presynaptic receptors**

Presynaptic neurotransmitter receptors powerfully modulate release at many synapses. Several types of metabotropic receptors have been found to regulate release, the three most well-characterized of which serve to decrease release probability: $GABA_B$ receptors (Takahashi et al., 1998), metabotropic glutamate receptors (mGluRs; Cartmell and Schoepp, 2000; Karim et al., 2000), and endocannabinoid receptors (Kreitzer and Regehr, 2002; Freund et al., 2003); although other, less-well characterized, receptors enhance release (e.g. the presynaptic adenosine receptor; Malva et al., 2003). The expression of presynaptic metabotropic receptors is not homogeneous, but is highly regulated. In fact, presynaptic mGluRs are present at CA3 terminals that contact inhibitory interneurons in CA1, but not at terminals that contact CA1 pyramidal cells (Scanziani et al., 1998). Thus, in addition to their role in regulating release, presynaptic metabotropic receptors may underlie some of the target-selective synaptic differences outlined above.

In contrast to presynaptic metabotropic receptors, little is known about the prevalence and functional role of presynaptic ionotropic receptors. The glycine receptor is a presynaptic chloride channel which has been observed at the Calyx of Held. There, it modulates release probability by depolarizing the presynaptic terminal which causes a small but significant increase in tonic calcium influx and serves to

enhance the probability of release when the next spike arrives (Turecek and Trussell 2001, 2002; Trussell 2002). The best-characterized presynaptic ionotropic glutamate receptor is the kainate receptor (KAR; Chittajallu et al., 1996). It is present at CA3 contacts onto CA1 pyramidal cells (Chittajallu et al., 1996) and onto some types of interneurons (Sun and Dobrunz, 2006), at parallel fiber to Purkinje synapses (Delaney and Jahr, 2002), at thalamacortical synapses (Kidd et al., 2002), and at synapses in L2/3 of rat prefrontal cortex (Campbell et al., *in press*). Interestingly, just as presynaptic mGluRs contribute to target-selective synaptic differences, presynaptic KARs have also been found to be expressed on CA3 terminals onto a subclass of somatostatin-positive, but not onto somatostatin negative, interneurons (Sun and Dobrunz, 2006). Taken together, these observations suggest that differential expression of presynaptic neurotransmitter receptors may be a common mechanism by which target-selective synaptic properties are achieved.

Classically, NMDA receptors (NMDARs) are thought to be involved in postsynaptic depolarization and calcium influx (see above). However, there has been an explosion of papers showing that non-postsynaptic NMDARs regulate release probability (Berretta and Jones 1996; Breukel et al., 1998; Hamada et al., 1998; Cochilla and Alford, 1999; Glitsch and Marty, 1999; MacDermott et al., 1999; Casado et al., 2000, 2002; Woodhall et al., 2001; Sjöström et al., 2003; Duguid and Smart, 2004; Engelman and MacDermott, 2004; Suárez et al., 2005; Fiszman et al., 2005; Yang et al., 2006; Lien et al., 2006; Suárez and Solís, 2006; Liu and Lachamp, 2006; Duguid and Sjöström, 2006; Li and Han, 2007; Corlew et al., *in press*). However, presynaptic NMDARs at the parallel fiber to Purkinje synapse in cerebellum, which

had been proposed to modulate plasticity (Casado et al., 2000, 2002) have since been determined to be present on another, non-postsynaptic cell (Shin and Linden, 2005). This explosion of papers is in part due to the discovery that inclusion of MK-801 in internal solution selectively blocks postsynaptic NMDARs (Fig. 1.3A-B; Berretta and Jones, 1996; Woodhall et al., 2001; Humeau et al., 2003; Samson and Pare, 2005; Mameli et al., 2005; Bender et al., 2006b; Corlew et al., *in press*), which has made the functional study of non-postsynaptic NMDARs more tractable.

In neocortex, presynaptic NMDARs have been found to regulate release and plasticity at synaptically coupled pairs of pyramidal cells in V1 (Sjostrom et al., 2003) and at the L4-L2/3 projection in V1 (Corlew et al., *in press*). Additionally, prior work from our lab has shown that a non-postsynaptic NMDAR is involved in tLTD, but not tLTP (Fig. 1.3). However, NMDARs have been observed only at a limited number of synaptic terminals in electron microscopy studies (e.g. 14% of terminals in Aoki et al., 1994), and it has not previously been determined whether their expression is systematically regulated at terminals arising from different cortical cells, or, as with mGluRs and KARs, at different collaterals from the same presynaptic cells. It is this question which we take up in Chapter 4.

**References**

Abbott LF, Nelson SB. (2000) Synaptic plasticity: taming the beast. Nat Neurosci 3:1178-83.

Aoki C, Venkatesan C, Go CG, Mong JA, Dawson TM (1994) Cellular and subcellular localization of NMDA-R1 subunit immunoreactivity in the visual cortex of adult and neonatal rats. J Neurosci 14:5202-5222.

Artola A, Singer W (1993) Long-term depression of excitatory synaptic transmission and its relationship to long-term potentiation. Trends Neurosci 16:480-487.

Bear MF, Cooper LN, Ebner FF (1987) A physiological basis for a theory of synapse modification. Science 237:42-48.

Bekkers JM, Richerson GB, Stevens CF (1990) Origin of variability in quantal size in cultured hippocampal neurons and hippocampal slices. Proc Natl Acad Sci U S A 87:5359-5362.

Bender VA, Bender KJ, Brasier DJ, Feldman DE (2006b) Two coincidence detectors for spike timing-dependent plasticity in somatosensory cortex. J Neurosci 26:4166-4177.

Berretta N, Jones RS (1996) Tonic facilitation of glutamate release by presynaptic N-methyl-D-aspartate autoreceptors in the entorhinal cortex. Neuroscience 75:339-344.

Bezprozvanny I, Watras J, Ehrlich BE (1991) Bell-shaped calcium-response curves of Ins(1,4,5)P3- and calcium-gated channels from endoplasmic reticulum of cerebellum. Nature 351:751-754.

Bi GQ, Poo MM (1998) Synaptic modifications in cultured hippocampal neurons: dependence on spike timing, synaptic strength, and postsynaptic cell type. J Neurosci 18:10464-10472.

Bienenstock EL, Cooper LN, Munro PW (1982) Theory for the development of neuron selectivity: orientation specificity and binocular interaction in visual cortex. J Neurosci 2:32-48.

Bliss TV, Lomo T (1973) Long-lasting potentiation of synaptic transmission in the dentate area of the anaesthetized rabbit following stimulation of the perforant path. J Physiol 232:331-356.

Bloodgood BL, Sabatini BL (2007) Ca(2+) signaling in dendritic spines. Curr Opin Neurobiol 17:345-351.

Breukel AI, Besselsen E, Lopes da Silva FH, Ghijsen WE (1998) A presynaptic N-methyl-D-aspartate autoreceptor in rat hippocampus modulating amino acid release from a cytoplasmic pool. Eur J Neurosci 10:106-114.

Campbell SL, Mathew SS, Hablitz JJ (2007) Pre- and postsynaptic effects of kainate on layer II/III pyramidal cells in rat neocortex. Neuropharmacology, *in press*.

Cartmell J, Schoepp DD (2000) Regulation of neurotransmitter release by metabotropic glutamate receptors. J Neurochem 75:889-907.

Casado M, Dieudonne S, Ascher P (2000) Presynaptic N-methyl-D-aspartate receptors at the parallel fiber-Purkinje cell synapse. Proc Natl Acad Sci U S A 97:11593-11597.

Casado M, Isope P, Ascher P (2002) Involvement of presynaptic N-methyl-D-aspartate receptors in cerebellar long-term depression. Neuron 33:123-130.

Celikel T, Szostak VA, Feldman DE (2004) Modulation of spike timing by sensory deprivation during induction of cortical map plasticity. Nat Neurosci 7:534-541.

Chittajallu R, Vignes M, Dev KK, Barnes JM, Collingridge GL, Henley JM (1996) Regulation of glutamate release by presynaptic kainate receptors in the hippocampus. Nature 379:78-81.

Cochilla AJ, Alford S (1999) NMDA receptor-mediated control of presynaptic calcium and neurotransmitter release. J Neurosci 19:193-205.

Corlew R, Wang Y, Ghermazien H, Erisir A, Philpot BD (2007) Developmental switch in the contribution of presynaptic and postsynaptic NMDA receptors to long-term depression. J Neurosci, *in press*.

Cormier RJ, Greenwood AC, Connor JA (2001) Bidirectional synaptic plasticity correlated with the magnitude of dendritic calcium transients above a threshold. J Neurophysiol 85:399-406.

Delaney AJ, Jahr CE (2002) Kainate receptors differentially regulate release at two parallel fiber synapses. Neuron 36:475-482.

Delmas P, Wanaverbecq N, Abogadie FC, Mistry M, Brown DA (2002) Signaling microdomains define the specificity of receptor-mediated InsP(3) pathways in neurons. Neuron 34:209-220.

Dingledine R, Borges K, Bowie D, Traynelis SF (1999) The glutamate receptor ion channels. Pharmacol Rev 51:7-61.

Duguid I, Sjöström PJ (2006) Novel presynaptic mechanisms for coincidence detection in synaptic plasticity. Curr Opin Neurobiol 16:312-322.

Duguid IC, Smart TG (2004) Retrograde activation of presynaptic NMDA receptors enhances GABA release at cerebellar interneuron-Purkinje cell synapses. Nat Neurosci 7:525-533.

Egger V, Feldmeyer D, Sakmann B (1999) Coincidence detection and changes of synaptic efficacy in spiny stellate neurons in rat barrel cortex. Nat Neurosci 2:1098-1105.

Engelman HS, MacDermott AB (2004) Presynaptic ionotropic receptors and control of transmitter release. Nat Rev Neurosci 5:135-145.

Feldman DE (2000) Timing-based LTP and LTD at vertical inputs to layer II/III pyramidal cells in rat barrel cortex. Neuron 27:45-56.

Feldman DE, Brecht M (2005) Map plasticity in somatosensory cortex. Science 310:810-815.

Fiszman ML, Barberis A, Lu C, Fu Z, Erdelyi F, Szabo G, Vicini S (2005) NMDA receptors increase the size of GABAergic terminals and enhance GABA release. J Neurosci 25:2024-20231.

Freund TF, Katona I, Piomelli D (2003) Role of endogenous cannabinoids in synaptic signaling. Physiol Rev 83:1017-1066.

Froemke RC, Dan Y (2002) Spike-timing-dependent synaptic modification induced by natural spike trains. Nature 416:433-438.

Froemke RC, Poo MM, Dan Y (2005) Spike-timing-dependent synaptic plasticity depends on dendritic location. Nature 434:221-225.

Glitsch M, Marty A (1999) Presynaptic effects of NMDA in cerebellar Purkinje cells and interneurons. J Neurosci 19:511-519.

Hamada T, Sonoda R, Watanabe A, Ono M, Shibata S, Watanabe S (1998) NMDA induced glutamate release from the suprachiasmatic nucleus: an in vitro study in the rat. Neurosci Lett 256:93-96.

Hebb DO (1949) Organization of Behavior. John Wiley & Sons, New York.

Holmgren CD, Zilberter Y (2001) Coincident spiking activity induces long-term changes in inhibition of neocortical pyramidal cells. J Neurosci 21:8270-8277.

Johnston D, Christie BR, Frick A, Gray R, Hoffman DA, Schexnayder LK, Watanabe S, Yuan LL (2003) Active dendrites, potassium channels and synaptic plasticity. Philos Trans R Soc Lond B Biol Sci 358:667-674.

Karim F, Bhave G, Gereau RW 4th (2001) Metabotropic glutamate receptors on peripheral sensory neuron terminals as targets for the development of novel analgesics. Mol Psychiatry 6:615-617.

Kidd FL, Coumis U, Collingridge GL, Crabtree JW, Isaac JT (2002) A presynaptic kainate receptor is involved in regulating the dynamic properties of thalamocortical synapses during development. Neuron 34:635-646.

Koester HJ, Johnston D (2005) Target cell-dependent normalization of transmitter release at neocortical synapses. Science 308:863-866.

Koester HJ, Sakmann B (1998) Calcium dynamics in single spines during coincident pre- and postsynaptic activity depend on relative timing of back-propagating action potentials and subthreshold excitatory postsynaptic potentials. Proc Natl Acad Sci U S A 95:9596-9601.

Kreitzer AC, Regehr WG (2002) Retrograde signaling by endocannabinoids. Curr Opin Neurobiol 12:324-330.

Li YH, Han TZ (2007) Glycine binding sites of presynaptic NMDA receptors may tonically regulate glutamate release in the rat visual cortex. J Neurophysiol 97:817-823.

Lien CC, Mu Y, Vargas-Caballero M, Poo MM (2006) Visual stimuli-induced LTD of GABAergic synapses mediated by presynaptic NMDA receptors. Nat Neurosci 9:372-380.

Lisman J (1989) A mechanism for the Hebb and the anti-Hebb processes underlying learning and memory. Proc Natl Acad Sci U S A 86:9574-9578.

Liu SJ, Lachamp P (2006) The activation of excitatory glutamate receptors evokes a long-lasting increase in the release of GABA from cerebellar stellate cells. J Neurosci 26:9332-9339.

MacDermott AB, Role LW, Siegelbaum SA (1999) Presynaptic ionotropic receptors and the control of transmitter release. Annu Rev Neurosci 22:443-485.

Malva JO, Silva AP, Cunha RA (2003) Presynaptic modulation controlling neuronal excitability and epileptogenesis: role of kainate, adenosine and neuropeptide Y receptors. Neurochem Res 28:1501-1515.

Markram H, Lubke J, Frotscher M, Sakmann B (1997) Regulation of synaptic efficacy by coincidence of postsynaptic APs and EPSPs. Science 275:213-215.

Martens S, Kozlov MM, McMahon HT (2007) How synaptotagmin promotes membrane fusion. Science 316:1205-1208.

Meliza CD, Dan Y (2006) Receptive-Field Modification in Rat Visual Cortex Induced by Paired Visual Stimulation and Single-Cell Spiking. Neuron 49, 183–189.

Murphy GJ, Glickfeld LL, Balsen Z, Isaacson JS (2004) Sensory neuron signaling to the brain: properties of transmitter release from olfactory nerve terminals. J Neurosci 24:3023-3030.

Murthy VN, Sejnowski TJ, Stevens CF (1997) Heterogeneous release properties of visualized individual hippocampal synapses. Neuron 18:599-612.

Nevian T, Sakmann B (2004) Single spine Ca2+ signals evoked by coincident EPSPs and backpropagating action potentials in spiny stellate cells of layer 4 in the juvenile rat somatosensory barrel cortex. J Neurosci 24:1689-1699.

Ngo-Anh TJ, Bloodgood BL, Lin M, Sabatini BL, Maylie J, Adelman JP (2005) SK channels and NMDA receptors form a Ca2+-mediated feedback loop in dendritic spines. Nat Neurosci 8:642-649.

Pinheiro PS, Perrais D, Coussen F, Barhanin J, Bettler B, Mann JR, Malva JO, Heinemann SF, Mulle C (2007) GluR7 is an essential subunit of presynaptic kainate autoreceptors at hippocampal mossy fiber synapses. Proc Natl Acad Sci U S A 104:12181-12186.

Reyes A, Lujan R, Rozov A, Burnashev N, Somogyi P, Sakmann B (1998) Target-cell-specific facilitation and depression in neocortical circuits. Nat Neurosci 1:279-285.

Sabatini BL, Oertner TG, Svoboda K (2002) The life cycle of Ca(2+) ions in dendritic spines. Neuron 33:439-452.

Samson RD, Pare D (2005) Activity-dependent synaptic plasticity in the central nucleus of the amygdala. J Neurosci 25:1847-1855.

Scanziani M, Gahwiler BH, Charpak S (1998) Target cell-specific modulation of transmitter release at terminals from a single axon. Proc Natl Acad Sci U S A 95:12004-12009.

Schneggenburger R, Sakaba T, Neher E (2002) Vesicle pools and short-term synaptic depression: lessons from a large synapse. Trends Neurosci 25:206-212.

Shin JH, Linden DJ (2005) An NMDA receptor/nitric oxide cascade is involved in cerebellar LTD but is not localized to the parallel fiber terminal. J Neurophysiol 94:4281-4289.

Shouval HZ, Bear MF, Cooper LN (2002) A unified model of NMDA receptor-dependent bidirectional synaptic plasticity. Proc Natl Acad Sci U S A 99:10831-10836.

Sjöström PJ, Turrigiano GG, Nelson SB (2001) Rate, timing, and cooperativity jointly determine cortical synaptic plasticity. Neuron 32:1149-1164.

Sjöström PJ, Turrigiano GG, Nelson SB (2003) Neocortical LTD via coincident activation of presynaptic NMDA and cannabinoid receptors. Neuron 39:641-654.

Silver RA, Lubke J, Sakmann B, Feldmeyer D (2003) High-probability uniquantal transmission at excitatory synapses in barrel cortex. Science 302:1981-1984.

Stevens CF, Wang Y (1995) Facilitation and depression at single central synapses. Neuron 14:795-802.

Suárez LM, Suárez F, del Olmo N, Ruiz M, González-Escalada JR, Solís JM (2005) Presynaptic NMDA autoreceptors facilitate axon excitability: a new molecular target for the anticonvulsant gabapentin. Eur J Neurosci 21:197-209.

Suárez LM, Solís JM (2006) Taurine potentiates presynaptic NMDA receptors in hippocampal Schaffer collateral axons. Eur J Neurosci 24:405-418.

Sudhof TC (2004) The synaptic vesicle cycle. Annu Rev Neurosci 27:509-547.

Sun HY, Dobrunz LE (2006) Presynaptic kainate receptor activation is a novel mechanism for target cell-specific short-term facilitation at Schaffer collateral synapses. J Neurosci 26:10796-10807.

Takahashi T, Kajikawa Y, Tsujimoto T (1998) G-Protein-coupled modulation of presynaptic calcium currents and transmitter release by a GABAB receptor. J Neurosci 18:3138-3146.

Trussell LO (2002) Modulation of transmitter release at giant synapses of the auditory system. Curr Opin Neurobiol 12:400-404.

Turecek R, Trussell LO (2001) Presynaptic glycine receptors enhance transmitter release at a mammalian central synapse. Nature 411:587-590.

Turecek R, Trussell LO (2002) Reciprocal developmental regulation of presynaptic ionotropic receptors. Proc Natl Acad Sci U S A 99:13884-13889.

Wadiche JI, Jahr CE (2001) Multivesicular release at climbing fiber-Purkinje cell synapses. Neuron 32:301-313.

Woodhall G, Evans DI, Cunningham MO, Jones RSG (2001) NR2B-containing NMDA autoreceptors at synapses on entorhinal cortical neurons. J Neurophysiol 86:1644-1651.

Yang SN, Tang YG, Zucker RS (1999) Selective induction of LTP and LTD by postsynaptic [Ca2+]i elevation. J Neurophysiol 81:781-787.

Yang J, Woodhall GL, Jones RS (2006) Tonic facilitation of glutamate release by presynaptic NR2B-containing NMDA receptors is increased in the entorhinal cortex of chronically epileptic rats. J Neurosci 26:406-410.

Zhu JJ, Connors BW (1999) Intrinsic firing patterns and whisker-evoked synaptic responses of neurons in the rat barrel cortex. J Neurophysiol 81:1171-1183.

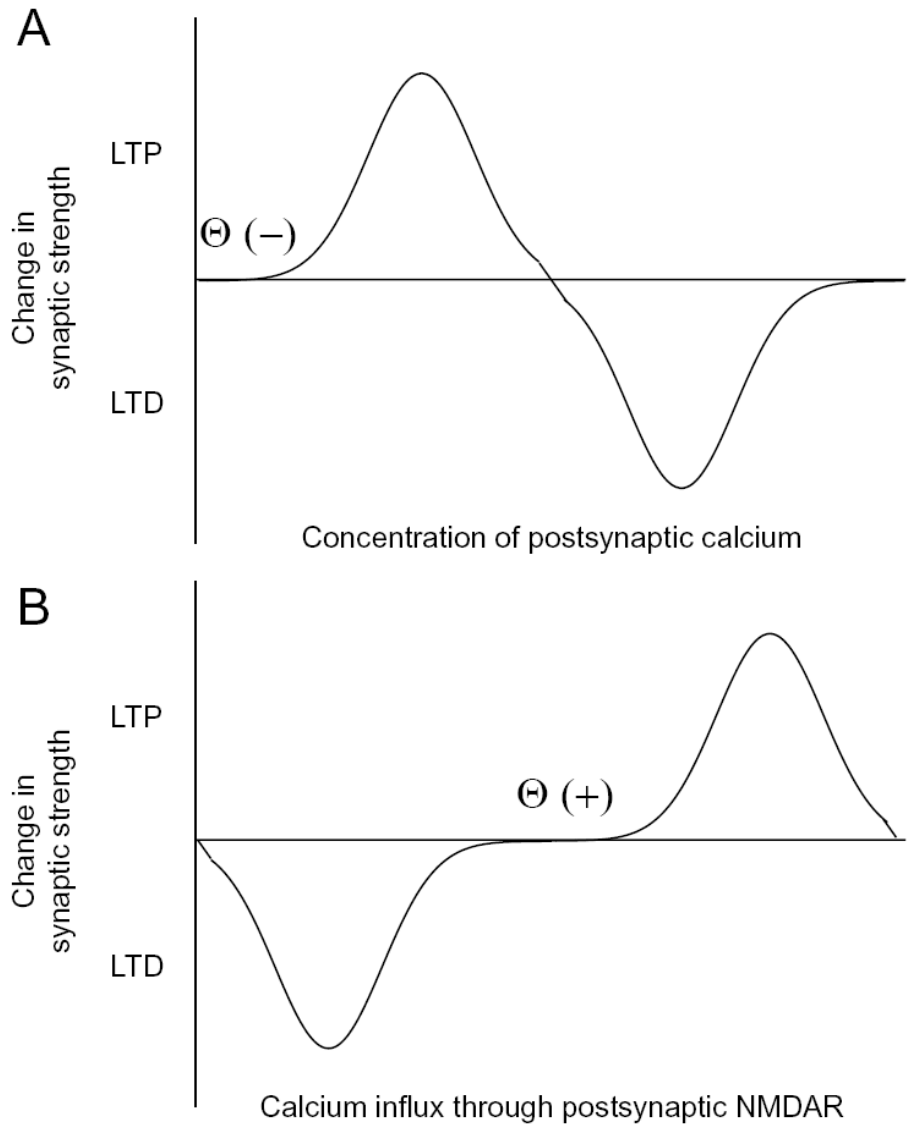



Fig. 1.1: Two models of postsynaptic calcium integration. Note: calcium is plotted in arbitrary, not-necessarily-linear units. A. The classic model first proposed by Bienenstock, Cooper, and Munro (1982). Baseline synaptic transmission causes small amount of calcium influx, insufficient for LTD or LTP ($\Theta^-$). Slight increases lead to LTD, greater increases lead to LTP. B. Model proposed by Froemke, Poo, and Dan (2005). Only calcium flowing through postsynaptic NMDARs can cause plasticity. Baseline transmission causes sufficient calcium influx to lie at the point between LTD and LTP ($\Theta^+$). (Adapted from Artola & Singer, 1993)

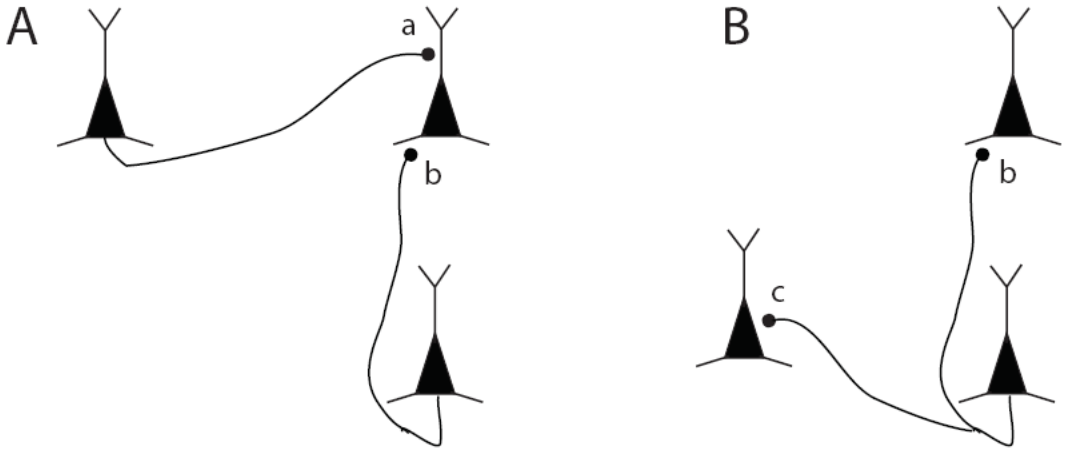



Fig. 1.2: Two types of synapse-specificity. A. "Input-selectivity": two excitatory synapses (a & b) converging onto a single postsynaptic excitatory cell from two different classes of presynaptic partners have different properties. B. "Target-selectivity": two axon collaterals from a single excitatory presynaptic cell make synaptic contacts (b & c) onto two different postsynaptic excitatory partners with different properties.

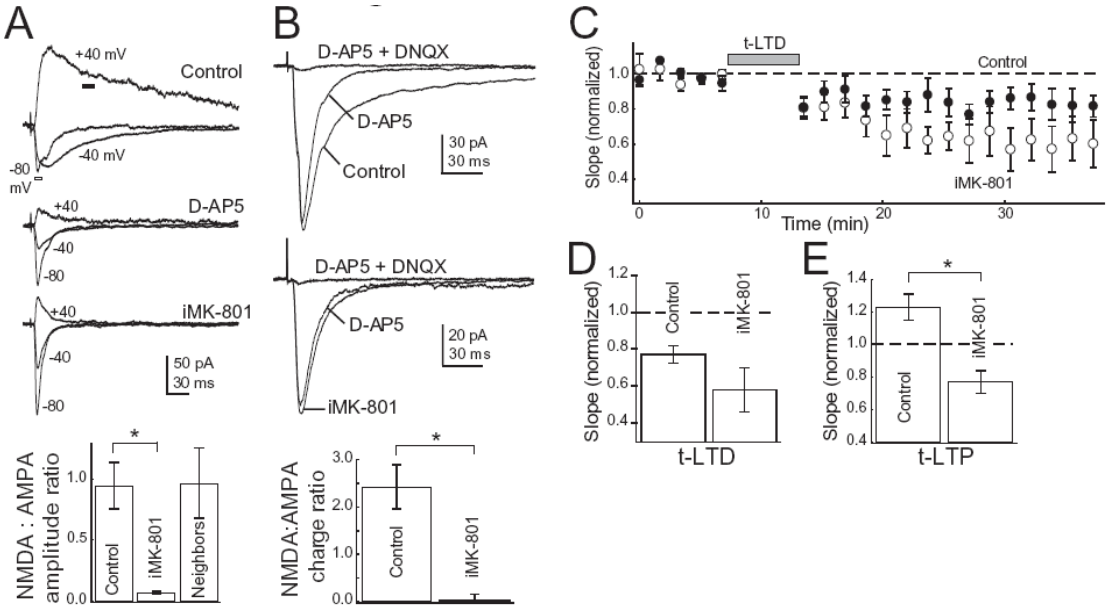



Fig. 1.3: Blockade of postsynaptic NMDA currents by internal MK-801 does not block t-LTD. A, iMK-801 (1 mM) substantially blocks NMDA currents measured at +40 mV. Top, representative EPSCs measured in control cells and in the presence of 50 μM D-AP5 and 1 mM internal MK-801. Holding potentials are indicated. Bottom, quantification of NMDA (amplitude of current at +40 mV at dark bar in $A_1$) to AMPA (amplitude of current at –80 mV at outlined bar in $A_1$) current ratios in control, D-AP5, iMK-801 conditions and cells recorded with normal internal within 10 μm of cells recorded with iMK-801 (neighbors). B, iMK-801 also blocks NMDA currents at –60 mV. Top, representative EPSCs recorded at –60 mV in low (0.4 mM) $Mg^{2+}$ Ringer's solution in control (top) and MK-801 (bottom) internals in normal Ringer's, 50 μM D-AP5 and 10 μM DNQX. Bottom, quantification of the NMDA:AMPA current integral ratio (see methods) for all cells tested. C, iMK-801 does not block t-LTD. Net effect of iMK-801 on t-LTD plotted with interleaved controls. Open circles, iMK-801. Closed circles, interleaved controls. D, Summary of effect of iMK-801 on t-LTD. E, iMK-801 does block t-LTP. Bars show mean ± SEM. (Reprinted from Bender et al., 2006 with permission from the authors.)

## II. Spike-timing dependent synaptic plasticity measured *in vivo* in primary somatosensory cortex


### Abstract

In spike-timing dependent plasticity (STDP), synaptic strength stably increases when presynaptic neurons reliably fire a few milliseconds before postsynaptic neurons, and stably decreases when the firing order is reversed. STDP has been clearly demonstrated *in vitro* in many systems and *in vivo* in *Xenopus* tectum, but has not yet been observed on the single-cell level in a mammalian system *in vivo*. Here, we attempted to induce STDP *in vivo* in urethane-anesthetized rat S1 (ages P27-30), using whole-cell recording. Sub-threshold whisker-evoked depolarizing postsynaptic potentials (wPSPs) were recorded in layer 2/3 neurons in response to deflection of the principal whisker (PW) and one adjacent whisker (AW). We attempted to induce STDP by pairing current-evoked spikes with wPSPs. When the postsynaptic spike preceded the wPSP, we observed a high degree of variability but several cells showed significant depression. However, control experiments in which wPSPs and spikes were uncorrelated also exhibited depression. When the wPSP preceded the postsynaptic spike, we observed consistent and significant synaptic potentiation in the small population of cells studied. These data suggest that appropriately timed spikes may be able to induce changes in synaptic strength *in vivo*.

This work represents preliminary data which is part of a larger study. At the time of the completion of the present chapter, only a subset of the data was available. The reader is referred to the completed study (Jacob et al., 2007) for the full data set.

It is important to note that the conclusions drawn at the time of this preliminary study differ both quantitatively and qualitatively from the conclusions that were reached by the full data set.

**Introduction**

Long-term potentiation and depression (LTP and LTD) of synaptic transmission are well-characterized forms of plasticity that occur in diverse brain areas and may mediate activity-dependent neuronal development and learning (Frégnac and Shulz, 1999; Abbott and Nelson, 2000; Feldman and Brecht, 2005). *In vitro* studies have shown that LTP and LTD can be induced by changes in the relative millisecond-scale timing of presynaptic and postsynaptic action potentials (spikes), termed spike-timing dependent plasticity (STDP) (Levy and Steward, 1983; Bell et al., 1997; Markram et al., 1997; Debanne et al., 1997; Bi and Poo, 1998; Nishiyama et al., 2000; Kobayashi and Poo, 2004; Wang et al., 2005; Meliza and Dan, 2006). In STDP at excitatory synapses on neocortical pyramidal cells, when a presynaptic spike and its evoked excitatory postsynaptic potential (EPSP) precede a postsynaptic spike by up to a few tens of milliseconds ("pre-leading-post"), synaptic potentiation is induced. Conversely, synaptic depression occurs when EPSP follow postsynaptic spikes ("post-leading-pre") (Feldman, 2000; Sjöström et al., 2001, Sjöström and Nelson, 2002; Froemke and Dan 2002).

Despite intensive study *in vitro*, it remains unresolved how, or whether, STDP is induced in mammalian cortex *in vivo*. STDP may differ *in vivo* from *in vitro* because of different spiking patterns, levels of inhibition, and neuromodulation, any of

which can affect the amount, likelihood, and duration of STDP (Froemke and Dan, 2002; Zhou et al., 2003; Lisman and Spruston, 2005). STDP has been inferred to occur in visual cortex *in vivo* based on receptive field changes that occur in response to precisely timed stimuli (Fu et al., 2002; René et al., 2003; Shuett et al., 2001, Yao and Dan, 2001, 2004). STDP has also been directly observed at the level of synaptic responses in visual cortex *in vivo* (Meliza and Dan, 2006). However, evidence for STDP in other cortical areas *in vivo* is lacking.

Here we studied whether STDP can be induced at the synaptic level in S1 cortex *in vivo*. We studied synaptic depression and potentiation, which both can be produced in layer (L) 2/3 pyramidal cells *in vitro* when postsynaptic spikes lead presynaptic spikes by up to 20-50 ms (Markram et al., 1997; Feldman, 2000; Sjostrom et al., 2001; Froemke and Dan, 2002). We tested for STDP using whole cell patch recording from L2/3 neurons *in vivo*, and inducing STDP by pairing current-evoked postsynaptic spikes with whisker deflections to activate presynaptic afferents at defined relative timing. Results from this protocol showed that pre-leading-post pairing drives potentiation of whisker responses, indicating that STDP-LTP can occur in S1 *in vivo*. Post-leading-pre pairing caused response depression, but this latter finding should be considered carefully, as control experiments in which spikes were paired at long delays which would be predicted to cause no change in PSP amplitude (Feldman, 2000), caused similar depression to post-before-pre pairings..

## Methods

**Surgical preparation.** All procedures were approved by the UCSD Institutional Animal Care and Use Committee. Long-Evans rats (age 27-32 days, 61-106 g) were anesthetized with urethane (1.5 g/kg, 25% in lactated Ringer's, i.p.) and given lactated Ringer's (2 mL, i.p.). The scalp was anesthetized with lidocaine and retracted, and a head bolt was attached to the skull with dental cement. The skull was thinned in a 2 x 2 mm region overlying S1, and a ~1 x 1 mm patch of bone was removed (centered 5.2 mm lateral, 2.5 mm caudal of Bregma; Celikel et al., 2004). This recording craniotomy was surrounded by a well of dental cement, which was filled with 0.9% saline. The dura was left intact. An Ag/AgCl pellet recording ground was placed below the caudal edge of the scalp, and moistened with 0.9% saline.

**Recording procedures.** During recording, anesthesia was maintained with supplemental doses of urethane (10% of original dose, i.p.). Supplemental urethane was given whenever limb withdrawal responses were present, whisker movements were observed, or breathing rate exceeded 120/min. Body temperature was maintained at 37°C with a feedback-controlled heating blanket.

Whisker deflection was performed using an array of 9 independent, computer-controlled piezoelectric actuators (Piezo Systems, Inc., Cambridge, MA), attached to individual whiskers in a 3 x 3 array. Whiskers were deflected with calibrated, 2° ramp-and-hold deflections (upward deflection, 4 ms ramp, 100 ms hold, applied 5-6.5 mm from the face).

Whole-cell recordings were made using blind patch techniques (Margrie et al., 2002). A small opening (~100 x 200 μm) was made in the dura for each penetration.

Standard borosilicate glass patch electrodes were used (3.0-5.5 MΩ tip diameter 2.5-3.5 μm). Electrodes were filled with internal solution containing (in mM): K gluconate 116; KCl 6; NaCl 2; HEPES 20; EGTA 0.5; MgATP 4-5; NaGTP 0.3; phosphocreatine 10; pH 7.20-7.25, 285-295 mOsm. The craniotomy was kept filled with 0.9% saline. High positive pressure (2.5 PSI) was applied while passing through the pia. After transiting the pia (~50-150 μm below the cortical surface), seals were sought in voltage clamp mode, using 5 mV seal test pulses, and low, intermittent pressure (0.1 - 0.2 PSI), while advancing the electrode in 2.5 μm steps. Penetrations were oriented 20° off the radial axis. "Strikes" onto putative neurons were recognized by a 2-fold increase in electrode resistance, accompanied by characteristic amplification of heartbeat/breathing artifact. After a strike, seal formation (>2GΩ) was obtained by release of pressure, gentle suction, and application of -70 mV holding potential. Whole-cell configuration was attained by applying a slow ramp of suction.

Whisker responses were recorded in current clamp mode (Axopatch-1D, 10x gain, 2 kHz low-pass filter, digitized at 5 kHz using a 12-bit National Instruments board). The bridge was generally not balanced, and Vm measurements were adjusted for uncompensated series resistance off-line. Vm was not adjusted for the liquid junction potential. Whisker deflection, data acquisition, and analysis were performed by custom-written routines in Igor (Wavemetrics, Lake Oswego, OR). Series and input resistance were measured in each sweep by responses to a square hyperpolarizing current injection (40-50 pA).

**STDP induction protocol.** PW and AW whiskers were deflected in alternation (1-1.5 s interstimulus interval) during baseline and test periods to elicit whisker-evoked subthreshold PSPs (wPSPs). For STDP induction, AW deflection was interrupted, and PW deflection was paired with current injection through the recording electrode (1.0 ± 0.3 nA, 15 to 30 ms) to induce a postsynaptic spike burst (1.5 ± 0.7 spikes) shortly before or after the PSP. One hundred pairings were performed, using the same inter-stimulus interval as during baseline. Spike bursts were used, rather than single spikes, because the relatively high series resistance *in vivo* prevented the rapid depolarization necessary to reliably elicit precisely timed single spikes. Pre-post spike delay ($\Delta t$) was calculated as the mean time of all evoked spikes in the postsynaptic burst minus the onset latency of the wPSP (Feldman, 2000). In the 5 pre-leading-post pairings, AW deflection was continued during PW pairing, interleaved but unpaired with current injection.

After PW pairing, PW and AW were again deflected in alternation to measure changes in wPSPs. At least 2.5 min (50 repetitions of each whisker) of post-pairing data were required for inclusion in analysis. In 15 of 36 neurons, only single pairings were performed. In 21 neurons, multiple (2 or 3) pairing periods, separated by ≥ 10 min, were performed. Plasticity in later pairings was not significantly different from that in early pairings (PSP amplitude: $p > 0.8$; PSP slope: $p > 0.4$, unpaired t-test). Thus, each pairing was considered a separate data point. A pairing was accepted for analysis only if series resistance and input resistance varied by < 20% between baseline and test periods, and if Vm varied by < 5 mV.

For each pairing, the wPSP amplitude (5 ms window) and initial slope (first 3.5 ms of wPSP) were calculated for the period (2.5-5 min before pairing) and the test period (first 5 min after pairing). Statistical significance of plasticity was determined using the non-parametric Kolmogorov-Smirnoff test (K-S test, significance threshold 0.01) comparing all responses in these intervals. Magnitude of plasticity was defined as $((Response_{test} - Response_{baseline}) / Response_{test})$, as standard in the *in vitro* literature (e.g., Feldman, 2000). All citations of plasticity magnitude in the text use this measure. All descriptive statistics are given as mean ± SEM unless stated otherwise.

**Results**

We used whole-cell recording *in vivo* to directly measure STDP of whisker-evoked subthreshold synaptic input. The strategy was to record whisker-evoked, subthreshold postsynaptic potentials (wPSPs), and then to induce STDP by pairing wPSPs (which represent activation of presynaptic inputs to the recorded neuron) with postsynaptic spikes produced by direct current injection into the neuron.

20 neurons were included in this study. Of these, 11 were regular spiking (Fig. 2.1A top), 4 were intrinsically bursting (Fig. 2.1A middle), and 5 were unclassified; unclassified neurons showed irregular firing patterns with no clear firing adaptation to 500-ms current injection. Fast-spiking neurons (putative interneurons, Fig. 2.1A bottom) were excluded from analysis because of well-known differences in plasticity rules at synapses on inhibitory vs. excitatory neurons (Bell et al., 1997, Bi and Poo, 1998, Tzounopoulos et al., 2004). All cells were located 220-730 μm (median 330

μm) below the pia, based on microdrive depth readings. These depths were shown previously to correspond to L2/3 (Celikel et al., 2004), though it is possible that a few of the deepest cells may have been in L4. We focused on L2/3 since L2/3 neurons exhibit well-characterized STDP *in vitro* (Feldman, 2000), and have been suggested to do so *in vivo* (Celikel et al., 2004). Mean series resistance was 120 MΩ, mean input resistance was 43 MΩ, and mean resting potential was -70 ± 11 mV (n=20).

**Induction of STDP in whole-cell recordings.** For each neuron, we first measured wPSPs evoked by each of 9 whiskers in a 3 x 3 array. The PW was identified as the whisker evoking the wPSP with the steepest initial slope and shortest latency (Fig. 2.1B and C) (Brecht et al., 2003). Deflections of the PW and one AW (typically the AW eliciting the largest wPSP) were then adjusted in amplitude and velocity to elicit roughly equal amplitude subthreshold wPSPs (7.2 ± 4.5 and 5.7 ± 3.7 mV for the PW and the AW, respectively). We tried to avoid driving whisker-evoked postsynaptic spikes, but such spikes did occasionally occur when PSPs coincided with large spontaneous depolarizations, as occur normally in S1 *in vivo* (Brecht et al., 2003; McCormick, 2005).

Baseline responses were measured to interleaved deflections of the PW and AW, with each whisker being deflected at 0.33-0.5 Hz in alternation. After a stable baseline (~5 min, 50-100 repetitions per whisker), we attempted to induce STDP by pairing deflection of the PW with current injection through the recording electrode to evoke one or more spikes in a short burst. The evoked spikes were timed to occur just before or after onset of the PW-PSP. PW pairing was repeated 100 times, without

altering stimulation rate, and the AW was not deflected (see Methods). The PW was chosen for pairing because PW responses in L2/3 neurons are mediated in large part by L4-to-L2/3 synapses, which show robust STDP *in vitro* (Feldman, 2000). After PW pairing, responses to interleaved PW and AW responses were again measured.

Figure 2.2 shows an example of a post-leading-pre pairing in a RS neuron which was subjected to postsynaptic spikes leading the PW-PSP by a mean of -26 ms (Fig. 2.2B). Pairing caused the amplitude of the PW-PSP to decrease from 19.7 ± 8.4 mV during baseline to 15.4 ± 10.1 mV in the first 5 min post-pairing (K-S, $p < 0.05$), and PSP initial slope to decrease from 1.8 ± 0.9 mV/ms to 1.2 ± 0.9 mV/ms, (K-S, $p<0.0001$). The depression lasted for the ten minutes of post-pairing recording and was specific to the paired PW whisker, since no significant change was observed for the unpaired AW whisker (baseline amplitude: 15.6 ± 8.9; post-pairing: 15.4 ± 7.6 mV, K-S, $p > 0.7$; baseline slope: 1.5 ± 0.7; post-pairing: 1.4 ± 0.7 mV/ms, K-S, $p>0.8$).

Figure 2.3 shows one example of potentiation, in a RS neuron (Fig. 2.3A) subjected to a +15 ms delay pairing of the PW response (Fig. 2.3B). After pairing, the PW-PSP increased from 6.8 ± 0.5 mV to 9.8 ± 0.7 mV (K-S, $p < 0.00001$) and the PSP slope increased from 1.6 ± 0.1 mV/ms to 2.2 ± 0.2 mV/ms post-pairing (K-S, $p < 0.00001$). Potentiation was accompanied by a change in the AW-PSP amplitude (3.6 ± 0.7 mV during baseline, 4.9 ± 0.6 mV in the period from 0-5 min post-pairing period, K-S, $p < 0.0005$) that was transient and that rapidly returned to the baseline values.

**The learning rule for spike timing-dependent synaptic depression *in vivo*.** The STDP learning rule across all pairings is shown in Fig. 2.4A. The magnitude of

plasticity for each pairing is represented as percent change in PW-PSP amplitude. Most post-leading-pre pairings produced some amount of depression of PW-PSP amplitude. 5 of 14 pairings showed significant depression of PSP amplitude, and no cases of significant potentiation were observed. Conversely, 3 of 5 pre-leading-post pairings showed significant potentiation of PSP amplitude, with no cases of significant depression observed.

Fig. 2.4B summarizes the data across the population. Post-leading-pre pairings caused -9 ± 3 % reduction in PW-PSP amplitude, although these results were not significant. By comparison, the AW-PSP exhibited an increase of 3 ± 5 % in amplitude suggesting that the changes observed in the PW were largely pathway-specific. However, in control pairings in which $\Delta t = 1$ s, a larger, significant degree of depression was observed ($\Delta$PW-PSP = -26 ± 6 %), with no change in the AW-PSP (1 ± 11 %). By comparison, pre-leading-post pairings caused significant increase in PW-PSP amplitude (24 ± 7 %). However, there was a similar amplitude increase in AW-PSP amplitude (20 ± 7 %), indicating that the changes are not pathway specific for potentiation. Taken together, these results indicate that post-leading-pre and long delay pairings cause a pathway-specific depression in paired wPSP amplitude, while pre-leading-post pairings cause robust, but pathway-non-specific potentiation in wPSP amplitude.

## Discussion

*In vitro*, excitatory synapses on cortical pyramidal neurons exhibit STDP in which pre-leading-post spiking drives LTP, while post-leading-pre spiking drives LTD. How STDP is induced *in vivo* has been less clear, in part because cortical neurons *in vivo* experience a strong bombardment of synaptic input, including GABAergic input that has been predicted to alter or prevent STDP (Lisman and Spruston, 2005). Understanding how, and whether, STDP is induced at excitatory cortical synapses *in vivo* is critical because STDP at these synapses has been proposed to mediate experience-induced changes in sensory representations and sensory perception (Schuett et al., 2001; Yao and Dan, 2001, 2004; Fu et al., 2002; René et al., 2003; Celikel et al., 2004; Feldman and Brecht, 2005; Meliza and Dan, 2006). While several prior studies have demonstrated STDP in the visual cortex *in vivo* (René et al., 2003; Schuett et al., 2001; Yao and Dan, 2001, Yao et al., 2004; Meliza and Dan, 2006), this is the first study that has tested STDP of synaptic inputs in S1 *in vivo*.

We observed consistent, pathway non-specific spike-timing dependent potentiation of wPSPs for pre-leading-post pairings. By comparison, PW-PSP amplitude decreased for both post-leading-pre pairings and long delay pairings, with no change in AW-PSP amplitude.

**Synaptic depression.** Plasticity was induced by pairing whisker-evoked subthreshold PSPs, which reflect spiking activity of presynaptic afferents, with postsynaptic spikes elicited by direct current injection into the recorded neuron. Recordings were made primarily in L2/3, and the PW was paired, rather than the AW. This was done because PW responses in L2/3 are primarily mediated by L4-L2/3

synapses (Armstrong-James et al., 1992), which exhibit well-defined STDP *in vitro*, thus facilitating comparison between *in vivo* and *in vitro* STDP rules.

Results showed that post-leading-pre pairing caused measurable depression of synaptic responses in most neurons (Fig. 2.4). Compared to STDP-LTD in pyramidal cells *in vitro* (Feldman, 2000; Celikel et al., 2004), cell-to-cell variability was high. However, 71% of neurons showed some depression, 36% showed significant depression, and no neurons showed significant potentiation following this protocol. Thus, we conclude that short post-leading-pre spike delays elicit depression of whisker-evoked synaptic responses in L2/3 pyramidal cells *in vivo*. (Recordings were likely from pyramidal cells because fast-spiking neurons were excluded.) Whether plasticity occurred mainly at L4-L2/3 synapses, which classically drive PW responses in L2/3 neurons, is unknown.

Depression persisted for 5 minutes, and in some cells for 12 min, the longest duration of stable recording (data not shown). This duration is considerable given the rapid reversal of plasticity that can occur *in vivo* (Zhou et al., 2003). However, the duration of our recordings does not allow us to conclude whether true LTD or a less persistent form of depression was induced.

We hypothesized that long delay ($\Delta t = 1$ s) pairings would produce no change. However, we observed a consistent and significant depression of the PW-PSP during long delay pairings. Although surprising, this observation is consistent with the fact that L4-L2/3 synapses exhibit an asymmetric STDP window *in vitro*, with a much broader window for LTD than LTP (Feldman, 2000; Celikel et al., 2004). It has been predicted that uncorrelated pre- and post-synaptic spiking would cause synaptic

depression (Feldman, 2000). Together with the fact that neurons *in vivo* exhibit spontaneous synaptic potentials at a high frequency (Brecht et al., 2003; Brasier, Shulz, and Feldman, unpublished observations), this observation may be because spontaneous PSPs paired randomly with long delay spikes and thus were uncorrelated and evoked synaptic depression. The reason why the mean depression is larger in uncorrelated controls than post-before-pre pairings is unknown but may reflect a novel mechanism by which uncorrelated inputs are selectively depressed. An alternative explanation of these data is that the timing window for synaptic depression is longer *in vivo* than *in vitro*.

**Synaptic potentiation.** In contrast to synaptic depression, the observed synaptic potentiation was more robust, albeit studied in fewer cells. Pre-leading-post pairing drove significant potentiation of PW-PSP amplitude (Fig. 2.4). Though the potentiation side of the STDP rule was not explored in detail, the delays at which it was measured is similar to STDP measured *in vivo* in visual cortex (Meliza and Dan, 2006) and *Xenopus* tectum (Dan and Poo, 2006). Surprisingly, unlike LTD, the LTP we observed was not pathway-specific, and comparable magnitude effects were seen on the unpaired AW and the paired PW. This may reflect heterosynaptic LTP expression *in vivo*. This is especially surprising considering that heterosynaptic LTD has been observed in some preparations, but LTP appears to always be homosynaptic *in vitro* (Muller et al., 1995; Bear and Abraham, 1996; Nishiyama et al., 2000). Alternatively, this observation could be due to the fact that AW deflection continued (without being paired with spikes) during PW-pairing for pre-leading-post, but not during post-leading-pre pairings. However, the reason why such a difference would

cause the plasticity to be expressed on both pathways is unclear and is difficult to reconcile with the observation that long delay pairings on the PW alone produced depression.

**Differences in STDP *in vivo* vs. *in vitro*.** Synaptic depression appeared less stable *in vivo* (5-10 min, though full duration may have been masked by limitations in recording duration) than *in vitro* (>30 min), consistent with the rapid reversal of LTP and LTD in active networks *in vivo* (Zhou et al., 2003). This may reflect (i) restriction of STDP by network activity, GABAergic inhibition, or neuromodulation *in vivo*, or (ii) a contribution to plasticity *in vivo* by non-L4-L2/3 synapses with STDP rules with shorter LTD windows (Froemke et al., 2005).

STPD induction *in vivo* occurs in the context of complex natural spike trains, compared to the simple spike trains typically used to study STDP *in vitro*. High-frequency natural spike trains impose multiple interactions between pre- and postsynaptic spike pairs, each of which may contribute to synaptic depression or potentiation (Sjöström et al., 2001; Froemke and Dan, 2002; Wang et al., 2005; Kobayashi and Poo, 2004; Froemke et al., 2006). The integration of multiple interspike interactions is described by second-order STDP rules that are more complex than first-order rules describing plasticity from isolated pre/post spike pairs.

**STDP as a potential mechanism for plasticity *in vivo*.** These results show that spike timing-dependent synaptic depression can be induced in S1 *in vivo* by the conjunction of appropriately timed natural sensory stimuli and evoked spikes. Pathway-specific depression was observed both for short-delay post-before-pre pairings and 1 s (long delay) pairings. Non-pathway-specific potentiation was

observed for pre-before-post pairings. These results support the idea that STDP is a relevant learning rule *in vivo*, and may contribute to map plasticity or learning.

**Acknowledgment**

These results represent preliminary data gathered as part of a larger study. The tentative conclusions drawn from these preliminary data differ from the conclusions that were drawn from the full data set at the completion of the study. The reader is referred to the completed study (Jacob et al., 2007) for the full data set and complete interpretation of the results.

This chapter is an early version of Jacob V, Brasier DJ, Erchova I, Feldman D, Shulz DE. Spike timing-dependent synaptic depression in the *in vivo* barrel cortex of the rat. J Neurosci. 2007 Feb 7; 27(6):1271-84. The data included in Chapter 2 only comprise those data for which the thesis author was primarily responsible. The portions present here are included with the permission of all the authors on the final publication. The co-authors on the final published paper are thanked for help in analysis for figures 2.1-2.3 and for substantial contribution to the text of this chapter.

**References**

Abbott LF, Nelson SB. (2000) Synaptic plasticity: taming the beast. Nat Neurosci 3:1178-83.

Armstrong-James M, Fox K, Das-Gupta A (1992) Flow of excitation within rat barrel cortex on striking a single vibrissa. J Neurophysiol68:1345-1358.

Bell CC, Han VZ, Sugawara Y, Grant K (1997) Synaptic plasticity in a cerebellum-like structure depends on temporal order. Nature 387:278-281.

Bi GQ, Poo MM (1998) Synaptic modifications in cultured hippocampal neurons: dependence on spike timing, synaptic strength, and postsynaptic cell type. J Neurosci 18:10464-10472.

Brecht M, Roth A, Sakmann B (2003) Dynamic receptive fields of reconstructed pyramidal cells in layers 3 and 2 of rat somatosensory barrel cortex. J Physiol 553:243-265.

Celikel T, Szostak VA, Feldman DE (2004) Modulation of spike timing by sensory deprivation during induction of cortical map plasticity. Nat Neurosci 7:534-541.

Debanne D, Gahwiler BH, Thompson SM (1997) Bidirectional associative plasticity of unitary CA3-CA1 EPSPs in the rat hippocampus in vitro. J Neurophysiol 77:2851-2855.

Feldman DE (2000) Timing-based LTP and LTD at vertical inputs to layer II/III pyramidal cells in rat barrel cortex. Neuron 27:45-56.

Feldman DE, Brecht M (2005) Map plasticity in somatosensory cortex. Science 310:810-815.

Frégnac Y, Shulz DE (1999) Activity-dependent regulation of receptive field properties of cat area 17 by supervised Hebbian learning. J Neurobiol 41:69-82.

Froemke RC, Dan Y (2002) Spike-timing-dependent synaptic modification induced by natural spike trains. Nature 416:433-438.

Froemke RC, Tsay IA, Raad M, Long JD, Dan Y. (2006) Contribution of individual spikes in burst-induced long-term synaptic modifications. J Neurophysiol 95:1620-1629

Fu YX, Djupsund K, Gao H, Hayden B, Shen K, Dan Y (2002) Temporal specificity in the cortical plasticity of visual space representation. Science 296: 1999-2003.

Jacob V, Brasier DJ, Erchova I, Feldman D, Shulz DE (2007) Spike timing-dependent synaptic depression in the in vivo barrel cortex of the rat. J Neurosci 27:1271-1284.

Kobayashi K, Poo MM (2004) Spike train timing-dependent associative modification of hippocampal CA3 recurrent synapses by mossy fibers. Neuron 41:445-454.

Levy WB and Steward O (1983) Temporal contiguity requirements for long-term associative potentiation/depression in the hippocampus. Neuroscience 8:791-797.

Lisman J and Spruston N (2005) Postsynaptic depolarization requirements for LTP and LTD: a critique of spike timing-dependent plasticity. Nat Neurosci 8:839-841

Markram H, Lubke J, Frotscher M, Sakmann B (1997) Regulation of synaptic efficacy by coincidence of postsynaptic APs and EPSPs. Science 275:213-215.

Meliza CD, Dan Y (2006) Receptive-Field Modification in Rat Visual Cortex Induced by Paired Visual Stimulation and Single-Cell Spiking. Neuron 49, 183–189.

McCormick DA (2005) Neuronal networks: flip-flops in the brain. Curr Biol15:R294-R296.

Muller D, Hefft S, Figurov A (1995) Heterosynaptic interactions between LTP and LTD in CA1 hippocampal slices. Neuron 14:599-605.

Nishiyama M, Hong K, Mikoshiba K, Poo MM, Kato K (2000) Calcium stores regulate the polarity and input specificity of synaptic modification. Nature 408:584-588.

René A, Huguet N, Pananceau M, Grant K, Frégnac Y. (2003) An in vivo generalisation of hebbian plasticity rules in adult visual cortex to multiple pre-post synaptic activity correlations. Society for Neuroscience Program No. 266.17.

Schuett S, Bonhoeffer T, Hubener M (2001) Pairing-induced changes of orientation maps in cat visual cortex. Neuron 32:325-337.

Sjöström PJ, Nelson SB (2002) Spike timing, calcium signals and synaptic plasticity. Curr Opin Neurobiol 12:305-314.

Sjöström PJ, Turrigiano GG, Nelson SB (2001) Rate, timing, and cooperativity jointly determine cortical synaptic plasticity. Neuron 32:1149-1164.

Tzounopoulos T, Kim Y, Oertel D, Trussell LO (2004) Cell-specific, spike timing-dependent plasticities in the dorsal cochlear nucleus. Nat Neurosci 7:719-725

Yao H, Dan Y (2001) Stimulus timing-dependent plasticity in cortical processing of orientation. Neuron 32:315-323.

Yao H, Shen Y, Dan Y (2004) Intracortical mechanism of stimulus-timing-dependent plasticity in visual cortical orientation tuning. Proc Natl Acad Sci U S A 101:5081-5086.

Wang HX, Gerkin RC, Nauen DW, Bi GQ (2005) Coactivation and timing-dependent integration of synaptic potentiation and depression. Nat Neurosci 8:187-193.

Zhou Q, Tao HW, Poo MM (2003) Reversal and stabilization of synaptic modifications in a developing visual system. Science 300:1953-1957.

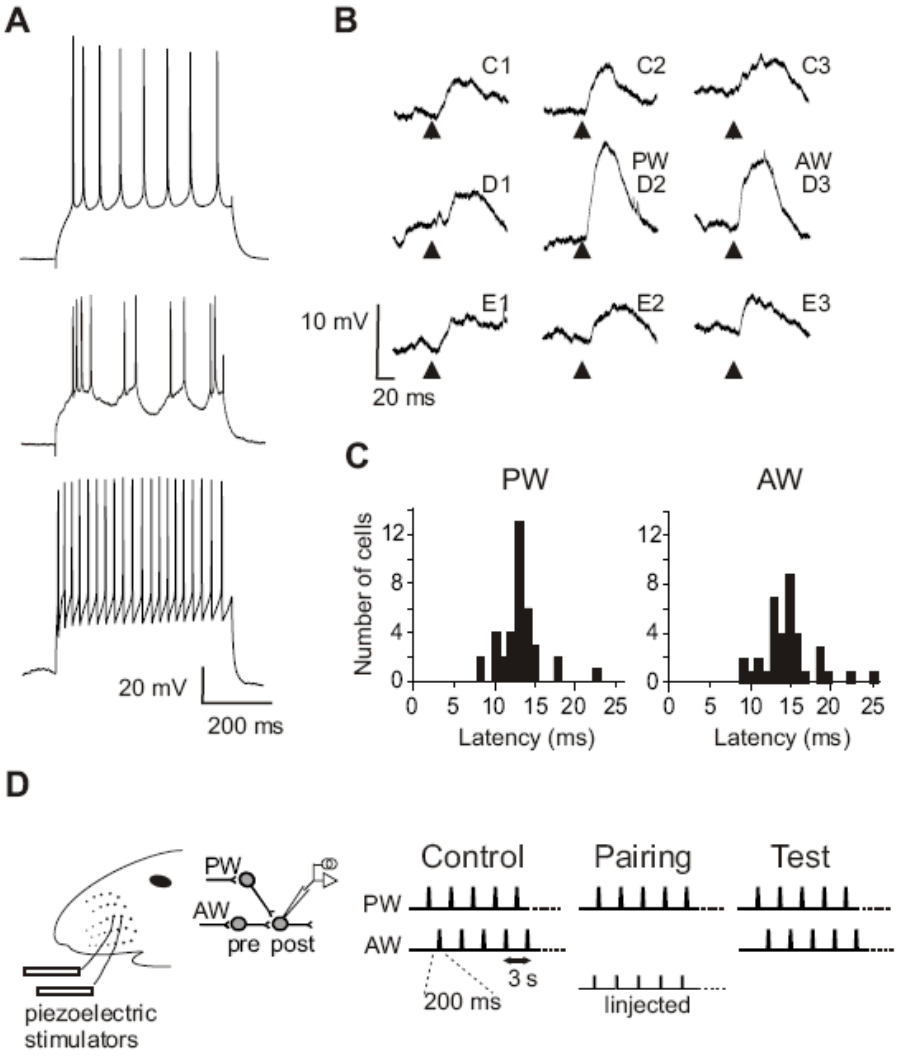



Fig. 2.1: Experimental protocol for whole-cell induction of STDP in vivo. A. Examples of regular spiking (putative pyramidal neuron, top), intrinsic bursting (putative pyramidal neuron, middle) and fast spiking (putative inhibitory interneuron, bottom) firing patterns. B. Subthreshold receptive field for one neuron. Each trace shows a wPSP elicited by the indicated whisker. The PW for this neuron was D2. C. Distribution of PSP latencies for the population of recorded neurons (n=36) in response to stimulation of the PW (left) and the AW (right). D. STDP protocol for whole-cell experiments. During the control and the test periods, the PW and the AW were deflected alternately. During pairing, PW deflection was paired with current injection to elicit postsynaptic spikes.

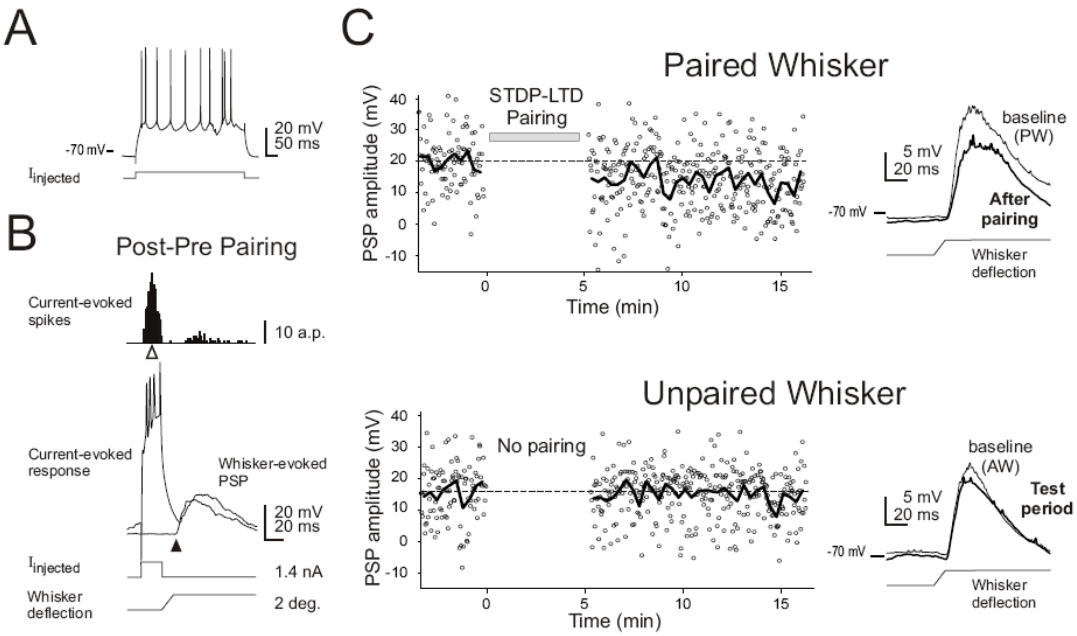



Fig. 2.2: Induction of tLTD in a representative neuron. A. Firing pattern in response to 500-ms current injection. B. Pairing protocol in which current-evoked spikes preceded the PW-evoked PSP. Histogram: distribution of times of all evoked spikes, relative to PSP onset (black arrowhead), during pairing. Mean ?t for this cell was -26 ms (white arrowhead). C. Results of pairing. Amplitude of each wPSP during the experiment (small points), and average of each 10 trials (thick line) for the paired PW (top) and unpaired AW (bottom) whiskers. On the right: wPSP averaged over 50 trials during baseline (thin line) and after pairing (thick line).

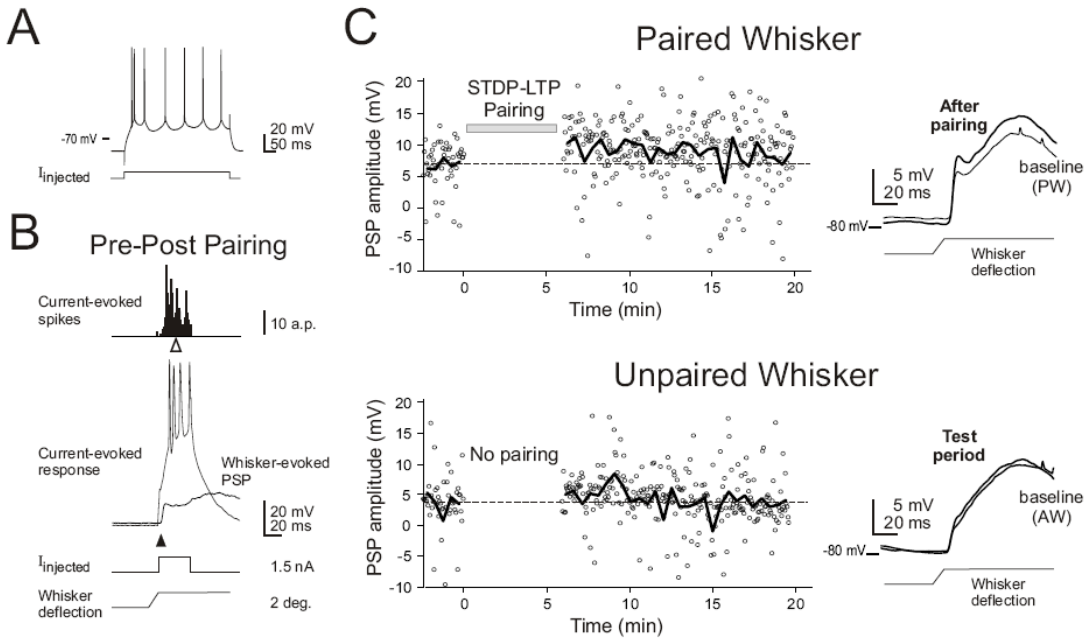



Fig. 2.3: Induction of spike timing-dependent synaptic potentiation in a representative neuron. A. Regular spiking pattern in response to 500-ms current injection. B. Pairing protocol in which current-evoked postsynaptic spikes followed the PW-evoked PSP. Mean ?t for this cell was +15 ms (white arrowhead). C. Results of pairing on PW (paired) and AW (unpaired) wPSPs. Conventions as in Fig. 2.2.

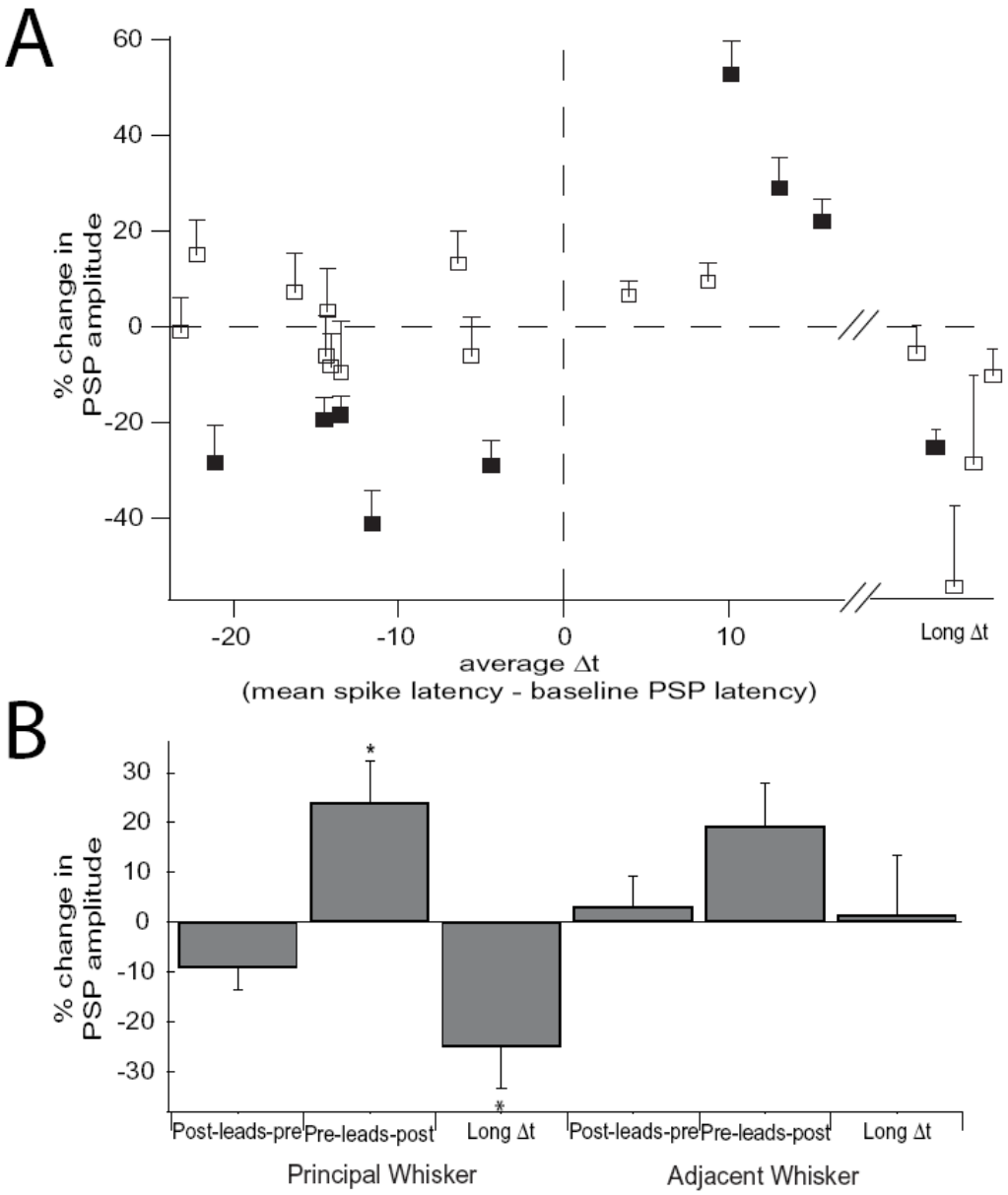



Fig. 2.4: Learning rule for spike timing-dependent synaptic plasticity in L2/3 in vivo. A. Pairing-induced changes in amplitude of the PW-PSP, as a function of delay between postsynaptic spikes and PW-PSP onset. Each point is one pairing. Filled symbols show statistically significant pairings (Student's t-test, $p<0.05$). Right, 1 s delay control pairings. B. Mean ± SEM for change in response of the PW (which was paired) and the surrounding unpaired AW for each of the three pairing protocols.

## III. Partial blockade of NMDA receptors is not sufficient to cause depression at synaptic inputs onto L2/3 pyramidal cells


### Abstract

Spike-timing dependent plasticity (STDP) is a physiologically relevant form of synaptic plasticity in which near-coincidence of pre- and postsynaptic action potentials causes synaptic long-term potentiation (LTP) or depression (LTD). While it is widely accepted that postsynaptic NMDA receptors (NMDARs) are the coincidence detector for STD-LTP, the identity of the coincidence detector for LTD remains illusive and controversial. Classically, LTD has been thought to be produced when calcium levels rise slightly above which normally occurs during baseline transmission, activating calcineurin which causes LTD. However, it has recently been observed in visual cortex that subsaturating blockade of NMDARs produces LTD, and it has been proposed that, rather than being downstream of coincidence detection, calcineurin detects postsynaptic spikes and causes NMDAR desensitization, providing the postsynaptic mechanism for coincidence detection. Here we attempted to induce LTD by partially blocking postsynaptic NMDARs, but were unable to do so at either the layer 4 to layer 2/3 projection or at local inputs onto the apical dendrites of layer 2/3 cells in somatosensory cortex. Thus it appears that this mechanism for coincidence detection is unique to visual cortex and, therefore, there may be multiple coincidence detectors for STD-LTD, specialized to individual cortical areas. Whether these differences are because of a difference between visual cortex and somatosensory cortex or some other, unidentified, difference between the studies is unknown.

## Introduction

How neurons detect near-coincident pre- and postsynaptic activity, and distinguish between pre-before-post and post-before-pre pairings is an important question to understanding the mechanism of spike-timing dependent plasticity (STDP), which is a physiologically relevant form of synaptic plasticity (Markram et al., 1997; Egger et al., 1999; Feldman, 2000; Abbott and Nelson, 2000; Holmgren and Zilberter, 2001; Sjöström et al., 2001; Bi and Poo; 2001; Froemke and Dan, 2002; Celikel et al., 2004; Young et al., 2007). A long standing model of the induction of long-term plasticity in general holds that moderate rises in postsynaptic calcium above that seen during normal baseline transmission cause LTD by activating calcium-dependent phosphatases such as calcineurin while more substantial rises in postsynaptic calcium activate calcium-dependent kinases such as CaMKII, resulting in LTP (Bienenstock et al., 1982; Bear et al., 1987; Lisman, 1989; Artola and Singer, 1993; Yang et al., 1999; Cormier et al., 2001).

In line with this theory, it has been observed that pre-before-post pairings cause a large, supralinear calcium signal in dendritic spines, while post-before-pre pairings cause a small, sublinear increase in calcium signal above baseline levels (Koester and Sakmann, 1998; Nevian and Sakmann, 2004). It has therefore been proposed that the postsynaptic NMDA receptor (NMDAR) serves as the coincidence detector for both spike-timing dependent LTP (tLTP) and tLTD (Shouval et al., 2002; Johnston et al., 2003). However, calcium influx into postsynaptic spines may be segregated spatially into microdomains (Delmas et al., 2002; Bloodgood and Sabatini,

2007) and it is therefore possible that even if post-before-pre pairings result in slight increases in total calcium signals above baseline levels, there is a decrease below baseline levels within a microdomain.

A recent study by Froemke and colleages (2005) proposes just that. They argue that rather than being downstream of coincidence detection and being a key player in expression of LTD, calcineurin actually serves as a critical player in coincidence detection. They propose a model whereby postsynaptic spikes cause an influx of calcium through voltage-sensitive calcium channels activating calcineurin, which causes calcium-dependent desensitization of postsynaptic NMDARs (Rosenmund et al., 1995; Tong et al., 1995; Umemiya et al., 2001). Subsequent glutamate release from the presynaptic terminal results in calcium influx through the postsynaptic NMDAR below that of baseline transmission. In contrast to the classical model, Froemke and colleagues (2005) propose that baseline synaptic activity causes NMDAR-mediated calcium influx that, rather than being so low as to cause no plasticity, is greater than the amount needed to induce LTD and less than that needed to induce LTP (Fig. 1.1B; Bienenstock et al., 1982; Bear et al., 1987; Lisman, 1989; Artola and Singer, 1993; Yang et al., 1999; Cormier et al., 2001). They made this conclusion based largely on the observation that partial blockade of postsynaptic NMDARs with a subsaturating concentration of APV caused long-lasting synaptic depression at local inputs onto the apical dendrite of L2/3 neurons

Here, we test whether the model proposed by Froemke and colleagues holds true at synaptic inputs onto L2/3 pyramidal cells in somatosensory cortex (S1). We find, unlike Froemke and colleagues (2005), that decreased NMDAR activity below

baseline levels does not result in LTD either at the ascending L4-L2/3 projection or at locally stimulated inputs to the apical dendrite. Our data thus indicate that calcium-dependent desensitization of postsynaptic NMDARs does not underlie coincidence detection in LTD at synapses in S1.

**Methods**

All procedures were approved by the UCSD Institutional Animal Care and Use Committee. Long-Evans rats (P14-22, either sex, Harlan Sprague Dawley) were anesthetized with isoflurane and decapitated, and the brain was rapidly removed in ice-cold oxygenated Ringer's solution (composition in mM: 119 NaCl, 26 NaHCO3, 11 D-(+)-Glucose, 2.5 KCl, 1.3 MgSO4, 1.0 NaH2PO4 , 2.5 CaCl2, pH 7.20-7.23, osmolarity 292 mOsm). Acute brain slices (350-400 μm) containing the posteromedial barrel subfield of primary somatosensory cortex (S1) were cut on a vibrating microtome (Leica VT1000S) at an oblique angle, 50o towards coronal from the midsaggital plane (Allen et al., 2003). After sectioning, slices were pre-incubated in Ringer's solution at 30$^{o}$ C for 30 min, and then incubated at room temperature (22-24$^{o}$ C) until use (0.5-8.5 hr). All recordings were made at room temperature. S1 was identified by the presence of three to five large (250–450 μm) barrels in L4, visible under transillumination (Feldman, 2000).

**Drugs.** D-2-Amino-5-phosphonovaleric acid (D-APV), and 6,7-dinitroquinoxaline-2,3-dione (DNQX), both from Tocris were dissolved in Ringer's and stored in stocks (1000x and 100x, respectively) at -20$^{o}$ C. Picrotoxin (Tocris) powder was dissolved directly in the Ringer's solution each day. 1,2-Bis(2-

aminophenoxy)ethane-N,N,N',N'-tetraacetic acid (BAPTA, 5 mM, Sigma) was dissolved directly into the internal solution.

**Statistics.** All comparisons were made by using a two-tailed unpaired Student's t-test, unless otherwise noted. The critical level of significance was $p < 0.05$. All data are presented as mean ± standard error, unless noted as standard deviation (SD).

**Whole Cell Recording.** Whole-cell recordings were made with 3-8 MΩ pipettes using an Axopatch 200B amplifier (Axon). Recordings were filtered at 2 kHz and digitized at 5 kHz using a 12 bit data acquisition board (National Instruments) and custom data acquisition and analysis routines running in Igor (Wavemetrics, Lake Oswego OR). Neurons with pyramidal shaped somata were selected for recording using infrared DIC optics. All cells exhibited regular spiking pattern characteristic of excitatory cells (Connors and Gutnick, 1990). A glass pipette (3-5 μm tip diameter) containing 5 mM bicuculline methiodide (BMI, Sigma) dissolved in Ringer's was placed in L2/3 within 100 μm of the recording electrode to block $GABA_A$ receptors locally (Castro-Alamancos et al., 1995; Feldman, 2000). For extracellular stimulation of the L4-L2/3 projection, a concentric bipolar stimulating electrode (FHC, Bowdoinham, ME) was placed at the base of a L4 barrel of the same column as the recorded pyramidal neuron. For local extracellular stimulation in L2/3, a glass pipette (3-5 μm tip diameter) containing Ringer's solution was placed at a point approximately 50 μm apical and 30 μm lateral to the recorded neuron; this location corresponds to proximal inputs which would be predicted to exhibit a symmetric STDP learning rule (Froemke et al., 2005); the ground for this electrode was

connected to the AgCl bath ground pellet. In both cases, just supratheshold stimulation was applied. Responses were either single-component EPSPs or multi-component EPSPs with well-isolated initial components (in which case only the first component was analyzed). All data were collected with stimulation at 0.1 Hz.

For voltage clamp experiments, the internal solution contained (in mM): 108 D-gluconic acid, 108 cesium OH, 20 HEPES, 5 TEACl, 2.8 NaCl, 0.4 EGTA, 0.3 GTP, 4 ATP, 10 phosphocreatine, adjusted to pH 7.30 with CsOH (290 mOsm). For current clamp experiments, the internal solution contained (in mM): 116 potassium gluconate, 20 HEPES, 6 KCl, 2 NaCl, 0.5 EGTA, 0.3 GTP, 4 ATP, 10 phosphocreatine, adjusted to pH 7.20 with KOH (290 mOsm). Initial membrane potential was -92 ± 4 mV (SD, n=14) after correcting for a junction potential of -12 mV. Cells hyperpolarized by an average of 4 mV during 50 minutes of recording. Series resistance was 21 ± 6 MΩ (SD). Input resistance was 91 ± 31 MΩ (SD): calculated from the response to a -100 pA step during each sweep.

For STDP experiments, current was injected via the recording electrode (5 ms duration) to elicit a spike 20 ms before the EPSP. 100-150 spikes were paired with EPSPs at 0.14 Hz (Bender et al., 2006). Following STDP induction, extracellular stimulation alone resumed at 0.1 Hz.

**Results**

If baseline (0.1 Hz) synaptic stimulation truly causes sufficient calcium influx thru NMDARs to exceed the LTD window lies on the cross-over point between LTD

and LTP (Fig. 1.1), we reasoned that a subsaturating dose of D-APV should reduce the calcium influx during 0.1 Hz stimulation to a level which will result in LTD.

**Partial block of NMDA currents with subsaturating D-APV.** We first found a dose of D-APV which reduced pharmacologically-isolated postsynaptic NMDA currents by 50%. NMDA currents were isolated in voltage-clamp (+30 mV holding potential) in 10 μM DNQX and 10 μM picrotoxin with 5 mM internal BAPTA. We applied increasing concentrations of D-APV (Fig. 3.1A). We, like Froemke and colleagues (2005), found that 2 μM D-APV resulted a partial block of postsynaptic NMDA currents which was not significantly different from 50% (55 ± 8% block, n=4, p = 0.62). Increasing concentration of D-APV resulted in a progressively larger blockade, which recovered to 93 ± 4% of baseline when D-APV was washed out (Fig. 3.1B). We therefore used 2 μM D-APV for the remainder of the experiments which matches the concentration used by Froemke and colleagues (2005).

**Subsaturating D-APV does not induce depression at L4-L2/3 synapses.** We next tested whether partial blockade of NMDARs with 2 μM D-APV caused synaptic depression at the L4-L2/3 projection. L4 afferents were stimulated at 0.1 Hz and EPSPs were recorded in the presence of local BMI. After a stable baseline, 2 μM D-APV was applied for 5-15 minutes and then washed out. As is illustrated by an example recording in figure 3.2A, EPSP slope and amplitude remained stable during application and washout of 2 μM D-APV. No changes in membrane potential or input resistance was observed during application or washout. Across a population of 7 cells, we observed no depression of EPSP slope and a slight increase in EPSP amplitude

(Fig. 3.2B). These results demonstrate that application of subsaturating D-APV does not cause synaptic depression at the L4-L2/3 projection in barrel cortex.

**The L4-L2/3 projection is competent to express STDP-LTD.** One possible explanation of the apparent discrepancy between our findings and Froemke and colleagues (2005) is that under the experimental conditions of our slices, the L4-L2/3 projection was incompetent to express tLTD. This could happen if some prior experience had induced synaptic depression in our slices (e.g. Allen et al., 2002) or if some uncontrolled difference in our recording condition were present. In order to ensure that this was not the case, in experiments interleaved with the last 4 cells from figure 3.2, we performed tLTD induction (Bender et al., 2006). Postsynaptic spikes preceded EPSPs by 20 ms for 100 to 150 pairings. We observed a consistent depression of both EPSP slope and amplitude as illustrated by an example recording (Fig. 3.3A), and across the population recorded (n=3; Fig. 3.3B). Thus, in our hands, the L4-L2/3 projection is competent to express tLTD.

**Subsaturating D-APV does not induce depression along the apical dendrite.** The apical dendrites of pyramidal cells in cortex and in hippocampus are large and therefore permit relatively easy imaging of calcium dynamics (e.g. Markram et al, 1995; Nakamura et al., 1999) and recording of electrical properties (e.g. Sah and Bekkers, 1996; Schiller et al., 1997; Johnston et al., 2003; Schaefer et al., 2003). By contrast, imaging in the basal dendrites is less common (Antic, 2003; Kampa and Stuart, 2006) and it has only recently become possible to perform intracellular recording (Nevian et al., 2007). Although it is now established that, like apical dendrites, somatic action potentials invade basal dendrites (Antic, 2003; Kampa and

Stuart, 2006; Nevian et al., 2007), it is unknown whether channel density is similar to apical dendrite, and given that the surface area to volume ratio is different in the two compartments, quantitative, and perhaps qualitative differences in how signals are processed is likely.

L4 excitatory cells in somatosensory cortex make 4-5 synaptic contacts onto postsynaptic L2/3 cells; the vast majority (~85%) of these contacts are made on the basal dendrites (Feldmeyer et al., 2002). Therefore, we reasoned that our failure to observe synaptic depression at the L4-L2/3 projection with application of subsaturating doses of D-APV may be because of a difference in LTD mechanism between synapses on the basal dendrites and those on the apical dendrite studied by Froemke and colleagues (2005). We therefore measured the effects of subsaturating D-APV on synapses onto the apical dendrites of L2/3 pyramidal cells. With focal BMI, we placed a glass stimulating electrode approximately 50 μm apical and 30 μm lateral to the recorded cell body. After a stable baseline of 0.1 Hz stimulation, we applied 2 μM D-APV for 10 minutes. We observed no change in EPSP amplitude or slope, either in an example cell (Fig. 3.4A) or across the population (n=4; Fig. 3.4B). A slight decrease in EPSP decay time is apparent in the example recording (Fig. 3.4A, inset), but this was not consistently observed across the population (data not shown). Taken together, our results indicate that inputs onto L2/3 pyramidal cells in barrel cortex do not exhibit depression when exposed to subsaturating D-APV. However, we did not perform a control to ensure that the proximal apical stimulation was competent to express tLTD in our preparation, which may explain our failure to see plasticity here.

## Discussion

We have shown here that a dose of D-APV which blocks postsynaptic NMDARs by approximately 50% does not cause depression of EPSPs recorded at resting membrane potential either during application or in a long-term manner following application. These results were observed at the L4-L2/3 projection as well as at local inputs onto the proximal segment of the apical dendrite of L2/3 cells. Despite our inability to induce an LTD-like depression with subsaturating D-APV, we did observe normal tLTD at the L4-L2/3 projection.

**Reconciling these findings with visual cortex.** Although these results seem at odds with those of Froemke and colleagues (2005), several differences exist between our studies. First, this difference could reflect a systematic difference between primary visual cortex and S1. Indeed, potential differences in synaptic transmission and plasticity may exist between the two regions (see Chapter 5), and this question has not been systematically addressed within a single lab. Alternatively, these differences may reflect a difference in synaptic dynamics between physiological temperature and room temperature. Such differences have been observed to govern release presynaptically (Sabatini and Regehr, 1996), and may also govern induction of plasticity postsynaptically through as yet undetermined mechanisms.

In fact, one possible explanation of these differences is that rather than inducing LTD, Froemke and colleagues depressed transmission by blocking presynaptic NMDARs. This possibility is supported by the fact that presynaptic NMDARs have been observed to tonically regulate release dynamics at physiological

temperatures in primary visual cortex at L5 excitatory pairs (Sjöström et al., 2003) and at unidentified inputs onto cells at several layers, including L2/3 of visual cortex (Corlew et al., in press). On this theory, rather than occluding LTD by applying subsaturating D-APV, Froemke and colleagues may have blocked LTD which depends on activity of presynaptic NMDARs (Sjostrom et al., 2003; Bender et al., 2006; Duguid and Sjöström, 2006; Corlew et al., in press). Thus, our inability to replicate the findings may reflect the fact that presynaptic NMDARs appear to be tonically active in slices from primary visual cortex at physiological temperatures (Sjostrom et al., 2003; Corlew et al., in press), but not in S1 at room temperature unless glutamate concentration is elevated (Bender et al., 2006; and this thesis, Chapter 4).

It has been shown that inhibitory transmission sculpts the rules governing plasticity of excitatory synapses in visual cortex (Kirkwood and Bear 1995; Hensch et al., 1998; Fagiolini and Hensch, 2000; Meredith et al., 2003). Froemke and colleagues performed their experiments either with inhibition intact (Froemke et al., 2005) or with inhibition globally blocked by picrotoxin (R. Froemke, personal communication). It is possible that by abolishing inhibition locally with BMI around the recorded cell, our preparation altered the rules governing LTD induction.

**Prospects for finding the coincidence detector for tLTD.** Although our results do not support the model that calcium-dependent desensitization of postsynaptic NMDARs act as a coincidence detector in tLTD in S1, as it appears to in visual cortex (Froemke et al., 2005), we have not ruled out the possibility that non-classical mechanisms of coincidence detection might exist. The existence of calcium microdomains in postsynaptic spines (Delmas et al., 2002; Bloodgood and Sabatini,

2007) calls into question the simple model of small increases in calcium mediating LTD and larger increases mediating LTP. We therefore conclude that neither model proposed in figure 1.1 is a full description of how tLTD coincidence is calculated in S1. Instead, a new model in which the spatial location at which calcium enters the spine must be considered. New models of coincidence detection for tLTD that rely on retrograde endocannabinoid signaling avoid these difficulties with simple, one compartment models of calcium dynamics (Sjostrom et al., 2003; Bender et al., 2006). We believe that the difference between our results and those of Froemke et al. (2005) represents a difference between S1 and visual cortex. Although, since we did not test whether visual cortex exhibited depression following partial blockade of NMDARs under our conditions, we cannot rule out the possibility that there was some other, uncontrolled difference between our experimental conditions and those of Froemke et al. (2005).

**References**

Abbott LF, Nelson SB (2000) Synaptic plasticity: taming the beast. Nat Neurosci 3:1178-1183.

Allen CB, Celikel T, Feldman DE (2003) Long-term depression induced by sensory deprivation during cortical map plasticity in vivo. Nat Neurosci 6:291-299.

Antic SD (2003) Action potentials in basal and oblique dendrites of rat neocortical pyramidal neurons. J Physiol 550:35-50.

Artola A, Singer W (1993) Long-term depression of excitatory synaptic transmission and its relationship to long-term potentiation. Trends Neurosci 16:480-487.

Bear MF, Cooper LN, Ebner FF (1987) A physiological basis for a theory of synapse modification. Science 237:42-48.

Bender VA, Bender KJ, Brasier DJ, Feldman DE (2006) Two coincidence detectors for spike timing-dependent plasticity in somatosensory cortex. J Neurosci 26:4166-4177.

Bi G, Poo M (2001) Synaptic modification by correlated activity: Hebb's postulate revisited. Annu Rev Neurosci 24:139-166.

Bienenstock EL, Cooper LN, Munro PW (1982) Theory for the development of neuron selectivity: orientation specificity and binocular interaction in visual cortex. J Neurosci 2:32-48.

Bloodgood BL, Sabatini BL (2007) Ca(2+) signaling in dendritic spines. Curr Opin Neurobiol 17:345-351.

Brasier DJ, Feldman DE (2007) Synapse specific modulation of transmission by presynaptic NMDA receptors in rat somatosensory cortex. J Neurosci. *submitted.*

Castro-Alamancos MA, Donoghue JP, Connors BW (1995) Different forms of synaptic plasticity in somatosensory and motor areas of the neocortex. J Neurosci 15:5324-5333.

Celikel T, Szostak VA, Feldman DE (2004) Modulation of spike timing by sensory deprivation during induction of cortical map plasticity. Nat Neurosci 7:534-541.

Connors BW, Gutnick MJ (1990) Intrinsic firing patterns of diverse neocortical neurons. Trends Neurosci 13:99-104.

Corlew R, Wang Y, Ghermazien H, Erisir A, Philpot BD (2007) Developmental switch in the contribution of presynaptic and postsynaptic NMDA receptors to long-term depression. J Neurosci, *in press*.

Cormier RJ, Greenwood AC, Connor JA (2001) Bidirectional synaptic plasticity correlated with the magnitude of dendritic calcium transients above a threshold. J Neurophysiol 85:399-406.

Dan Y, Poo MM (2004) Spike timing-dependent plasticity of neural circuits. Neuron 44:23-30.

Delmas P, Wanaverbecq N, Abogadie FC, Mistry M, Brown DA (2002) Signaling microdomains define the specificity of receptor-mediated InsP(3) pathways in neurons. Neuron 34:209-220.

Duguid I, Sjöström PJ (2006) Novel presynaptic mechanisms for coincidence detection in synaptic plasticity. Curr Opin Neurobiol 16:312-322.

Egger V, Feldmeyer D, Sakmann B (1999) Coincidence detection and changes of synaptic efficacy in spiny stellate neurons in rat barrel cortex. Nat Neurosci 2:1098-1105.

Fagiolini M, Hensch TK (2000) Inhibitory threshold for critical-period activation in primary visual cortex. Nature 404:183-186.

Feldman DE (2000) Timing-based LTP and LTD at vertical inputs to layer II/III pyramidal cells in rat barrel cortex. Neuron 27:45-56.

Feldmeyer D, Lubke J, Silver RA, Sakmann B (2002) Synaptic connections between layer 4 spiny neurone-layer 2/3 pyramidal cell pairs in juvenile rat barrel cortex: physiology and anatomy of interlaminar signaling within a cortical column. J Physiol 538:803-822.

Froemke RC, Dan Y (2002) Spike-timing-dependent synaptic modification induced by natural spike trains. Nature 416:433-438.

Froemke RC, Poo MM, Dan Y (2005) Spike-timing-dependent synaptic plasticity depends on dendritic location. Nature 434:221-225.

Hensch TK, Fagiolini M, Mataga N, Stryker MP, Baekkeskov S, Kash SF (1998) Local GABA circuit control of experience-dependent plasticity in developing visual cortex. Science 282:1504-1508.

Holmgren CD, Zilberter Y (2001) Coincident spiking activity induces long-term changes in inhibition of neocortical pyramidal cells. J Neurosci 21:8270-8277.

Johnston D, Christie BR, Frick A, Gray R, Hoffman DA, Schexnayder LK, Watanabe S, Yuan LL (2003) Active dendrites, potassium channels and synaptic plasticity. Philos Trans R Soc Lond B Biol Sci 358:667-674.

Kampa BM, Stuart GJ (2006) Calcium spikes in basal dendrites of layer 5 pyramidal neurons during action potential bursts. J Neurosci 26:7424-7432.

Kirkwood A, Bear MF (1995) Elementary forms of synaptic plasticity in the visual cortex. Biol Res 28:73-80.

Koester HJ, Sakmann B (1998) Calcium dynamics in single spines during coincident pre- and postsynaptic activity depend on relative timing of back-propagating action potentials and subthreshold excitatory postsynaptic potentials. Proc Natl Acad Sci U S A 95:9596-9601.

Lisman J (1989) A mechanism for the Hebb and the anti-Hebb processes underlying learning and memory. Proc Natl Acad Sci U S A 86:9574-9578.

Markram H, Helm PJ, Sakmann B (1995) Dendritic calcium transients evoked by single back-propagating action potentials in rat neocortical pyramidal neurons. J Physiol 485:1-20.

Markram H, Lubke J, Frotscher M, Sakmann B (1997) Regulation of synaptic efficacy by coincidence of postsynaptic APs and EPSPs. Science 275:213-215.

Meredith RM, Floyer-Lea AM, Paulsen O (2003) Maturation of long-term potentiation induction rules in rodent hippocampus: role of GABAergic inhibition. J Neurosci 23:11142-11146.

Nakamura T, Barbara JG, Nakamura K, Ross WN (1999) Synergistic release of Ca2+ from IP3-sensitive stores evoked by synaptic activation of mGluRs paired with backpropagating action potentials. Neuron 24:727-737.

Nevian T, Sakmann B (2004) Single spine Ca2+ signals evoked by coincident EPSPs and backpropagating action potentials in spiny stellate cells of layer 4 in the juvenile rat somatosensory barrel cortex. J Neurosci 24:1689-1699.

Nevian T, Larkum ME, Polsky A, Schiller J (2007) Properties of basal dendrites of layer 5 pyramidal neurons: a direct patch-clamp recording study. Nat Neurosci 10:206-214.

Rosenmund C, Feltz A, Westbrook GL (1995) Calcium-dependent inactivation of synaptic NMDA receptors in hippocampal neurons. J Neurophysiol 73:427-430.

Sabatini BL, Regehr WG (1996) Timing of neurotransmission at fast synapses in the mammalian brain. Nature 384:170-172.

Sah P, Bekkers JM (1996) Apical dendritic location of slow afterhyperpolarization current in hippocampal pyramidal neurons: implications for the integration of long-term potentiation. J Neurosci 16:4537-4542.

Schaefer AT, Larkum ME, Sakmann B, Roth A (2003) Coincidence detection in pyramidal neurons is tuned by their dendritic branching pattern. J Neurophysiol 89:3143-3154.

Schiller J, Schiller Y, Stuart G, Sakmann B (1997) Calcium action potentials restricted to distal apical dendrites of rat neocortical pyramidal neurons. J Physiol 505:605-616.

Shouval HZ, Bear MF, Cooper LN (2002) A unified model of NMDA receptor-dependent bidirectional synaptic plasticity. Proc Natl Acad Sci U S A 99:10831-10836.

Sjostrom PJ, Turrigiano GG, Nelson SB (2001) Rate, timing, and cooperativity jointly determine cortical synaptic plasticity. Neuron 32:1149-1164.

Sjostrom PJ, Turrigiano GG, Nelson SB (2003) Neocortical LTD via coincident activation of presynaptic NMDA and cannabinoid receptors. Neuron 39:641-654.

Tong G, Shepherd D, Jahr CE (1995) Synaptic desensitization of NMDA receptors by calcineurin. Science 267:1510-1512.

Umemiya M, Chen N, Raymond LA, Murphy TH (2001) A calcium-dependent feedback mechanism participates in shaping single NMDA miniature EPSCs. J Neurosci 21:1-9.

Yang SN, Tang YG, Zucker RS (1999) Selective induction of LTP and LTD by postsynaptic [Ca2+]i elevation. J Neurophysiol 81:781-787.

Young JM, Waleszczyk WJ, Wang C, Calford MB, Dreher B, Obermayer K (2007) Cortical reorganization consistent with spike timing-but not correlation-dependent plasticity. Nat Neurosci 10:887-895.

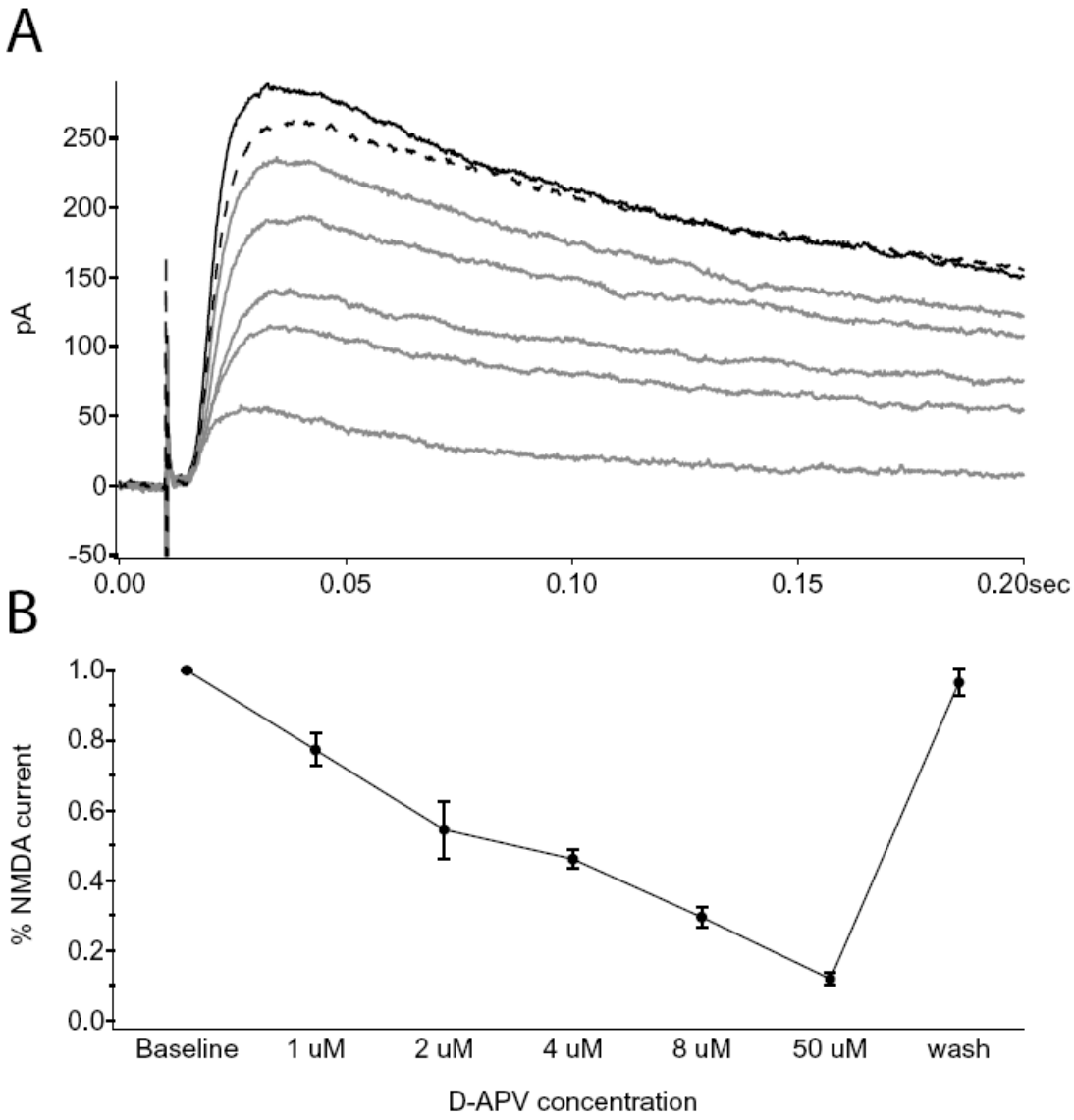



Fig. 3.1: Effects of increasing concentration of D-APV on postsynaptic NMDA currents. A. Traces from an example L2/3 pyramidal cell in which increasing D-APV concentration was applied during 0.1 Hz stimulation of the L4-L2/3 pathway. Baseline (black) NMDA currents showed greater reduction with increasing D-APV concentration (1, 2, 4, 8, and 50 μM; grey traces). The current returned to near-baseline levels after D-APV was removed (dashed black trace). B. Normalized NMDA current for 4 such experiments.

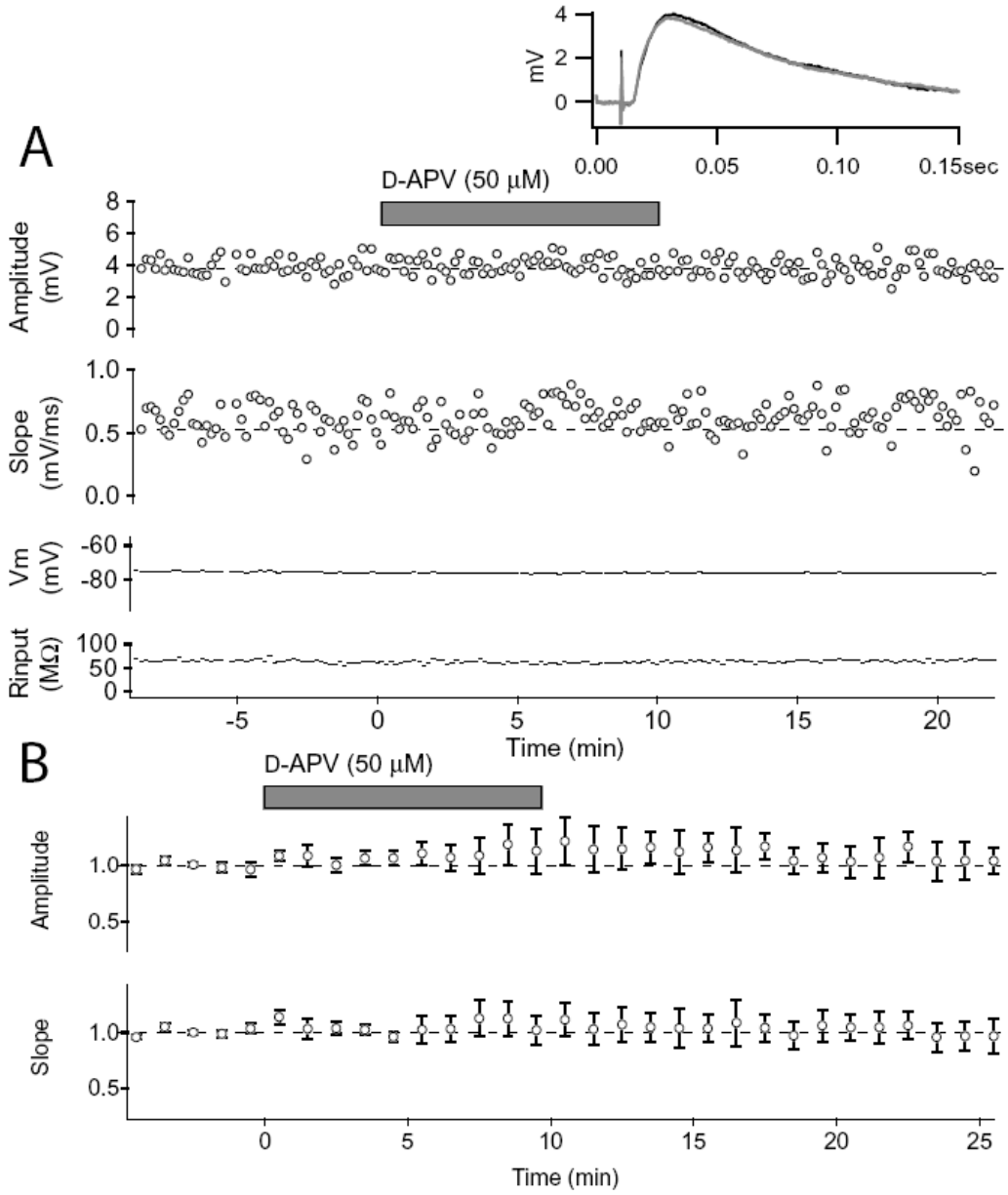



Fig. 3.2: 2 µM D-APV does not cause depression at the L4-L2/3 projection. A. Example recording in which 2 µM D-APV was applied during 0.1 Hz L4-L2/3 stimulation. Top: EPSP amplitude throughout the experimen. Middle: EPSP slope. Bottom: membrane potential and input resistance during the experiment. Inset: Average of 15 sweeps before and after 2 µM D-APV application. B. Normalized timecourse for EPSP amplitude (top) and slope (bottom) with D-APV application, n=7.

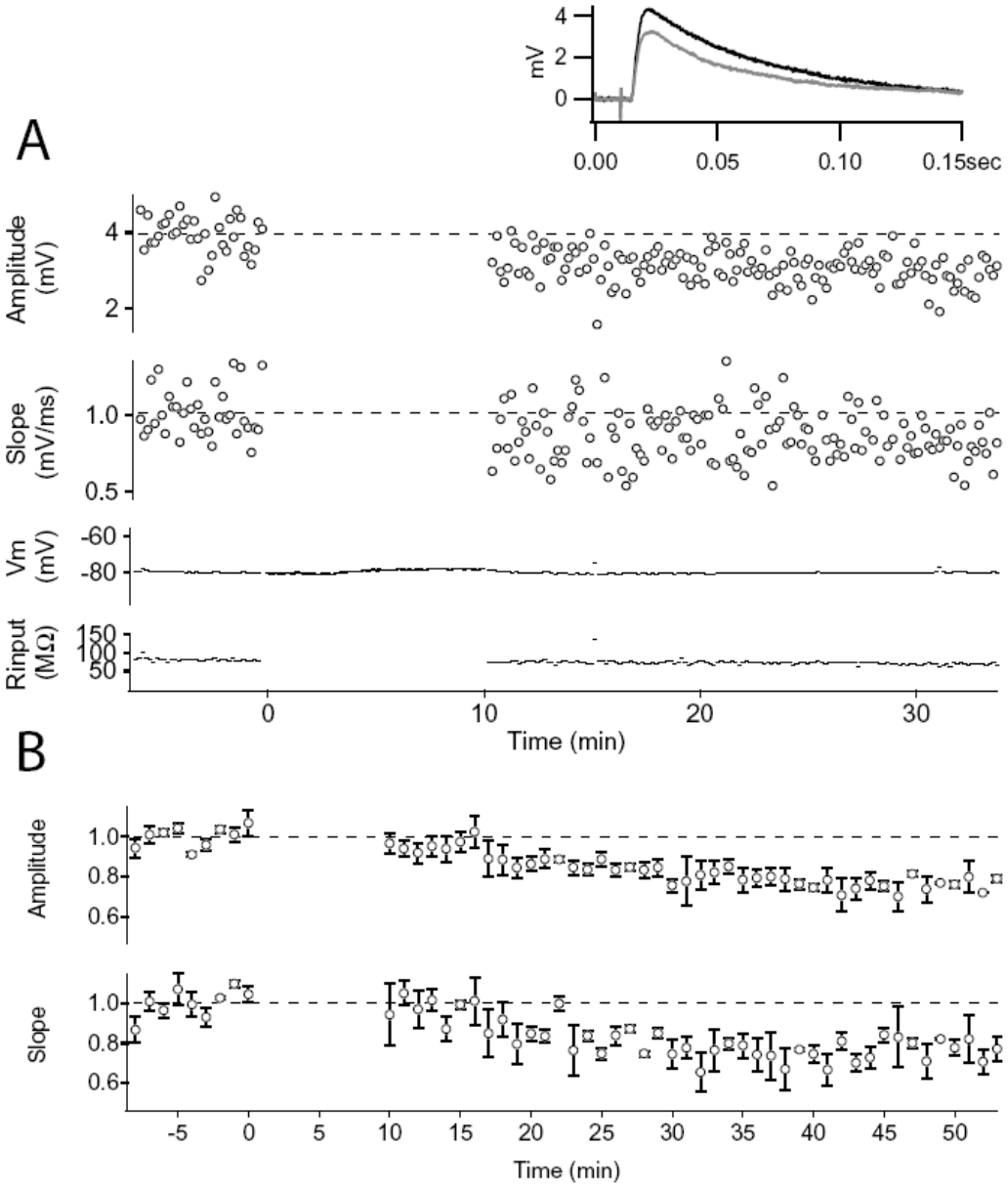



Fig. 3.3: Induction of tLTD at the L4-L2/3 projection. A. Example recording in which 150 post-leads-pre pairings at 0.14 Hz caused tLTD. (Conventions as in figure 3.2A.) B. Mean timecourse of tLTD induction across a population of 3 cells. Pairing protocol took between 7 and 10 minutes depending on if 150 pairings (n=2) or 100 pairings (n=1) were applied. Baseline times were aligned to the final sweep before tLTD induction and post-pairing times were aligned to the first sweep after pairing, m=3. (Other conventions as in figure 3.2B.)

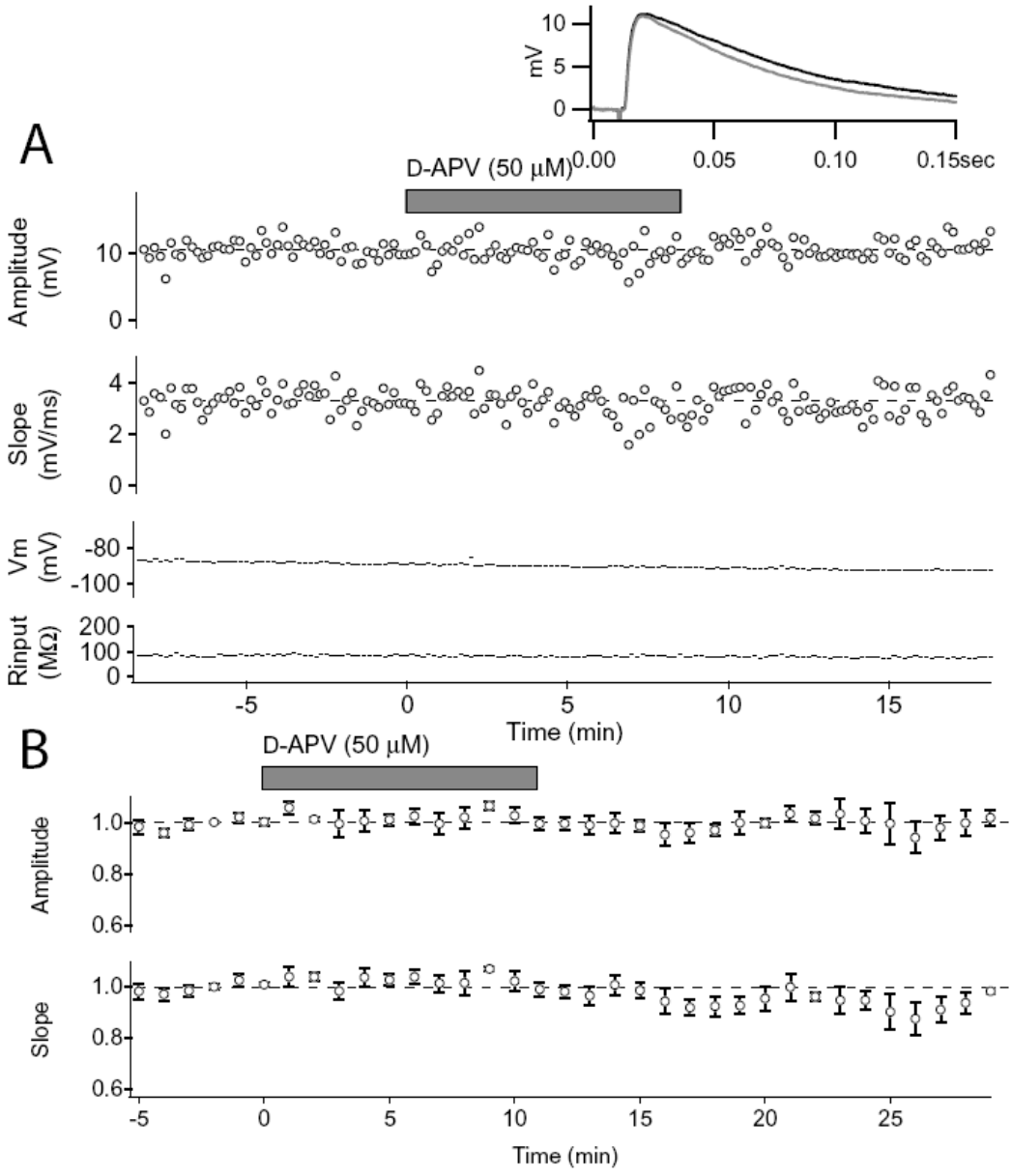



Fig. 3.4: 2 µM D-APV does not cause depression at local inputs onto the proximal segment of the apical dendrite of L2/3 pyramidal cells. A. Example recording in which 2 µM D-APV was applied during 0.1 Hz focal stimulation with a glass pipette along the proximal segment of the apical dendrite (approx. 50 µm apical and 30 µm lateral to the recorded soma). (Conventions as in figure 3.2A.) B. Normalized timecourse, n=4. (Conventions as in figure 3.2B.)

## IV. Synapse specific expression of functional presynaptic NMDA receptors in rat somatosensory cortex


### Abstract

Presynaptic NMDA receptors (NMDARs) modulate release and plasticity at many glutamatergic synapses, but the specificity of their expression across synapse classes has not been systematically examined. We found that non-postsynaptic, likely presynaptic NR2B-containing NMDARs enhanced AMPA receptor-mediated postsynaptic currents (EPSCs) at layer (L) 4 to L2/3 (L4-L2/3) synapses in juvenile rat barrel cortex when they are activated by elevated extracellular glutamate. In contrast, presynaptic NMDARs did not modulate L4-L4 synapses, which originate from the same presynaptic neurons, or cross-columnar L2/3-L2/3 horizontal projections onto the same postsynaptic target neurons. Blockade of these NMDARs depressed unitary and extracellularly evoked EPSCs, accompanied by changes in paired-pulse ratio and coefficient of variation indicative of a decrease in presynaptic release probability. NMDAR agonists increased miniature EPSC frequency in L2/3 neurons, without altering mEPSC amplitude or kinetics. Focal application of NMDAR antagonist revealed that the NMDARs that modulate L4-L2/3 transmission are located in L2/3, not L4, consistent with localization on terminals or axons of L4-L2/3 synapses, rather than on the somatodendritic compartment of presynaptic L4 neurons. Thus, presynaptic NMDARs selectively modulate L4-L2/3 synapses, relative to other synapses made by the same neurons. Existence of these receptors may support specialized processing or plasticity by L4-L2/3 synapses.

## Introduction

Synapse efficacy, dynamics, modulation, and plasticity vary markedly across classes of excitatory synapses, a heterogeneity that greatly increases the computing power of neural circuits (Murthy et al., 1997; Reyes et al., 1998; Tóth and McBain, 2000; Koester and Johnston, 2005). This functional heterogeneity reflects, in part, differential expression across synapses of presynaptic neurotransmitter receptors, which powerfully modulate release dynamics and plasticity. Among presynaptic receptors that modulate release are metabotropic receptors, including $GABA_B$ receptors (Takahashi et al., 1998), endocannabinoid receptors (Kreitzer and Regehr, 2002; Freund et al., 2003), and metabotropic glutamate receptors (Cartmell and Schoepp, 2000; Karim et al., 2000) which have been well characterized in many systems, and have been shown to modulate release properties in a target-cell selective manner (Scanziani et al., 1998). More recently, presynaptic ionotropic receptors have also been found to regulate release (MacDermott et al., 1999; Schmitz et al., 2000; Contractor et al., 2001; Engelman and MacDermott, 2004). One presynaptic ionotropic receptor, the kainate receptor, is differentially expressed at hippocampal Schaffer collateral synapses onto different types of interneurons (Sun and Dobrunz, 2006), and at parallel fiber synapses onto Purkinje cells and stellate cells (Delaney and Jahr, 2002), in both cases they contribute to target-cell specific differences in release dynamics. However, whether other presynaptic ionotropic receptors are also differentially expressed and modulate function of specific synapse classes is not known.

We focused on NMDA receptors (NMDARs), which classically exist in postsynaptic densities of excitatory synapses and contribute to depolarization and calcium influx during neurotransmission and synaptic plasticity (Dingledine et al., 1999). Presynaptic NMDARs (PreNMDARs) have been reported at many cortical synapses, including synapses between layer (L) 5 pyramidal cells in visual cortex (Sjöström et al., 2003), synapses from L4 cells onto L2/3 pyramidal cells (L4-L2/3 synapses) in somatosensory cortex (S1; Bender et al., 2006b), and unidentified synapses onto L2/3, L4, and L5 cells in visual cortex (Corlew et al., 2007) and onto L2 & L5 cells in entorhinal cortex (Berretta and Jones, 1996; Woodhall et al., 2001; Yang et al., 2006). PreNMDARs modulate both release probability and long-term synaptic depression at cortical synapses (Sjöström et al., 2003; Bender et al., 2006b; Duguid and Sjöström, 2006; Corlew et al., 2007). In contrast to the abundance of cortical synapses that show functional, physiological regulation by PreNMDARs, electron microscopy (EM) studies have typically found presynaptic NMDARs expressed at only a small subset of cortical excitatory terminals (Aoki et al., 1994; Conti et al., 1997; Charton et al., 1999), though prevalence may be greater in early postnatal development (P23; Corlew, et al., 2007).

This apparent discrepancy suggests two alternative models of PreNMDAR abundance. First, PreNMDARs may indeed regulate transmission broadly across many cortical excitatory synapse classes, but occur at a relatively small, random subset of terminals within each class. Alternatively, PreNMDARs may be selectively expressed at a small, specific subset of synapse classes, and be entirely absent from other classes of synapses. If PreNMDAR expression is synapse-class specific, it

would indicate that neurons selectively form and traffic these receptors to govern the functional properties of specific synapses.

We showed previously that non-postsynaptic NMDARs are required for spike-timing dependent long-term depression (tLTD) at presumptive L4-L2/3 synapses in S1. These receptors acutely regulated release probability when activated by enhanced extracellular glutamate (i.e., high-frequency burst firing, or when glutamate transporters were partially blocked) (Bender et al., 2006b). Here we show that PreNMDARs selectively modulate L4-L2/3 synapses, but not L4-L4 synapses, which originate from the same presynaptic cell class, or cross-columnar, horizontal inputs onto the same postsynaptic L2/3 pyramidal cells. Thus, PreNMDARs may be selectively localized to L4-L2/3 synapses, relative to other synapses made by the same pre- and postsynaptic neurons. Portions of this work have been previously presented in abstract form (Brasier and Feldman, 2006).

**Methods**

All procedures were approved by the UCSD Institutional Animal Care and Use Committee. Long-Evans rats (P14-22, either sex, Harlan Sprague Dawley) were anesthetized with isoflurane and decapitated, and the brain was rapidly removed in ice-cold oxygenated Ringer's solution (composition in mM: 119 NaCl, 26 NaHCO3, 11 D-(+)-Glucose, 2.5 KCl, 1.3 $MgSO_4$, 1.0 $NaH_2PO4$ , 2.5 $CaCl_2$, pH 7.20-7.23, osmolarity 292 mOsm). Acute brain slices (350-400 μm) containing the posteromedial barrel subfield of primary somatosensory cortex were cut on a vibrating microtome (Leica VT1000S) at an oblique angle, $50^o$ towards coronal from the

midsaggital plane (Allen et al., 2003). In some experiments, the rostral pole of the brain was tilted 10$^{o}$ up during cutting (Feldmeyer et al., 2002), which increased the rate of finding synaptic connected L4-L2/3 neuron pairs (from 2.2% to 4.3%). After sectioning, slices were pre-incubated in Ringer's solution at 30$^{o}$C for 30 min, and then incubated at room temperature (22-24$^{o}$C) until use (0.5-8.5 hr). All recordings were made at room temperature unless otherwise noted in the text. For recordings at 30$^{o}$C, a feedback-controlled automatic temperature controller (model TC-344B, Warner Instruments, Hamden, CT) was used to heat the recording stage and the Ringer's inflow. The temperature of the bath was recorded to be 30-32$^{o}$C. S1 was identified by the presence of three to five large (250–450 μm) barrels in L4, visible under transillumination (Feldman, 2000).

**Whole Cell Recording.** Whole-cell recordings were made with 3-8 MΩ pipettes using an Axopatch 200B amplifier (Axon). Recordings were filtered at 2 kHz and digitized at 5 kHz using a 12 bit data acquisition board (National Instruments) and custom data acquisition and analysis routines running in Igor (Wavemetrics, Lake Oswego OR). Neurons with pyramidal shaped somata were selected for recording using infrared DIC optics. A glass pipette (3-5 μm tip diameter) containing 5 mM bicuculline methiodide (BMI, Sigma) in Ringer's solution was placed in L2/3 within 100 μm of the recording electrode to block GABAA receptors focally (Castro-Alamancos et al., 1995; Feldman, 2000). For extracellular stimulation of the L4-L2/3 projection, a concentric bipolar stimulating electrode (FHC, Bowdoinham, ME) was placed at the base of a L4 barrel of the same column as the recorded pyramidal neuron. For extracellular stimulation of the horizontal L2/3-L2/3 projection, an identical

stimulating electrode was placed in L2/3 of the neighboring column centered above the neighboring barrel and at the same sub-pial depth as the recorded neuron.

For voltage clamp experiments, the internal solution contained (in mM): 108 D-gluconic acid, 108 cesium OH, 20 HEPES, 5 TEACl, 2.8 NaCl, 0.4 EGTA, 0.3 GTP, 4 ATP, 10 phosphocreatine, adjusted to pH 7.30 with CsOH (290 mOsm). Membrane potential (measured immediately after break-in) was -82 ± 3.4 mV (SD; n=28 cells). Membrane potentials and holding potentials were corrected for the liquid junction potential of -12 mV. Holding potential was -90 mV unless otherwise noted. Initial holding current was -47 ± 36 pA (SD) and increased by an average of -23 pA during 50 minutes of recording. Cells were excluded if holding current increased by more than -200 pA. Series resistance and input resistance were calculated from the response to a -5 mV step during each sweep. The mean series resistance was 15 ± 4 MΩ (SD). The mean input resistance was 340 ± 186 MΩ (SD). Just supratheshold extracellular stimulation was applied. Responses were either single-component EPSCs or multi-component EPSCs with well-isolated initial components (in which case only the first component was analyzed). Pairs of stimuli (30 Hz ) were delivered every 30 sec. The amplitude of the first EPSC was 123 ± 68 pA (SD).

All experiments were performed by recording isolated AMPA receptor-mediated EPSCs (AMPA-EPSCs), except where noted in Results. AMPA-EPSCs were isolated by holding the postsynaptic cell held at -90 mV to block voltage-dependent postsynaptic NMDARs. In addition, postsynaptic NMDARs were blocked pharmacologically in most experiments by loading the postsynaptic cell internally with the NMDA channel blocker MK-801 (iMK-801, 1 mM) via the recording pipette,

which selectively blocks postsynaptic NMDA currents without affecting NMDA currents in neighboring cells (Berretta and Jones, 1996; Woodhall et al., 2001; Humeau et al., 2003; Samson and Pare, 2005; Mameli et al., 2005; Bender et al., 2006b; Corlew et al., 2007). No attempt was made to block kainate receptor-mediated EPSCs, which may account for a small component of the primarily AMPA-EPSCs that were studied.

**Drugs.** Ifenprodil, D-2-Amino-5-phosphonovaleric acid (D-APV), tetrodotoxin citrate (TTX), 6,7-dinitroquinoxaline-2,3-dione (DNQX), homoquinolinic acid (HQA), DL-threo-ß-benzyloxyaspartic acid (TBOA), and picrotoxin (all from Tocris) were dissolved in Ringer's and stored as stock solutions (100x to 1000x) at -20$^{o}$C. The final concentration of TBOA used here would be predicted to block most activity of presynaptic and postsynaptic neuronal EAATs, but only affect a subset of glial EAATs (Shigeri et al., 2004). (+)-5-methyl-10,11-dihydro-5H-dibenzo[a,d]cyclohepten-5,10-imine maleate (MK-801, 1 mM, Tocris) and 1,2-Bis(2-aminophenoxy)ethane-N,N,N',N'-tetraacetic acid (BAPTA, 5 mM, Sigma) were dissolved directly into the internal solution.

**Focal D-APV puffing.** For experiments in which D-APV was applied via focal puffing in L2/3, a glass pipette (3-5 μm tip diameter) containing 2.5 mM D-APV dissolved in Ringer's solution was positioned near the recorded neuron, at a distance of 106 ± 28 μm (SD; range: 70 – 160 μm). For focal puffing of D-APV in L4, the puffer pipette was positioned in the center of the L4 barrel approximately 100 μm apical to the L4 stimulating electrode. Sweeps were collected at a 30 s inter-sweep interval and D-APV was puffed 15 s before each sweep by applying a 20 ms burst

pressure (5 PSI, compressed nitrogen) using a PV830 Pneumatic PicoPump (WPI, Sarasota FL).

**Synaptically connected pairs.** *L4-L2/3 pairs*. For synaptically coupled L4 to L2/3 pairs, we made a whole-cell voltage clamp recording from a postsynaptic L2/3 pyramidal cell using $Cs^+$-internal with iMK-801. A 6-8 MΩ glass recording electrode containing (in mM): 116 potassium gluconate, 20 HEPES, 6 KCl, 2 NaCl, 0.5 EGTA, 0.3 GTP, 4 ATP, 10 phosphocreatine, adjusted to pH 7.20 with KOH (290 mOsm) was then positioned just over the surface of the slice in L4. The potassium-based internal solution was puffed manually at random points throughout the L4 barrel while whole-cell currents in the L2/3 cell were visually monitored using an oscilloscope. "Hot spots" of connectivity were identified by a dramatic increase in synaptic currents in the L2/3 cell.

Once a "hot spot" was found, a whole-cell recording was established with a regular spiking L4 neuron (mean Vm: -84 ± 7 mV [SD], input resistance 299 ± 96 MΩ [SD], series resistance 19 ± 8 MΩ [SD], statistics are from 25 presynaptic L4 neurons for L4-L2/3 cell pairs as well as L4-L4 cell pairs). In 3/119 cases, this cell was synaptically connected to the L2/3 neuron. In the remaining cases, the electrode was withdrawn from the cell and reused to form a loose seal (< 1 GΩ) on another L4 spiny neuron which was stimulated in cell-attached mode as described elsewhere (Feldmeyer et al., 1999; 2002). Briefly, the presynaptic loose patch was hyperpolarized to approximately -50 mV (in current clamp) and one or more action potentials were elicited by applying at 10 ms current pulse (1-6 nA) which were usually visible as small deflections in the voltage trace. If the L4 neuron elicited an

EPSC, indicating a connected pair, the loose seal electrode was withdrawn and the cell repatched with a new electrode. Once a connected L4-L2/3 pair was found, presynaptic action potentials were evoked by 10 ms presynaptic current injection to evoke unitary AMPA-EPSCs (AMPA-uEPSCs). Pairs of AMPA-uEPSCs were evoked at 30 Hz with 30 s between sweeps.

*L4-L2/3 connectivity rates*. 132 postsynaptic L2/3 pyramidal cells were recorded. In 119, a L4 "hot spot" was identified in which 968 potential presynaptic L4 cells were tested for connectivity. 5.9% of L4 cells within "hot spots" appeared connected during loose-patch stimulation; 59.6% (n=28) of those that survived repatching were found to be actually connected with the postsynaptic neuron. Thus, we estimate the overall connectivity rate within a "hot spot" to be 3.6% (5.9% apparent connectivity during loose-patch stimulation * 59.6% of apparently connected cells actually connected). This may underestimate true connectivity because it assumes that every cell which did not appear connected by loose-patch stimulation was not actually connected. An additional 117 L4 cells outside of "hot spots" were tested for connectivity, but no pairs were found, suggesting that L4 cells projecting to a single L2/3 target neuron exist in clusters. Of 28 connected pairs, 17 were discarded because one cell was lost before the experiment was completed or because of significant run-down in baseline transmission.

*L4-L4 pairs*. 68 simultaneous recordings were made between adjacent L4 excitatory cells. 12 were synaptically coupled (connectivity rate = 18%), of which 5 were discarded because one cell died before completion of the experiment. 10 coupled cell pairs were tested for reciprocal connectivity, of which 1 was found to be

reciprocally connected; in that pair, the experiment was performed on the stronger connection. All 6 pairs that were tested for sensitivity to 1 μM DNQX showed significant blockade of the unitary EPSC (mean blockade: 51 ± 6%), confirming that these were excitatory connections.

**Miniature EPSCs.** Spontaneous AMPA-mediated miniature EPSCs (mEPSCs) were recorded using the same whole-cell voltage clamp methods as above except that 500 nM TTX and 100 μM picrotoxin were included in the Ringer's solution, and focal BMI was omitted. All mEPSCs were measured in iMK-801. mEPSC frequency, amplitude, and other parameters were analyzed offline using MiniAnalysis software (Synaptosoft, Decatur GA) with a mEPSC threshold set at 4.5 pA (approx. 2.5 times root-mean-square noise). Automated detection of mEPSCs was verified by visual inspection, with the experimenter blind to the experimental condition during analysis. Input and series resistance were monitored by applying -5 mV holding potential steps (3-5 pulses at 0.14 Hz every 5 minutes during recording). mEPSCs were recorded during an initial 10 min baseline period, followed by application of NMDAR agonists or antagonists for 10 min each. Only the last 5 minutes of each 10 minute recording epoch was analyzed to ensure that drugs had fully equilibrated.

**Statistics.** All comparisons were made by using a two-tailed paired Student's t-test (for single comparisons) or a repeated measures ANOVA (for multiple comparisons), unless otherwise noted. The critical level of significance was $p < 0.05$. All data are presented as mean ± standard error, unless noted as standard deviation (SD).

## Results

**Non-postsynaptic, potentially presynaptic NMDARs are required for t-LTD.** To study L4-L2/3 excitatory synaptic responses, we made whole-cell recordings from single L2/3 pyramidal neurons in acute slices of S1 cortex from P14-22 Long-Evans rats, while stimulating with just suprathreshold extracellular stimulation in the underlying L4 barrel. As an initial test for the existence of functional presynaptic NMDA receptors, we tested whether these receptors acutely modulate release probability, as found in L5 of V1 (Sjostrom et al., 2003). To do this, we measured the effect of D-APV wash-in on the amplitude and PPR of EPSCs , measured in voltage clamp at -90 mV. Under standard conditions, D-APV did not significantly alter EPSC amplitude when EPSCs were evoked singly at 0.1 Hz, or in bursts of 5 EPSCs at 30 Hz (EPSC amplitude relative to pre-drug baseline, 0.1 Hz: 1.13 ± 0.07, n=5, paired t-test, $p = 0.11$; 30 Hz, 0.90 ± 0.05, $p = 0.07$; Fig. 4.1A, C).

However, increasing glutamate levels with the broad-spectrum glutamate transport blocker TBOA (25 μM, Shigeri et al., 2004), revealed the presence of functional, non-postsynaptic NMDA receptors that regulate release (Lien et al., 2006). TBOA alone evoked a small increase in holding current (62 ± 23 pA at -90 mV, $n = 6$; $p < 0.05$), consistent with increased ambient glutamate, but had no significant effect on AMPA-EPSC amplitude (0.91 ± 0.05, $n = 7$, $p = 0.24$). Application of D-APV (50 μM) in the TBOA background significantly decreased EPSC amplitude, measured using pairs of stimuli at 30 Hz (first EPSC: 0.80 ± 0.04, $p < 0.02$; second EPSC: 0.90 ± 0.03, $p < 0.02$; $n = 8$; Fig. 4.1B-C), and increased PPR (before D-APV: 0.92 ± 0.08;

after D-APV: 1.03 ± 0.08, paired t-test, $p < 0.03$), consistent with a modest decrease in presynaptic release probability. Similar results occurred using higher frequency bursts (7 EPSCs at 50 Hz) without TBOA (first EPSC: 0.74 ± 0.06, $p < 0.05$; second EPSC: 0.71 ± 0.06, $p < 0.01$; $n = 8$; Fig. 4.1A, C), although with no change in PPR (before D-APV: 0.62 ± 0.12; after D-APV: 0.56 ± 0.11, paired t-test, $p = 0.46$). Thus, increasing ambient glutamate either with TBOA or high-frequency bursts revealed the presence of NMDA receptors that regulate release.

**NMDARs that regulate evoked release at L4-2/3 synapses are non-postsynaptic.** To confirm that the NMDARs that modulate release at L4-L2/3 synapses were non-postsynaptic, we recorded isolated AMPA-mediated EPSCs (AMPA-EPSCs) with iMK-801 (1 mM) at -90 mV in the presence of TBOA (15 μM), with BMI applied locally to block $GABA_A$-mediated inhibition (Feldman, 2000; Castro-Alamancos et al., 1995); two pulses at 30 Hz were applied every 30 s. We asked whether D-APV reduced AMPA-EPSCs and/or changed paired-pulse ratio (PPR) under these conditions, when postsynaptic NMDA currents were already blocked with iMK-801. In an example cell (Fig. 4.2A), bath application of 50 μM D-APV caused a decrease in the amplitude of evoked AMPA currents and an increase in PPR, without coincident changes in holding current, series resistance, or input resistance. This decrease in AMPA-EPSC and increase in PPR is consistent with a decrease in presynaptic release probability (Dobrunz and Stevens, 1997; Zucker and Regehr, 2002; Sun et al., 2005). Both of these effects recovered with washout of D-APV.

Across the population of neurons, brief D-APV applications (n=5 cells) reversibly decreased AMPA-EPSCs and increased PPR (Fig. 4.2B&D, filled diamonds). Baseline PPR was slightly, but not significantly, less than 1.0 (PPR = 0.920 ± 0.056, n=15, p = 0.17, unpaired t-test), consistent with prior studies of extracellular stimulation at this projection (Bender et al., 2006a). Longer duration D-APV application (n=5 cells) produced a similar magnitude effect, indicating that the maximal effect had been reached by brief D-APV application (Fig. 4.2C-D, filled circles). Interleaved control experiments confirmed that the presence of TBOA itself, without D-APV application, did not cause a decrease in AMPA-EPSC amplitude or a change in PPR (n=5, Fig. 4.2C-D, open circles). These data indicate that in the presence of TBOA (which increases extracellular glutamate concentration), blockade of non-postsynaptic, putatively presynaptic NMDARs decreases release probability.

**PreNMDARs regulate mEPSC frequency.** If PreNMDARs modulate release probability, activation of PreNMDARs should alter frequency, but not amplitude or kinetics, of AMPA-mediated miniature EPSCs (mEPSCs). mEPSCs were measured at -90 mV from L2/3 pyramidal neurons in TTX (500 nM) and picrotoxin (100 μM), with iMK-801 (1 mM) to block postsynaptic NMDARs (no TBOA was present in mEPSC experiments). mEPSCs were recorded under baseline conditions (10 min), after which 15 μM NMDA was bath applied to activate NMDARs (10 min), and then D-APV was added to antagonize the effect (10 min, Fig. 4.3A). NMDA caused a small but significant increase in mean mEPSC frequency (Fig. 4.3C), which was evident as a leftward shift in the cumulative probability histogram of inter-mEPSC interval compiled across 7 cells (Fig. 4.3B, 25291 total individual mEPSCs). Addition

of D-APV returned mEPSC frequency to baseline levels (Fig. 4.3C; baseline = 6.6 ± 0.9 Hz, NMDA = 7.6 ± 1.0 Hz, NMDA+D-APV = 6.4 ± 0.9 Hz; $p < 0.0001$, repeated measures ANOVA; *post hoc* pairwise-comparison p-values in Fig. 4.3). In contrast, NMDA and D-APV did not alter mEPSC amplitude (Fig. 4.3D; Baseline = 9.5 ± 0.4 pA, NMDA = 9.7 ± 0.2, NMDA+D-APV = 9.4 ± 0.2, $p = 0.58$). NMDA and D-APV also did not alter mEPSC kinetics, consistent with the interpretation that mEPSCs at -90 mV represent AMPA but not NMDA currents (Fig. 4.3B, inset; rise time: baseline = 2.1 ± 0.1 ms, NMDA = 2.2 ± 0.2 ms, NMDA+D-APV = 2.2 ± 0.2 ms, $p = 0.34$; decay time: baseline = 4.9 ± 0.4 ms, NMDA = 5.2 ± 0.5 ms, NMDA+D-APV = 5.2 ± 0.6 ms, $p = 0.24$). These data indicate that activation of PreNMDARs by exogenous agonist modestly but significantly increases release probability.

To test whether PreNMDARs actively promote release under normal baseline conditions in the slice, we applied D-APV without NMDA in 6 cells. Under these conditions, D-APV had no effect on mEPSC frequency (baseline = 5.90 ± 1.22 Hz, D-APV = 5.89 ± 1.23 Hz, $p = 0.96$) or amplitude (baseline = 8.8 ± 0.3 pA ± 8.7 ± 0.3 pA, $p = 0.56$). This indicates that, at least at room temperature, PreNMDARs promote release only under conditions of exogenous NMDAR agonist, or (as with TBOA application above) conditions of enhanced extracellular glutamate. Other studies suggest that at physiological temperatures, extracellular glutamate is elevated sufficiently to activate NMDARs (Sah et al., 1989; see Fig. 4.9).

**Localization of PreNMDARs on L4-2/3 terminals.** Presynaptic ionotropic receptors could influence release by being located on the presynaptic terminal and locally influencing membrane potential (Turecek and Trussell 2001, 2002; Trussell

2002) or directly supplying calcium (Chen et al., 2000; Chávez et al., 2006). Alternatively, they could be located on the presynaptic somatodendritic compartment and generate somatic depolarization that spreads down the axon to influence release, as has been shown to occur with subthreshold depolarization at some terminals (Alle and Geiger, 2006; Shu et al., 2006). To determine the location of the PreNMDARs that modulate release at L4-L2/3 synapses, we focally puffed D-APV (2.5 mM via a picospritzer pipette) in L2/3. We first verified that the focal D-APV puffing protocol blocked local NMDARs on neural elements in L2/3, but not in L4, by recording pharmacologically isolated postsynaptic NMDAR currents at +30 mV from L2/3 and L4 neurons (in 10 μM DNQX and 100 μM picrotoxin, with 5 mM internal BAPTA). Focal D-APV puffing in L2/3 blocked 77.4 ± 10.8% (n=4) of synaptically evoked, postsynaptic NMDA currents recorded in L2/3 neurons 103 ± 30 μm (SD) away from the puffer pipette, but only 16.7 ± 5.3% (n=4) of synaptically evoked NMDA currents recorded in L4 neurons in the underlying barrel (Fig. 4.4A, insets). Thus, this protocol blocked NMDARs located in L2/3 (presumably including the presynaptic axons and terminals of L4 cells that extended into L2/3), relatively selectively compared to L4.

Next, we tested whether focal D-APV puffing in L2/3 modulated L4-L2/3 AMPA-EPSCs. We stimulated in L4 while recording AMPA-EPSCs in 15 μM TBOA, focal BMI, and iMK-801. After a stable baseline in which two AMPA-EPSCs were evoked at 30 Hz every 30 s, 2.5 mM D-APV was puffed focally in L2/3, 108 ± 29 μm (SD) away from the postsynaptic cell 15 s before each sweep (Fig. 4.4A). Fig. 4.4B shows an example cell in which this protocol caused a rapid decrease in AMPA-EPSC amplitude and an increase in PPR, which recovered after puffing was stopped.

This effect was consistent across a population of 12 cells (Fig. 4.4C&G, filled circles). To ensure specificity of puffing effects, in interleaved control experiments (n=5 cells), we focally puffed Ringer's solution using the same protocol, and observed no change in evoked EPSC amplitude or PPR (Fig. 4.4C&G, open circles).

To ensure that this effect was not due to the modest blockade of L4 NMDARs produced by D-APV puffing in L2/3, we performed the converse experiment, focally puffing D-APV in the center of the L4 barrel (about 100 μm apical to the site of stimulation), to block NMDARs in the somatodendritic compartment of L4 neurons (Fig. 4.4D). D-APV puffing in L4 blocked 80.6 ± 2.4% (n=4) of pharmacologically isolated postsynaptic NMDA currents in local L4 neurons, but only 20.5 ± 11.7% (n=3) of synaptically evoked postsynaptic NMDA currents in overlying L2/3 neurons (Fig. 4.4D, *insets*). Thus, puffing in L4 preferentially blocked NMDARs located in L4. D-APV puffing in L4 did not affect AMPA-EPSCs at L4-L2/3 synapses (n=10 cells; Fig. 4.4E-F), and did not change PPR (Fig. 4.4G, open squares). Together, these results indicate D-APV modulates release by acting on non-postsynaptic NMDARs that are located in L2/3, rather than in L4, consistent with localization on L4 axons or terminals in L2/3, rather than on L4 cell bodies or dendrites.

**PreNMDARs contain NR2B subunits.** NMDARs are heterotetrameric channels made up of two NMDA receptor 1 (NR1) subunits and two NR2 subunits (Dingledine et al., 1999). Of the four types of NR2 subunits, cortical neurons preferentially express NR2A and/or NR2B (Monyer et al., 1994). In cortex, postsynaptic NMDARs undergo an early postnatal developmental switch from NR2B-containing to NR2A-containing receptors (Monyer et al., 1994; Flint et al., 1997;

Stocca and Vicini, 1998; Kew et al., 1998; Tovar and Westbrook, 1999; Liu et al., 2004), while PreNMDARs are thought to preferentially retain NR2B subunits (Woodhall et al., 2001; Sjöström et al., 2003; Yang et al., 2006). To determine the subunit composition of PreNMDARs at L4-L2/3 synapses, we applied the NR2B-selective antagonist ifenprodil (Williams, 1993). We first tested whether NR2B receptors were largely absent from postsynaptic NMDARs, as expected by this age (Flint et al., 1997), by measuring L4-evoked postsynaptic NMDA currents in L2/3 pyramidal cells (+30 mV holding potential, in 10 μM DNQX and 100 μM picrotoxin, 5 mM internal BAPTA), and applying increasing concentrations of ifenprodil. Postsynaptic NMDA currents were almost completely insensitive to 3 μM ifenprodil (4.3 ± 0.1% block, n=3), but were progressively blocked by higher ifenprodil concentrations, consistent with the weak affinity of ifenprodil for postsynaptic NR2A-containing NMDARs (Fig. 4.5A; Williams, 1993).

To test whether NR2B-containing receptors regulated release at L4-L2/3 synapses, we applied 3 μM ifenprodil while measuring L4-2/3 EPSCs recorded at -90 mV in the presence of 15 μM TBOA and focal BMI. iMK-801 was not present in these experiments. Pairs of EPSCs (30 Hz) were evoked every 30 sec. After a stable baseline period, 3 μM ifenprodil was applied. Ifenprodil caused a decrease in EPSC amplitude and an increase in PPR, indicating a decrease in release probability (Fig. 4.5B-D, filled symbols). Interleaved experiments without ifenprodil confirmed that, no change in EPSC amplitude or PPR was observed under these conditions (Fig. 4.5B-C, open symbols).

In addition to NR2A and NR2B subunits, NR2C and 2D subunits are also present in cortex, though in low abundance (Monyer et al., 1994). To further determine whether PreNMDARs preferentially contain 2A/B or 2C/D subunits, we measured the effect of the NR2A- and NR2B-preferring NMDAR agonist HQA (20 μM) on mEPSC frequency (de Carvalho et al., 1996; Woodhall et al., 2001). mEPSCs were measured (500 nM TTX, 100 μM picrotoxin and 1 mM iMK-801) during a baseline period (10 min), after addition of HQA (20 μM, 10 min), and after subsequent addition of ifenprodil (3 μM, 10 min, Fig. 4.5E). HQA caused an increase in mEPSC frequency, which was reversed by ifenprodil (Fig. 4.5F, baseline = 7.4 ± 0.9 Hz, HQA = 8.7 ± 1.1 Hz, HQA+ifenprodil = 7.3 ± 1.0 Hz, $p < 0.0001$). There was no effect on mEPSC amplitude (baseline = 9.1 ± 0.4 pA, HQA = 8.8 ± 0.3 pA, HQA+ifenprodil = 9.0 ± 0.4 pA, $p = 0.68$), rise time (baseline = 1.93 ± 0.06 ms, HQA = 2.04 ± 0.04 ms, HQA+ifenprodil = 2.06 ± 0.09 ms, $p = 0.16$), or decay time (baseline = 5.0 ± 0.3 ms, HQA = 4.8 ± 0.3 ms, HQA+ifenprodil = 4.9 ± 0.3 ms, $p = 0.68$). Together, these results are consistent with the hypothesis that the PreNMDARs that modulate release onto L2/3 pyramidal cells preferentially contain NR2B subunits.

**Synapse specificity of PreNMDARs.** We examined the presence of functional PreNMDARs with respect to two types of synapse-specificity: first, input specificity, in which PreNMDARs are not localized on all excitatory synaptic inputs to a neuron, but are instead localized to one class of inputs; and second, target specificity, in which PreNMDARs are not expressed on all axonal terminals of a neuron, but only those terminals that contact a specific target neuron class.

*Input specificity*. We first tested whether PreNMDARs are selectively expressed at L4-L2/3 inputs onto L2/3 pyramidal cells, relative to other excitatory inputs onto these same cells. We therefore tested for functional PreNMDARs at horizontal, cross-columnar L2/3 inputs onto L2/3 neurons. We recorded AMPA-EPSCs from a single L2/3 pyramidal cell in one barrel column in 15 in μM TBOA and iMK-801 with focal BMI. We placed one extracellular stimulating electrode in L4 of the same column to activate the L4-L2/3 pathway (as above), and another in L2/3 of a neighboring column to activate the cross-columnar L2/3-L2/3 pathway (Fig. 4.6B). We alternately stimulated each pathway with two pulses (30 Hz), with 15 s between pathways, and tested whether D-APV (50 μM) modulated release on either pathway. In an example cell, D-APV decreased AMPA-EPSC amplitude and increased PPR on the L4-L2/3 pathway, but caused no change in either AMPA-EPSC amplitude or PPR on the simultaneously recorded L2/3 cross-columnar pathway (Fig. 4.6A). Similar results were obtained across 8 cells (Fig. 4.6C-D). Thus, PreNMDARs functionally regulate L4 inputs onto L2/3 pyramidal cells, but not cross-columnar L2/3 inputs onto L2/3 pyramidal cells, indicating that the presence of PreNMDARs is dependent on the origin of presynaptic input.

*Target specificity*. To test whether the presence of functional PreNMDARs is dependent on the postsynaptic cell that different axon collaterals target, we asked whether other synapses made by L4 neurons, besides L4-L2/3 synapses, also express functional PreNMDARs. In addition to projecting to L2/3, L4 excitatory neurons are extensively interconnected in their home barrels (Feldmeyer et al., 1999; Petersen and Sakmann, 2000). We therefore tested whether unitary connections between L4

neurons are regulated by PreNMDARs (Fig. 4.7A). We recorded unitary AMPA-EPSCs (AMPA-uEPSCs) from 12 synaptically connected L4-L4 pairs in the presence of 15 μM TBOA. 7 pairs survived long enough to assess the effects of D-APV application. Two presynaptic action potentials (30 Hz) were evoked every 30 s. After a stable baseline, 50 μM D-APV was applied. D-APV application caused no change in the amplitude of the first AMPA-uEPSC or PPR as seen in a single, representative cell (Fig. 4.7B) and across a population of 7 cells (Fig. 4.7C-D). These results indicate that PreNMDARs functionally regulate L4-L2/3 synapses, but not L4-L4 synapses.

Because L4 neurons densely innervate each other, spontaneous mEPSCs on L4 neurons will reflect, to a large degree, inputs from other L4 cells. Therefore, as a second test of whether functional PreNMDARs regulate release at L4-L4 synapses, we measured the effects of the NMDAR agonist HQA on mEPSCs in L4 excitatory neurons in 500 nM TTX, 100 μM picrotoxin, and 1 mM iMK-801 (holding potential = -90 mV). Bath application of HQA (20 μM) did not affect mEPSC frequency (Fig. 4.7E, baseline = 7.3 ± 0.9 Hz, HQA = 7.6 ± 0.8 Hz, $p = 0.35$), amplitude (baseline = 7.8 ± 0.1 pA, HQA = 7.9 ± 0.1 pA, $p = 0.30$), rise time (baseline = 2.03 ± 0.04 ms, HQA = 2.08 ± 0.05 ms, $p = 0.14$), or decay time (baseline = 5.0 ± 0.2 ms, HQA = 5.0 ± 0.1 ms, $p = 0.60$). Together, these results indicate that PreNMDARs regulate release on L4-L2/3 synapses, but not at L4-L4 synapses or horizontal L2/3-L2/3 synapses. Thus, functional PreNMDARs exhibit both target specificity and input specificity.

**Confirmation of functional PreNMDARs at unitary L4-2/3 synapses.** To verify that PreNMDAR regulation of synaptic transmission occurs specifically at L4-

L2/3 synapses, as opposed to other synapses that may be activated by extracellular L4 stimulation, we tested whether PreNMDARs regulated release probability at synaptically coupled pairs of presynaptic L4 excitatory cells and postsynaptic L2/3 pyramidal cells (Feldmeyer et al., 2002). To obtain dual recordings, the postsynaptic L2/3 pyramidal cell was whole-cell voltage-clamped at -90 mV with iMK-801, and the presynaptic L4 cell was identified by loose-patch stimulation and repatched in whole-cell current clamp mode using $K^+$-gluconate internal. We tested 1085 pairs, of which 28 were connected, and 11 remained stable long enough for analysis. PPR was measured in 8 pairs (prior to TBOA addition) to be 0.95 ± 0.15 at 20 ms isi and 0.65 ± 0.06 at 200 ms isi, which were not different from PPR previously measured at L4-L2/3 inputs using extracellular L4 stimulation ($p = 0.87$ for 20 ms, $p = 0.15$ for 200 ms; Bender et al., 2006a; K. Bender and D. Feldman unpublished observations). In 2 cells, AMPA-uEPSC reversal potential was measured to be +7 mV, consistent with glutamatergic transmission. All L4 cells exhibited a regular-spiking pattern consistent with excitatory spiny stellate or star pyramidal cells (Fig. 4.8A, *inset*; Connors and Gutnick, 1990; Feldmeyer, et al., 2002)

We tested the effects of D-APV application on AMPA-uEPSCs (30 Hz, 30 s inter-sweep interval, n=7 pairs) in the presence of 15 μM TBOA and postsynaptic iMK-801 (postsynaptic holding potential = -90 mV). In an example pair, D-APV application caused a reduction in amplitude of the first AMPA-uEPSC, and an increase in PPR, without any coincident changes in presynaptic membrane potential or input resistance, or postsynaptic holding current, input resistance, or series resistance (Fig. 4.8A). Across the population, D-APV consistently decreased first AMPA-

uEPSC amplitude (Fig. 4.8B) and increased PPR (Fig. 4.8C). To ensure that this effect did not represent non-specific synaptic rundown, we performed interleaved control experiments in which we recorded unitary L4-L2/3 connections in the presence of TBOA, but did not apply D-APV. In these experiments (n=4 pairs), no change was observed in the amplitude of the first AMPA-uEPSC, and no consistent change in PPR (Fig. 4.8B-C).

As an additional test to determine whether D-APV affected presynaptic release, we calculated the coefficient of variation (CV) for the first AMPA-uEPSC amplitude before and after D-APV application. Manipulations that cause postsynaptic depression are associated with a decrease in mean EPSC amplitude without change in $CV^{-2}$, while depression of presynaptic release is expected to cause a decrease in $CV^{-2}$ greater than the decrease in mean EPSC amplitude (Malinow and Tsien, 1990; Faber and Korn, 1991; Larkman et al., 1992; Sjöström et al., 2003). We observed that D-APV treatment caused $CV^{-2}$ to decrease significantly more than mean EPSC amplitude (Fig. 4.8D; $CV^{-2}_{APV}/CV^{-2}_{baseline} = 0.42 \pm 0.08$, $mean_{APV}/mean_{baseline} = 0.61 \pm 0.07$; $p = 0.03$), consistent with a presynaptic locus of depression. In contrast, control cell pairs in which D-APV was not applied exhibited no change in mean ($mean_{APV}/mean_{baseline} = 0.98 \pm 0.06$, $p = 0.81$, unpaired t-test) or $CV^{-2}$ ($CV^{-2}_{APV}/CV^{-2}_{baseline} = 1.08 \pm 0.33$, $p = 0.83$, unpaired t-test; Fig. 4.8D). These results indicate that PreNMDARs regulate presynaptic release probability at unitary L4-L2/3 synaptic connections.

**PreNMDARs tonically enhance release probability at physiological temperatures.** In contrast to our observation that, at room temperature PreNMDARs require enhanced extracellular glutamate (Fig. 4.1; Bender et al., 2006b) or application

of exogenous agonist (Fig. 4.3) in order to be activated, other groups have previously found that neocortical PreNMDARs are tonically activate at physiological temperatures (Sjostrom et al., 2003; Corlew et al., 2007). It is known that postsynaptic NMDARs can be tonically activated by ambient glutamate at physiological temperatures (Sah et al., 1989). We therefore tested whether the effects on mEPSCs we have observed are still present at 30-32$^{o}$C and whether D-APV application causes a reduction in mEPSC frequency below baseline rates.

mEPSCs were recorded from L2/3 pyramidal neurons at 30-32$^{o}$C as above (holding potential = -90 mV) in TTX (500 nM) and picrotoxin (100 μM), with iMK-801 (1 mM). After a 10 minutes baseline period, 15 μM HQA was applied to activate non-postsynaptic NMDARs, causing an increase in mEPSC frequency (Fig. 4.9A, upper 2 traces). Subsequent addition of 50 μM D-APV caused a reduction in mEPSC frequency below baseline levels (Fig. 4.9A). These effects were consistent across the population of 6 cells recorded as seen by the cumulative probability histogram for inter-mEPSC interval (Fig. 4.9B) and the mean mEPSC frequency for each cell (Fig. 4.9C, upper panel). There was no change in mEPSC amplitude (Fig. 4.9B, lower panel; baseline = 10.2 ± 0.7 pA, HQA = 9.9 ± 0.6 pA, HQA+APV = 10.1 ± 0.9 pA, p = 0.64), rise time (baseline = 1.94 ± 0.09 ms, HQA = 1.99 ± 0.09 ms, HQA+APV = 1.91 ± 0.09 ms, p = 0.10), or decay time (baseline = 4.7 ± 0.3 ms, HQA = 4.6 ± 0.4 ms, HQA+APV = 4.6 ± 0.3 ms, p = 0.57).

To test whether inputs onto L4 neurons exhibit functional PreNMDARs at physiological temperatures, we recorded mEPSCs from L4 excitatory neurons as above. Neither HQA nor subsequent application of D-APV altered mEPSC frequency

in L4 as shown in example recordings (Fig. 4.9D), cumulative probability histogram for inter-mEPSC interval (Fig. 4.9E), and mean mEPSC frequency (Fig. 4.9F, upper trace). Drug application did not alter mESPC amplitude (Fig. 4.9F, lower trace; baseline = 10.7 ± 0.8 pA, HQA = 10.4 ± 0.9 pA, HQA+APV = 10.2 ± 1.0 pA, p = 0.50), rise time (baseline = 1.76 ± 0.04 ms, HQA = 1.89 ± 0.07 ms, HQA+APV = 1.92 ± 0.14 ms, p = 0.26), or decay time (baseline = 4.0 ± 0.2 ms, HQA = 4.0 ± 0.3 ms, HQA+APV = 4.0 ± 0.3 ms, p = 0.98). These results indicate that tonically active PreNMDARs are present on inputs to L2/3, but not L4 excitatory cells at physiological temperatures.

**Discussion**

Functional PreNMDARs have been observed at many excitatory cortical synapses (Berretta and Jones 1996; Woodhall et al., 2001; Sjöström et al., 2003; Yang et al., 2006; Corlew et al., 2007), particularly during the first 3 weeks of postnatal development (Fiszman et al.,2005; Mameli et al., 2005; Corlew et al., 2007). Our results demonstrate that functional, NR2B-containing PreNMDARs are present in S1, but are restricted to a specific subset of terminals in P15-P22 rats. Specifically, they are present at excitatory feedforward L4-L2/3 synapses, but not at other synapses made by L4 cells (L4-L4 synapses) or at other inputs onto L2/3 cells (synapses of the cross-columnar L2/3-L2/3 projection). Thus the expression of functional PreNMDARs depends both on the origin and the target of synaptic inputs. This demonstrates for the first time that functional expression of PreNMDARs is not a general property of developing cortical synapses, but is highly targeted to specific

synapses within and across neurons. These results also demonstrate, for the first time, that synapses of single cortical excitatory neurons onto different excitatory postsynaptic targets can have distinct, target-specific properties.

**Activation and detection of PreNMDARs.** NMDARs require binding of glutamate for activation. Glutamate for PreNMDAR activation could arise from (i) local, phasic glutamate release by the synapses expressing PreNMDARs; (ii) tonic, ambient glutamate pooled from other nearby neurons, as has been shown to activate postsynaptic NMDARs in some preparations (Sah et al., 1989; Le Meur et al., 2007); or (iii) glutamate released from non-neuronal sources, chiefly synaptically-associated astrocytes, which have been reported to release glutamate to activate PreNMDARs in hippocampus (Jourdain et al., 2007). Our results show that PreNMDARs are activated at room temperature only after elevation of ambient glutamate by TBOA or by high-frequency bursts (Bender et al., 2006b), indicating that pooled ambient glutamate can activate these receptors. However, at physiological temperatures, PreNMDAR blockade shows strong effects without TBOA or bursts, suggesting that ambient glutamate may be sufficiently elevated at physiological temperature to activate cortical PreNMDARs (Fig. 4.9; Berretta and Jones 1996; Woodhall et al., 2001; Sjöström et al., 2003; Corlew et al., 2007). The ability of ambient glutamate to tonically activate PreNMDARs is in contrast to observed phasic activation of presynaptic kainate receptors (Sun and Dobrunz, 2006), and may reflect the low glutamate affinity of presynaptic kainate receptors (Pinheiro et al., 2007) relative to NMDARs. A third possibility is that glutamate is released in a regulated manner from a third cell, such as a synaptically associated glial as has been seen for PreNMDARs in hippocampus

(Jourdain et al., 2007). We cannot rule out the possibility that such regulated release of glutamate from synaptically associated glia is temperature-dependent. It is therefore possible that elevating the temperature to 30-32$^{o}$C does not elevate ambient glutamate in the entire slice, but rather enhances glia-mediated release of glutamate onto PreNMDARs.

Previous studies have identified functional cortical PreNMDARs primarily by applying antagonists and looking for decreases in mEPSC frequency or evoked EPSCs (Berretta and Jones 1996; Woodhall et al., 2001; Sjöström et al., 2003; Corlew et al., 2007). This approach will only identify synapses that both have functional PreNMDARs, and which are exposed to sufficient glutamate to tonically activate these receptors under slice conditions. In contrast, our goal was to identify which synapses had functional PreNMDARs, irrespective of whether tonic glutamate was sufficient in the slice to activate them. Thus, we artificially activated PreNMDARs with NMDAR agonists and by using TBOA to increase basal glutamate concentrations. This approach will be highly sensitive to identifying synapses with and without functional PreNMDARs.

**Localization of NMDARs to presynaptic terminals.** We infer that the NMDARs that modulate release at L4-L2/3 synapses are not located on the postsynaptic neuron, because their function was not blocked by postsynaptic hyperpolarization or internal MK-801, manipulations that nearly completely block postsynaptic NMDAR currents in L2/3 neurons (Bender et al., 2006b; D. Brasier, V. Bender, and D. Feldman, unpublished observations). These findings also rule out the possibility that the relevant NMDARs are extrasynaptic postsynaptic receptors, which,

like presynaptic NMDARs, are also enriched for NR2B-containing NMDARs (Tovar and Westbrook, 1999, but see Thomas et al., 2006). Postsynaptic NMDARs receptors are also excluded because 3 μM ifenprodil powerfully reduced AMPA-EPSCs without affecting postsynaptic NMDAR currents. Finally, D-APV does not reduce AMPA-mediated transmission by a non-selective effect on L2/3 neurons, because D-APV selectively reduced L4-L2/3 synaptic responses, but not horizontal L2/3-L2/3 synaptic responses when recorded at the same time onto the same postsynaptic target.

Given that the relevant receptors are not postsynaptic, they could be located on the somatodendric compartment of the presynaptic cell, the presynaptic terminal itself, or on a third cell. We were able to exclude the somatodendritic compartment of the presynaptic L4 cell, because focal application of D-APV in L2/3 reduced release at L4-L2/3 synapses, while focal application in L4, where presynaptic somata and dendrites are located, did not. Thus, the relevant NMDARs must be located in L2/3, either on the axons or terminals of presynaptic L4 cells, or on an unknown third cell. This third cell could be a synaptically associated glial cell (DeBiasi et al., 1996; Conti et al., 1996, 1999; Lalo et al., 2006; Verkhratsky and Kirchhoff, 2007). However, the locus of expression of NMDAR effects at L4-L2/3 synapses is clearly a decrease in release probability within the presynaptic terminal, as evidenced by the increased PPR and decreased $CV^{-2}$ when NMDARs are blocked, and by the increased mEPSC frequency when NMDARs are activated . In addition, electron microscopic evidence places NMDAR protein on axon terminals in L2/3 of visual cortex (Aoki et al., 1994; Conti et al., 1997; Charton et al., 1999; Corlew et al., 2007). Therefore, we conclude that the simplest possible location of the NMDARs that modulate release is the

presynaptic L4-L2/3 terminal. PreNMDARs on terminals could readily enhance release probability by depolarizing the terminal (Turecek and Trussell 2001, 2002; Trussell 2002) or by providing direct influx of calcium (Chen et al., 2000; Chávez et al., 2006).

**Synapse-specificity of PreNMDARs.** PreNMDARs have been observed functionally at multiple excitatory synapses in primary visual cortex (Sjöström et al., 2003; Corlew et al., 2007) and entorhinal cortex (Berretta and Jones 1996; Woodhall et al., 2001), and electron microscopy indicates broad expression of PreNMDAR protein in visual cortex in early postnatal development (<P23, overlapping with the ages studied here; Corlew et al., 2007). In contrast, our data demonstrate that in juvenile S1, functional PreNMDARs are not universal, but instead regulate release at a highly specific subset of excitatory synapses, at least within L4 and L2/3. This specificity is apparent at the cellular level, with functional PreNMDARs evident at L4-L2/3 synapses, but not at horizontal, cross-columnar synapses onto the same postsynaptic L2/3 neurons, or at L4-L4 synapses made by the same presynaptic neurons onto a different target cell. Thus, the molecular targeting or functional regulation of PreNMDARs must be tightly spatially controlled in L4 neurons. Differences between our results in S1 those of Corlew et al. (2007) in visual cortex may reflect circuit specializations or different developmental programs within these two sensory areas.

Excitatory synapses made by collaterals from the same presynaptic axon can have markedly different release properties, dynamics (Reyes et al., 1998; Scanziani et al., 1998; Tóth and McBain, 2000; Koester and Johnston, 2005), and expression of

presynaptic neurotransmitter receptors (Scanziani et al., 1998; Sun and Dobrunz, 2006). Our results indicate that PreNMDARs can also be expressed in a target-specific manner. Thus, differential expression of presynaptic receptors (including ionotropic receptors) may be a general mechanism by which a single presynaptic cell regulates release dynamics and other synapse properties at its many terminals in a target-cell specific manner.

**Potential functional role of PreNMDARs.** When activated by sufficient glutamate, PreNMDARs help to maintain high release probability at L4-L2/3 synapses. This suggests that the presence of PreNMDARs may offset the synaptic depression that occurs with even modest sustained activity at this synapse (Feldmeyer et al., 2002). Assuming that neural activity increases local ambient glutamate, this offset may increase dynamically with local cortical activity. The selective expression of PreNMDARs at feedforward L4-L2/3 synapses, rather than at cross-columnar L2/3-L2/3 synapses or at L4-L4 synapses, suggests that PreNMDARs may function to promote feedforward activation within S1. In this model, activation of PreNMDARs during rapid trains of sensory-evoked responses (Bender et al., 2006b) or during cortical up states (McCormick, 2005), could serve to enhance ascending columnar transmission preferentially relative to lateral spread of excitation. This could sharpen functional boundaries between columns *in vivo*. This type of activity-dependent sharpening of columnar transmission may contribute to the more spatially restricted spread of excitation that is observed in S1 of active vs. passive mice (Ferezou et al., 2006).

Understanding the synapse selective targeting of PreNMDARs may also be important for understanding the role of these receptors in epilepsy, where they have recently emerged as a potential therapeutic target (Suárez et al., 2005; Yang et al., 2006), and in activity-dependent plasticity, because these receptors are known to mediate or regulate spike timing-dependent long-term synaptic depression (LTD) at cortical synapses (Sjöström et al., 2003; Bender et al., 2006b; Duguid and Sjöström, 2006). Thus, PreNMDARs serve to enhance excitatory synaptic transmission selectively at the feedforward L4-L2/3 projection in S1.

**Acknowledgment**

This chapter is original work submitted as Brasier DJ, Feldman DE. Synapse specific expression of functional presynaptic NMDA receptors in somatosensory cortex. J Neurosci. 2007, *submitted*. It has been reformatted and restructured from the submitted version to include data that was published in figure 8 of Bender VA, Bender KJ, Brasier DJ, Feldman DE. Two coincidence detectors for spike timing-dependent plasticity in somatosensory cortex. J Neurosci. 2006 Apr 19; 26(16):4166-77, for which the thesis author was primarily responsible and which has been incorporated into this chapter as figure 4.1 with permission from all the paper's authors.

**References**

Alle H, Geiger JR (2006) Combined analog and action potential coding in hippocampal mossy fibers. Science. 311:1290-1293.

Allen CB, Celikel T, Feldman DE (2003) Long-term depression induced by sensory deprivation during cortical map plasticity in vivo. Nat Neurosci 6:291-299.

Aoki C, Venkatesan C, Go CG, Mong JA, Dawson TM (1994) Cellular and subcellular localization of NMDA-R1 subunit immunoreactivity in the visual cortex of adult and neonatal rats. J Neurosci 14:5202-5222.

Bender KJ, Allen CB, Bender VA, Feldman DE (2006a) Synaptic basis for whisker deprivation-induced synaptic depression in rat somatosensory cortex. J Neurosci 26:4155-4165.

Bender VA, Bender KJ, Brasier DJ, Feldman DE (2006b) Two coincidence detectors for spike timing-dependent plasticity in somatosensory cortex. J Neurosci 26:4166-4177.

Berretta N, Jones RS (1996) Tonic facilitation of glutamate release by presynaptic N-methyl-D-aspartate autoreceptors in the entorhinal cortex. Neuroscience 75:339-344.

Brasier DJ, Feldman, DF (2006) Presynaptic NMDA receptors modulate release at the layer 4 to layer 2/3 synapse in rat somatosensory cortex (S1). Program No. 534.4. Neuroscience Meeting Planner. Atlanta, GA: Society for Neuroscience. *Online*.

Cartmell J, Schoepp DD (2000) Regulation of neurotransmitter release by metabotropic glutamate receptors. J Neurochem 75:889-907.

Castro-Alamancos MA, Donoghue JP, Connors BW (1995) Different forms of synaptic plasticity in somatosensory and motor areas of the neocortex. J Neurosci 15:5324-5333.

Charton JP, Herkert M, Becker CM, Schroder H (1999) Cellular and subcellular localization of the 2B-subunit of the NMDA receptor in the adult rat telencephalon. Brain Res 816:609-617.

Chávez E, Singer JH, Diamond JS (2006) Fast neurotransmitter release triggered by Ca influx through AMPA-type glutamate receptors. Nature 443:705-708.

Chen WR, Xiong W, Shepherd GM (2000) Analysis of relations between NMDA receptors and GABA release at olfactory bulb reciprocal synapses. Neuron 25:625-633.

Connors BW, Gutnick MJ (1990) Intrinsic firing patterns of diverse neocortical neurons. Trends Neurosci 13:99-104.

Conti F, DeBiasi S, Minelli A, Melone M (1996) Expression of NR1 and NR2A/B subunits of the NMDA receptor in cortical astrocytes. Glia 17:254-258.

Conti F, Minelli A, DeBiasi S, Melone M (1997) Neuronal and glial localization of NMDA receptors in the cerebral cortex. Mol Neurobiol 14:1-18.

Conti F, Barbaresi P, Melone M, Ducati A (1999) Neuronal and glial localization of NR1 and NR2A/B subunits of the NMDA receptor in the human cerebral cortex. Cereb Cortex 9:110-120.

Contractor A, Swanson G, Heinemann SF (2001) Kainate receptors are involved in short- and long-term plasticity at mossy fiber synapses in the hippocampus. Neuron 29:209-216.

Corlew R, Wang Y, Ghermazien H, Erisir A, Philpot BD (2007) Developmental switch in the contribution of presynaptic and postsynaptic NMDA receptors to long-term depression. J Neurosci, *in press*.

de Carvalho LP, Bochet P, Rossier J (1996) The endogenous agonist quinolinic acid and the non endogenous homoquinolinic acid discriminate between NMDAR2 receptor subunits. Neurochem Int 28:445-452.

DeBiasi S, Minelli A, Melone M, Conti F (1996) Presynaptic NMDA receptors in the neocortex are both auto- and heteroreceptors. Neuroreport 7:2773-2776.

Delaney AJ, Jahr CE (2002) Kainate receptors differentially regulate release at two parallel fiber synapses. Neuron 36:475-482.

Dingledine R, Borges K, Bowie D, Traynelis SF (1999) The glutamate receptor ion channels. Pharmacol Rev 51:7-61.

Dobrunz LE, Stevens CF (1997) Heterogeneity of release probability, facilitation, and depletion at central synapses. Neuron 18:995-1008.

Duguid I, Sjostrom PJ (2006) Novel presynaptic mechanisms for coincidence detection in synaptic plasticity. Curr Opin Neurobiol 16:312-322.

Engelman HS, MacDermott AB (2004) Presynaptic ionotropic receptors and control of transmitter release. Nat Rev Neurosci 5:135-145.

Faber DS, Korn H (1991) Applicability of the coefficient of variation method for analyzing synaptic plasticity. Biophys J 60:1288-94.

Feldman DE (2000) Timing-based LTP and LTD at vertical inputs to layer II/III pyramidal cells in rat barrel cortex. Neuron 27:45-56.

Feldmeyer D, Egger V, Lubke J, Sakmann B (1999) Reliable synaptic connections between pairs of excitatory layer 4 neurones within a single 'barrel' of developing rat somatosensory cortex. J Physiol 521:169-190.

Feldmeyer D, Lubke J, Silver RA, Sakmann B (2002) Synaptic connections between layer 4 spiny neurone-layer 2/3 pyramidal cell pairs in juvenile rat barrel cortex: physiology and anatomy of interlaminar signaling within a cortical column. J Physiol 538:803-822.

Ferezou I, Bolea S, Petersen CC (2006) Visualizing the cortical representation of whisker touch: voltage-sensitive dye imaging in freely moving mice. Neuron 50:617-629.

Fiszman ML, Barberis A, Lu C, Fu Z, Erdelyi F, Szabo G, Vicini S (2005) NMDA receptors increase the size of GABAergic terminals and enhance GABA release. J Neurosci 25:2024-20231.

Flint AC, Maisch US, Weishaupt JH, Kriegstein AR, Monyer H (1997) NR2A subunit expression shortens NMDA receptor synaptic currents in developing neocortex. J Neurosci 17:2469-2476.

Freund TF, Katona I, Piomelli D (2003) Role of endogenous cannabinoids in synaptic signaling. Physiol Rev 83:1017-1066.

Humeau Y, Shaban H, Bissiere S, Luthi A (2003) Presynaptic induction of heterosynaptic associative plasticity in the mammalian brain. Nature 426:841-845.

Jourdain P, Bergersen LH, Bhaukaurally K, Bezzi P, Santello M, Domercq M, Matute C, Tonello F, Gundersen V, Volterra A (2007) Glutamate exocytosis from astrocytes controls synaptic strength. Nat Neurosci 10:331-339.

Karim F, Bhave G, Gereau RW 4th (2001) Metabotropic glutamate receptors on peripheral sensory neuron terminals as targets for the development of novel analgesics. Mol Psychiatry 6:615-617.

Kew JN, Richards JG, Mutel V, Kemp JA (1998) Developmental changes in NMDA receptor glycine affinity and ifenprodil sensitivity reveal three distinct populations of NMDA receptors in individual rat cortical neurons. J Neurosci 18:1935-1943.

Koester HJ, Johnston D (2005) Target cell-dependent normalization of transmitter release at neocortical synapses. Science 308:863-866.

Kreitzer AC, Regehr WG (2002) Retrograde signaling by endocannabinoids. Curr Opin Neurobiol 12:324-330.

Lalo U, Pankratov Y, Kirchhoff F, North RA, Verkhratsky A (2006) NMDA receptors mediate neuron-to-glia signaling in mouse cortical astrocytes. J Neurosci 26:2673-2683.

Larkman A, Hannay T, Stratford K, Jack J (1992) Presynaptic release probability influences the locus of long-term potentiation. Nature 360:70-73.

Le Meur K, Galante M, Angulo MC, Audinat E (2007) Tonic activation of NMDA receptors by ambient glutamate of non-synaptic origin in the rat hippocampus. J Physiol 580:373-383.

Lien CC, Mu Y, Vargas-Caballero M, Poo MM (2006) Visual stimuli-induced LTD of GABAergic synapses mediated by presynaptic NMDA receptors. Nat Neurosci 9:372-380.

Liu XB, Murray KD, Jones EG (2004) Switching of NMDA receptor 2A and 2B subunits at thalamic and cortical synapses during early postnatal development. J Neurosci 24:8885-8895.

MacDermott AB, Role LW, Siegelbaum SA (1999) Presynaptic ionotropic receptors and the control of transmitter release. Annu Rev Neurosci 22:443-485.

Malinow R, Tsien RW (1990) Presynaptic enhancement shown by whole-cell recordings of long-term potentiation in hippocampal slices. Nature 346:177-180.

Mameli M, Carta M, Partridge LD, Valenzuela CF (2005) Neurosteroid-induced plasticity of immature synapses via retrograde modulation of presynaptic NMDA receptors. J Neurosci 25:2285-2294.

McCormick DA (2005) Neuronal networks: flip-flops in the brain. Curr Biol15:R294-R296.

Monyer H, Burnashev N, Laurie DJ, Sakmann B, Seeburg PH (1994) Developmental and regional expression in the rat brain and functional properties of four NMDA receptors. Neuron 12:529-540.

Murthy VN, Sejnowski TJ, Stevens CF (1997) Heterogeneous release properties of visualized individual hippocampal synapses. Neuron 18:599-612.

Petersen CC, Sakmann B (2000) The excitatory neuronal network of rat layer 4 barrel cortex. J Neurosci 20:7579-7586.

Pinheiro PS, Perrais D, Coussen F, Barhanin J, Bettler B, Mann JR, Malva JO, Heinemann SF, Mulle C (2007) GluR7 is an essential subunit of presynaptic kainate autoreceptors at hippocampal mossy fiber synapses. PNAS. in press.

Reyes A, Lujan R, Rozov A, Burnashev N, Somogyi P, Sakmann B (1998) Target-cell-specific facilitation and depression in neocortical circuits. Nat Neurosci 1:279-285.

Sah P, Hestrin S, Nicoll RA (1989) Tonic activation of NMDA receptors by ambient glutamate enhances excitability of neurons. Science 246:815-818.

Samson RD, Pare D (2005) Activity-dependent synaptic plasticity in the central nucleus of the amygdala. J Neurosci 25:1847-1855.

Scanziani M, Gahwiler BH, Charpak S (1998) Target cell-specific modulation of transmitter release at terminals from a single axon. Proc Natl Acad Sci U S A 95:12004-12009.

Schmitz D, Frerking M, Nicoll RA (2000) Synaptic activation of presynaptic kainate receptors on hippocampal mossy fiber synapses. Neuron 27:327-338.

Shigeri Y, Seal RP, Shimamoto K (2004) Molecular pharmacology of glutamate transporters, EAATs and VGLUTs. Brain Res Brain Res Rev 45:250-265.

Shu Y, Hasenstaub A, Duque A, Yu Y, McCormick DA (2006) Modulation of intracortical synaptic potentials by presynaptic somatic membrane potential. Nature 441:761-765.

Sjöström PJ, Turrigiano GG, Nelson SB (2003) Neocortical LTD via coincident activation of presynaptic NMDA and cannabinoid receptors. Neuron 39:641-654.

Stocca G, Vicini S (1998) Increased contribution of NR2A subunit to synaptic NMDA receptors in developing rat cortical neurons. J Physiol 507:13-24.

Suárez LM, Suárez F, del Olmo N, Ruiz M, González-Escalada JR, Solís JM (2005) Presynaptic NMDA autoreceptors facilitate axon excitability: a new molecular target for the anticonvulsant gabapentin. Eur J Neurosci 21:197-209.

Sun HY, Lyons SA, Dobrunz LE (2005) Mechanisms of target-cell specific short-term plasticity at Schaffer collateral synapses onto interneurones versus pyramidal cells in juvenile rats. J Physiol 568:815-840.

Sun HY, Dobrunz LE (2006) Presynaptic kainate receptor activation is a novel mechanism for target cell-specific short-term facilitation at Schaffer collateral synapses. J Neurosci 26:10796-10807.

Takahashi T, Kajikawa Y, Tsujimoto T (1998) G-Protein-coupled modulation of presynaptic calcium currents and transmitter release by a GABAB receptor. J Neurosci 18:3138-3146.

Thomas CG, Miller AJ, Westbrook GL (2006) Synaptic and extrasynaptic NMDA receptor NR2 subunits in cultured hippocampal neurons. J Neurophysiol 95:1727-1734.

Tóth K, McBain CJ (2000) Target-specific expression of pre- and postsynaptic mechanisms. J Physiol 525:41-51.

Tovar KR, Westbrook GL (1999) The incorporation of NMDA receptors with a distinct subunit composition at nascent hippocampal synapses in vitro. J Neurosci 19:4180-4188.

Trussell LO (2002) Modulation of transmitter release at giant synapses of the auditory system. Curr Opin Neurobiol 12:400-404.

Turecek R, Trussell LO (2001) Presynaptic glycine receptors enhance transmitter release at a mammalian central synapse. Nature 411:587-590.

Turecek R, Trussell LO (2002) Reciprocal developmental regulation of presynaptic ionotropic receptors. Proc Natl Acad Sci U S A 99:13884-13889.

Verkhratsky A, Kirchhoff F (2007) NMDA Receptors in glia. Neuroscientist 13:28-37.

Williams K (1993) Ifenprodil discriminates subtypes of the N-methyl-D-aspartate receptor: selectivity and mechanisms at recombinant heteromeric receptors. Mol Pharmacol 44:851-859.

Woodhall G, Evans DI, Cunningham MO, Jones RSG (2001) NR2B-containing NMDA autoreceptors at synapses on entorhinal cortical neurons. J Neurophysiol 86:1644-1651.

Yang J, Woodhall GL, Jones RS (2006) Tonic facilitation of glutamate release by presynaptic NR2B-containing NMDA receptors is increased in the entorhinal cortex of chronically epileptic rats. J Neurosci 26:406-410.

Zucker RS, Regehr WG (2002) Short-term synaptic plasticity. Annu Rev Physiol 64:355-405.

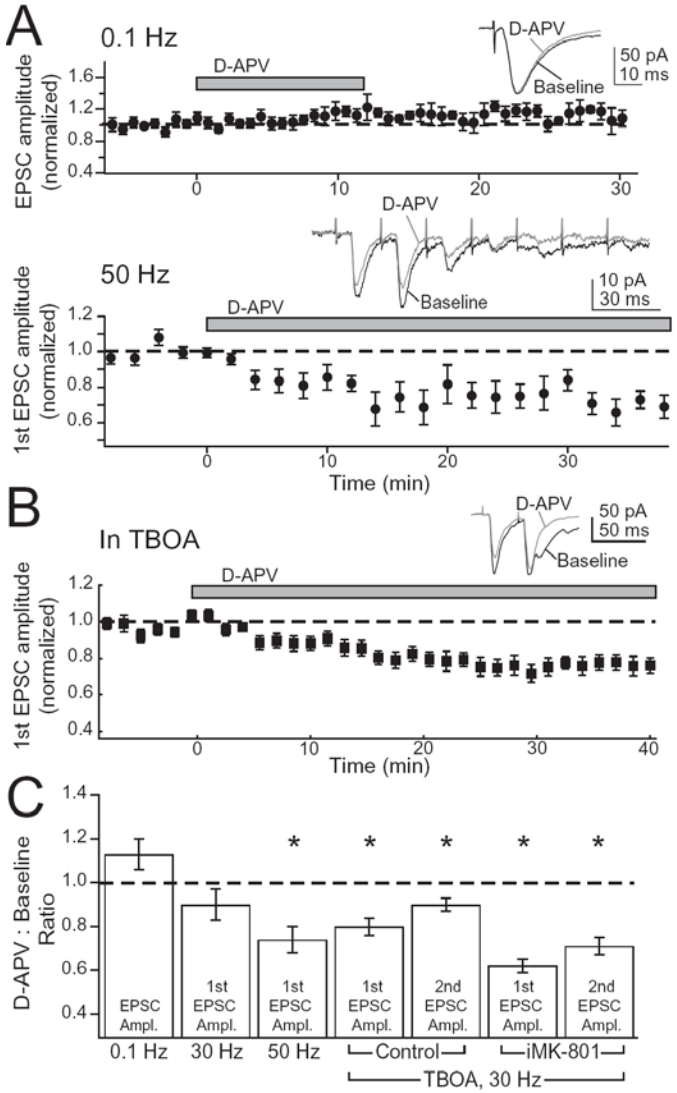



Fig. 4.1: Putatively presynaptic NMDARs regulate release at the L4-L2/3 projection when extracellular glutamate concentration is enhanced. A, D-APV does not block synaptically evoked AMPA receptor currents measured in voltage clamp at -90 mV in single pulses at 0.1 Hz (top), but does block currents when 7 pulses are evoked at 50 Hz (bottom). Insets, single examples of AMPA currents before (black) and after D-AP5 (grey). B, D-APV does block AMPA currents measured at –90 mV in trains of 2 pulses at 30 Hz in the presence of 25 μM TBOA. Inset, single example of AMPA currents before (black) and after D-APV (grey). C, Summary of effects of D-APV on the amplitudes of the first and second EPSCs at 0.1, 30, and 50 Hz and 30 Hz in the presence of TBOA, under normal conditions (control) and for a subset of the data in the presence of internal MK-801 (iMK-801). Asterisks indicated significance from baseline using a paired t-test.

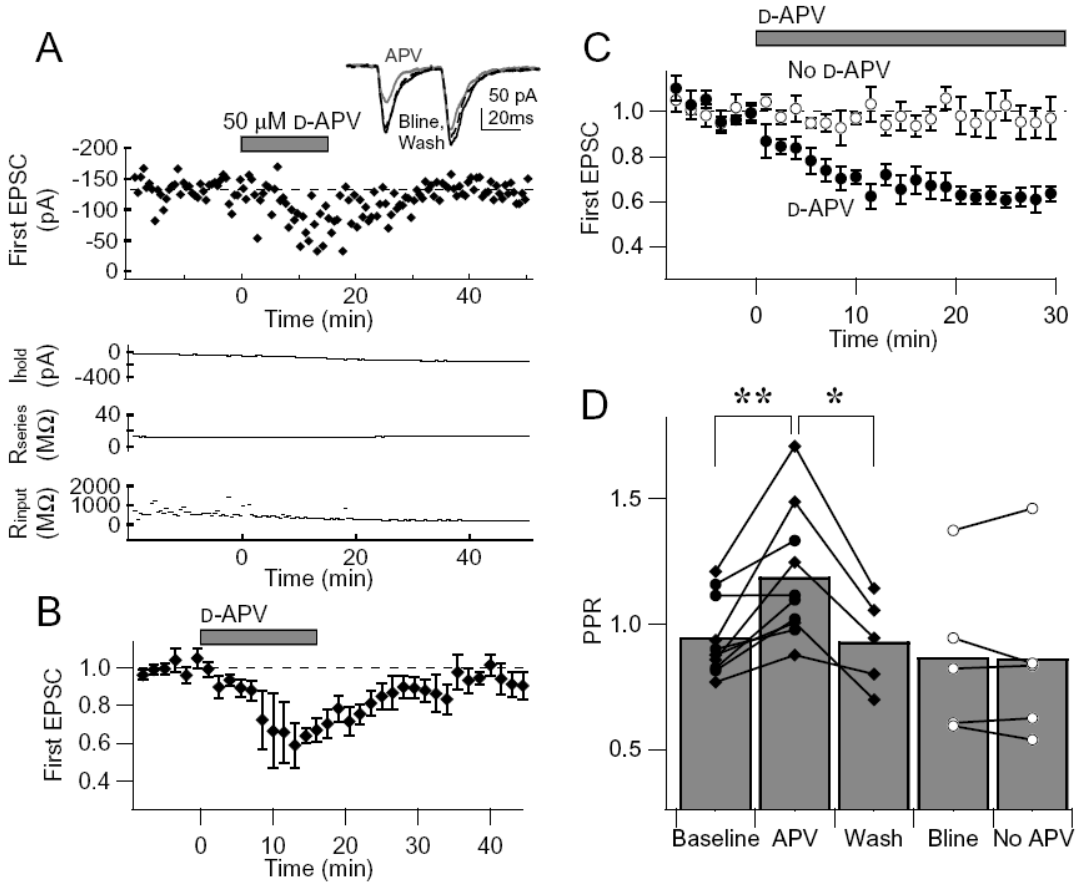



Fig. 4.2: Non-postsynaptic NMDARs modulate synaptic transmission at L4-L2/3 synapses in S1. All recordings were in 15 μM TBOA, focal BMI, and iMK-801. A, AMPA-EPSCs recorded in L2/3 pyramidal neurons evoked by stimulation of L4 barrel. Inset: Representative pair of EPSCs (30 Hz) during baseline (black), with 50 μM D-APV (grey), and after D-APV washout (dashed black). Top: Amplitude of the first EPSC throughout the recording for this cell. Bottom: Holding current, series resistance, and input resistance. B, Normalized timecourse of the first EPSC amplitude for 14 minute application of 50 μM D-APV with washout (n=5). C, Normalized timecourse of the first EPSC amplitude for 30 minute application of 50 μM D-APV (filled squares, n=5) and for control experiments (open squares, n=5). D, PPR for 14 minute (filled diamonds) and 30 minute (filled squares) D-APV application were pooled for analysis; PPR for control experiments (open squares) early and late in the recording are also plotted; bars represent mean PPR for each group (** = $p < 0.01$, * = $p < 0.05$).

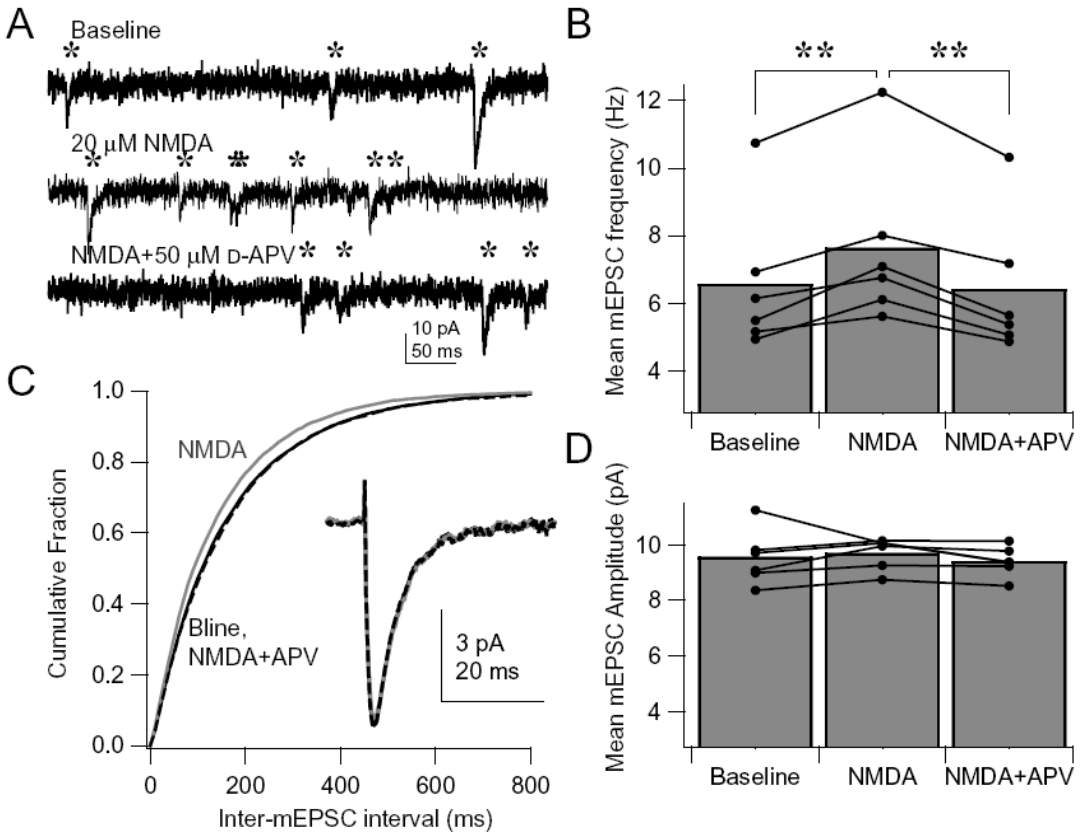



Fig. 4.3: Activation of PreNMDARs increase the frequency of mEPSCs on L2/3 pyramidal neurons. All recordings in 500 nM TTX, 100 μM picrotoxin, and iMK-801. A, Representative mEPSC from a single L2/3 pyramidal neuron during baseline (top), 15 μM NMDA application (middle), and 15 μM NMDA + 50 μM D-APV application (bottom). B, Mean cumulative probability histogram for inter-mEPSC interval during baseline (solid black), NMDA (grey), and NMDA+APV (dashed black); ($p < 0.01$ for baseline vs. NMDA and for NMDA vs. NMDA+APV, $p > 0.05$ for baseline vs. NMDA+APV, Kolmogorov-Smirnov test). Inset: Average mEPSC waveform across the population (black: baseline, grey: NMDA, dashed: NMDA+APV). C, Mean frequency for each cell during each condition, bars represent population mean (** = $p < 0.01$). D, Mean amplitude for each cell during each condition, bars represent population mean.

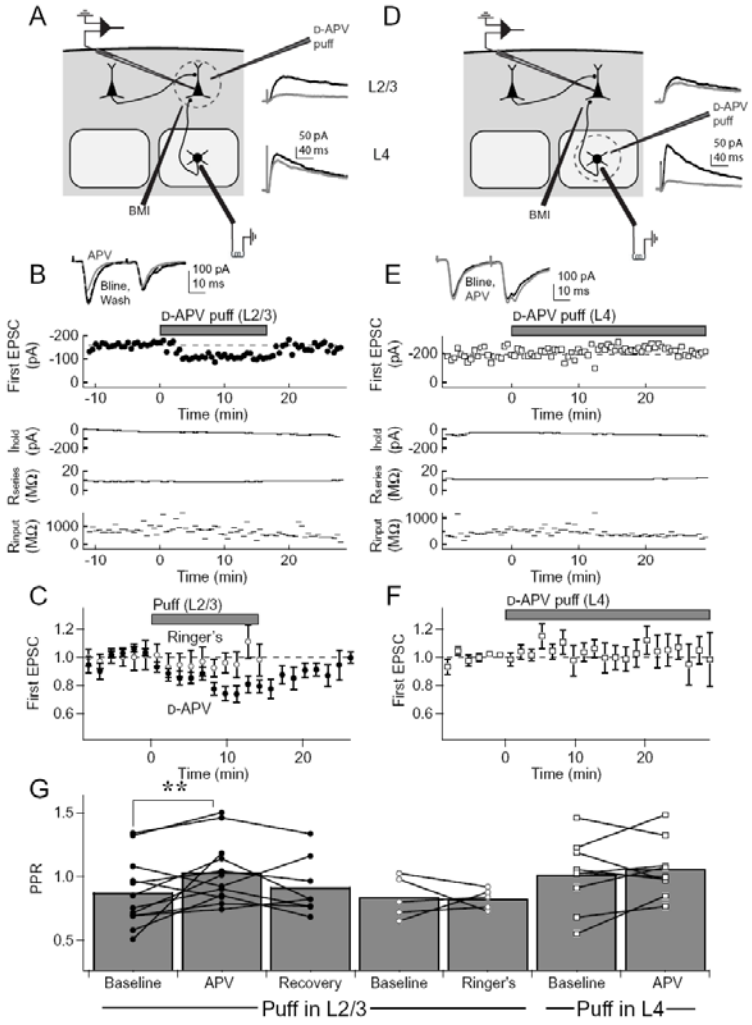



Fig. 4.4: PreNMDARs at the L4-L2/3 projection exist on L4 terminals located in L2/3. A&D, Recording schematic for focal puffing of D-APV or Ringer's in L2/3 (A) or L4 (D). Insets: Representative traces from L2/3 (upper) and L4 (lower) excitatory cells before (black) and during (grey) focal 2.5 μM D-APV puffing in L2/3. B&E, Example recordings from cells with focal D-APV puffing in L2/3 (B) or L4 (E). Inset: Mean EPSCs during baseline (black), focal 2.5 μM D-APV puffing (grey), and after cessation of puffing (black, dashed, B only). Top: Amplitude of the first EPSC throughout the recording for these cells. Bottom: Holding current, series resistance, and input resistance. C, Normalized timecourse of the first EPSC amplitude during focal 2.5 μM D-APV puffing in L2/3 (n=12, filled circles) and during focal Ringer's puffing in L2/3 (n=5, open circles). F, Normalized timecourse of the first EPSC amplitude during focal 2.5 μM D-APV puffing L4 (n=9, open squares). G, PPR for focal L2/3 D-APV puffing (filled circles), focal L2/3 Ringer's puffing (open circles), and focal L4 D-APV puffing (open squares), bars represent population means (* = $p<0.05$).

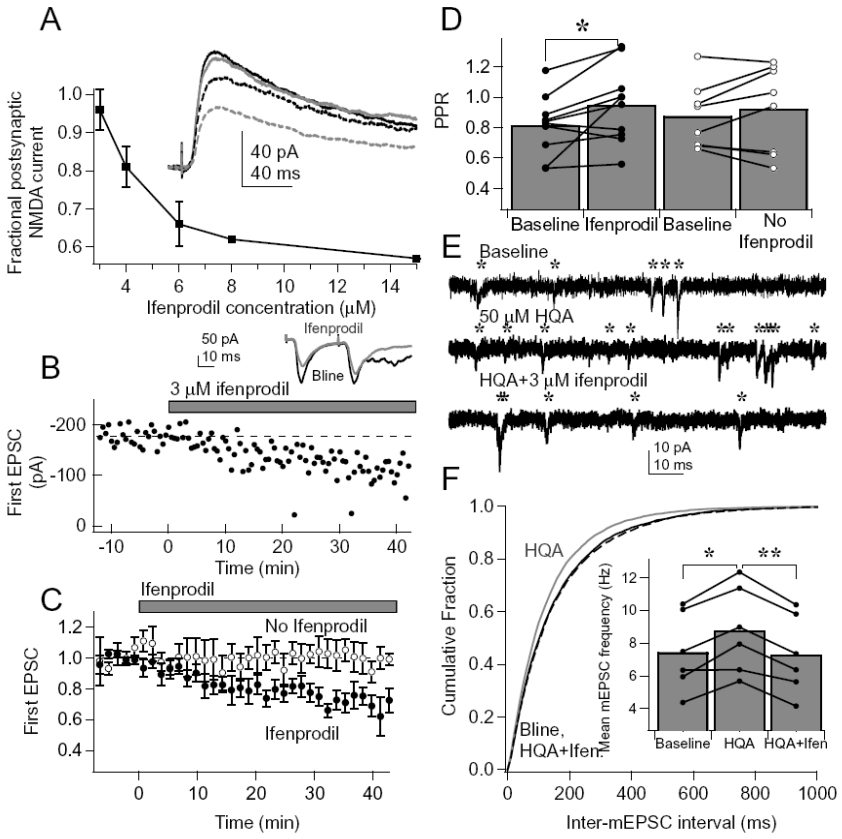



Fig. 4.5: PreNMDARs preferentially contain NR2B subunits. A, Mean decrease in pharmacologically-isolated postsynaptic NMDA-mediated EPSCs during successively increased ifenprodil concentration. Inset: representative traces from a single cell during baseline (solid black), 3 μM ifenprodil (solid grey), 4 μM ifenprodil (dashed black), and 6 μM ifenprodil (dashed grey). B, Amplitude of the first EPSC during 3 μM ifenprodil application for a representative cell. Inset: mean EPSCs before (black) and during (grey) 3 μM ifenprodil application. C, Normalized timecourse of the first EPSC amplitude during 3 μM ifenprodil application (n=10, filled circles) and for control experiments without ifenprodil (n=8, open circles). D, PPR for 3 μM ifenprodil application (filled circles) and control (open circles), bars represent population means (* = $p < 0.05$). E, Representative mEPSC from a single L2/3 pyramidal neuron during baseline (top), 20 μM HQA application (middle), and 20 μM HQA + 3 μM ifenprodil application (bottom). F, Mean cumulative probability histogram for inter-mEPSC interval during baseline (solid black), HQA (grey), and HQA+ifenprodil (dashed black); ($p < 0.01$ for baseline vs. HQA and for HQA vs. HQA+ifenprodil, $p > 0.05$ for baseline vs. HQA+ifenprodil, Kolmogorov-Smirnov test). Inset: Mean frequency for each cell during each condition, bars represent population mean (** = $p < 0.01$, *** = $p < 0.001$).

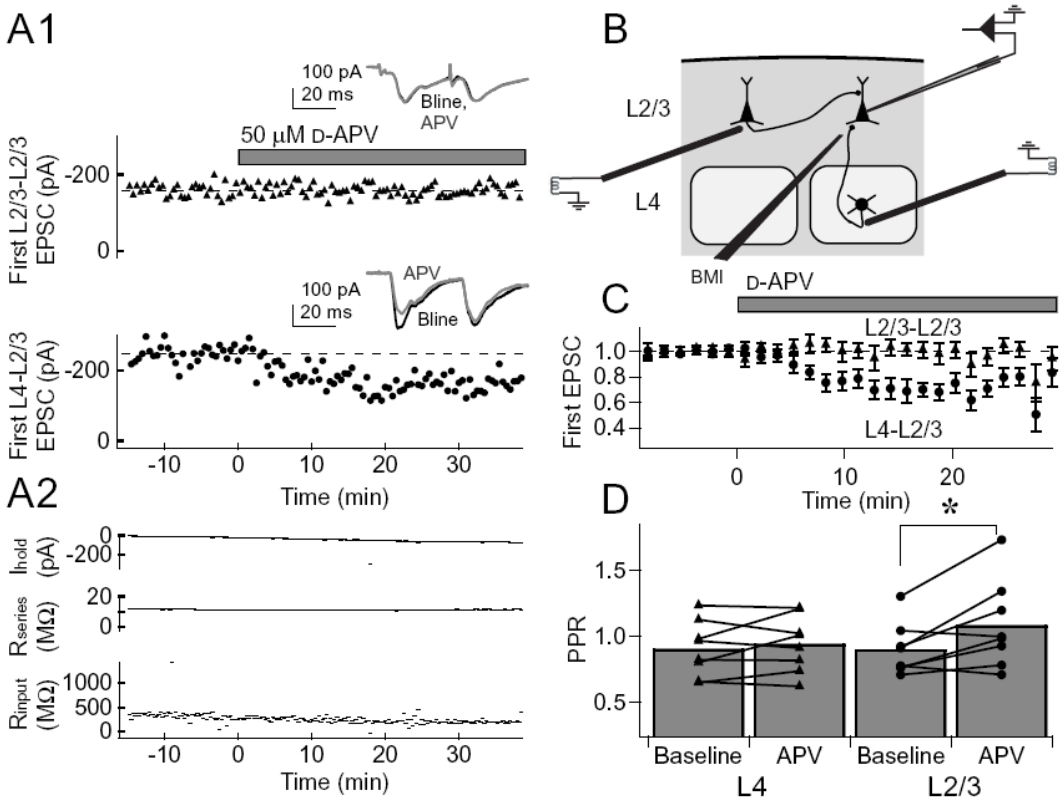



Fig. 4.6: PreNMDARs are located on the L4-2/3 projection, but not on other cortical inputs to L2/3. A1, Top: Amplitude of the first EPSC at the L2/3 cross-columnar projection during 50 μM D-APV application for a representative cell. Bottom: Amplitude of the first EPSC at the L4-L2/3 ascending projection for the same cell. Insets: Mean EPSCs before (black) and during (grey) D-APV application. A2, Holding current, series resistance, and input resistance for this cell. B, Recording set-up for these experiments. C, Normalized timecourse of the first EPSC amplitude during D-APV application for L2/3 cross-columnar (triangles) and L4 ascending (circles) inputs, n=8. D, PPR for L2/3 cross-columnar (triangles) and L4 ascending (circles) inputs, bars represent population means (* = $p < 0.05$).

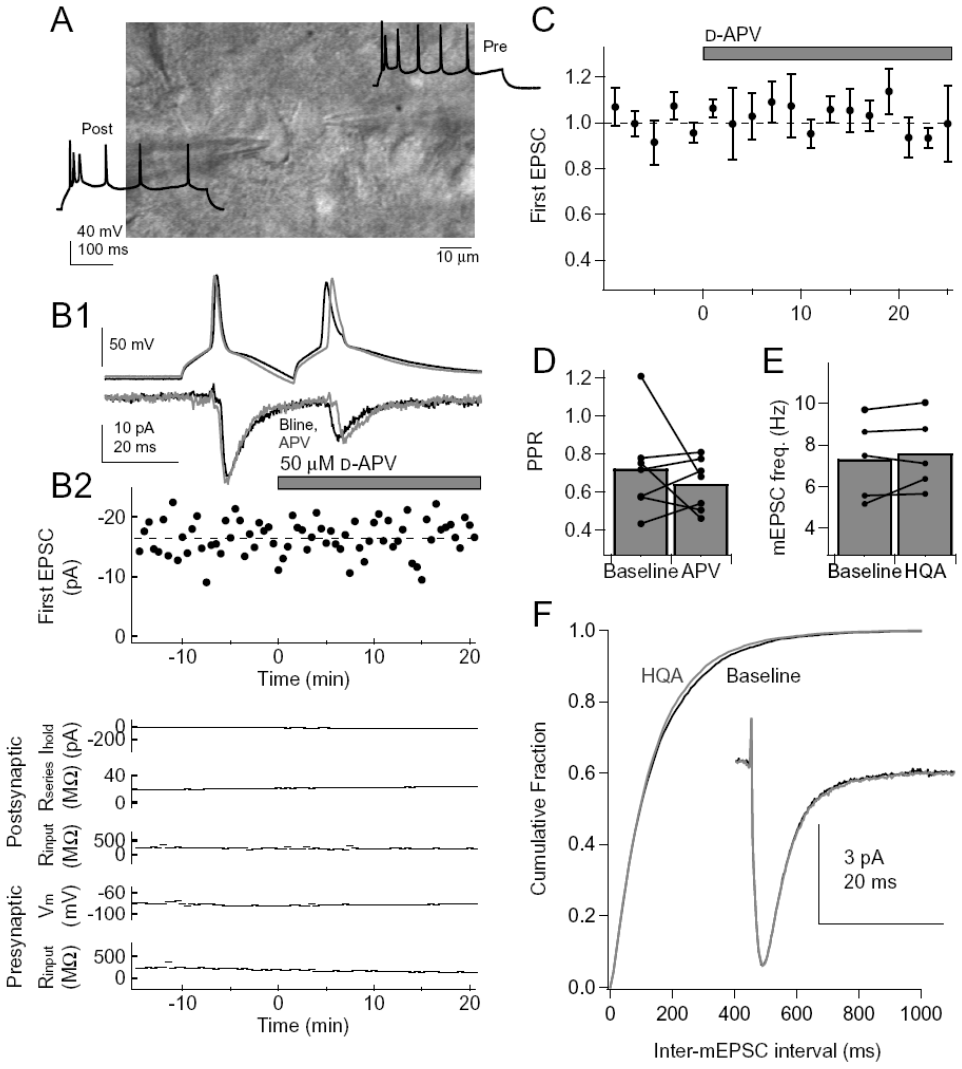



Fig. 4.7: There are not PreNMDARs at local synapses between L4 excitatory cells. A, Image of example synaptically coupled L4 excitatory cells; insets: regular-spiking pattern for example cells. B1, Average presynaptic membrane potential and postsynaptic response during two AMPA-uEPSCs before (black) and after (grey) 50 µM D-APV application for the regular-spiking pair above. B2, Top: Amplitude of the first AMPA-uEPSC during D-APV application. Bottom: postsynaptic holding current, postsynaptic series resistance, postsynaptic input resistance, presynaptic membrane potential, and presynaptic input resistance for this pair. C, Normalized timecourse of the first AMPA-uEPSC amplitude during D-APV application. D, PPR during D-APV application, bars represent population means. E, Mean mEPSC frequency for 5 L4 cells before and after 20 µM HQA application. F, Cumulative probability histogram before (black) and after (grey) HQA application ($p > 0.1$, Kolmogorov-Smirnov test). Inset: mean mEPSC before (black) and after (grey) HQA application.

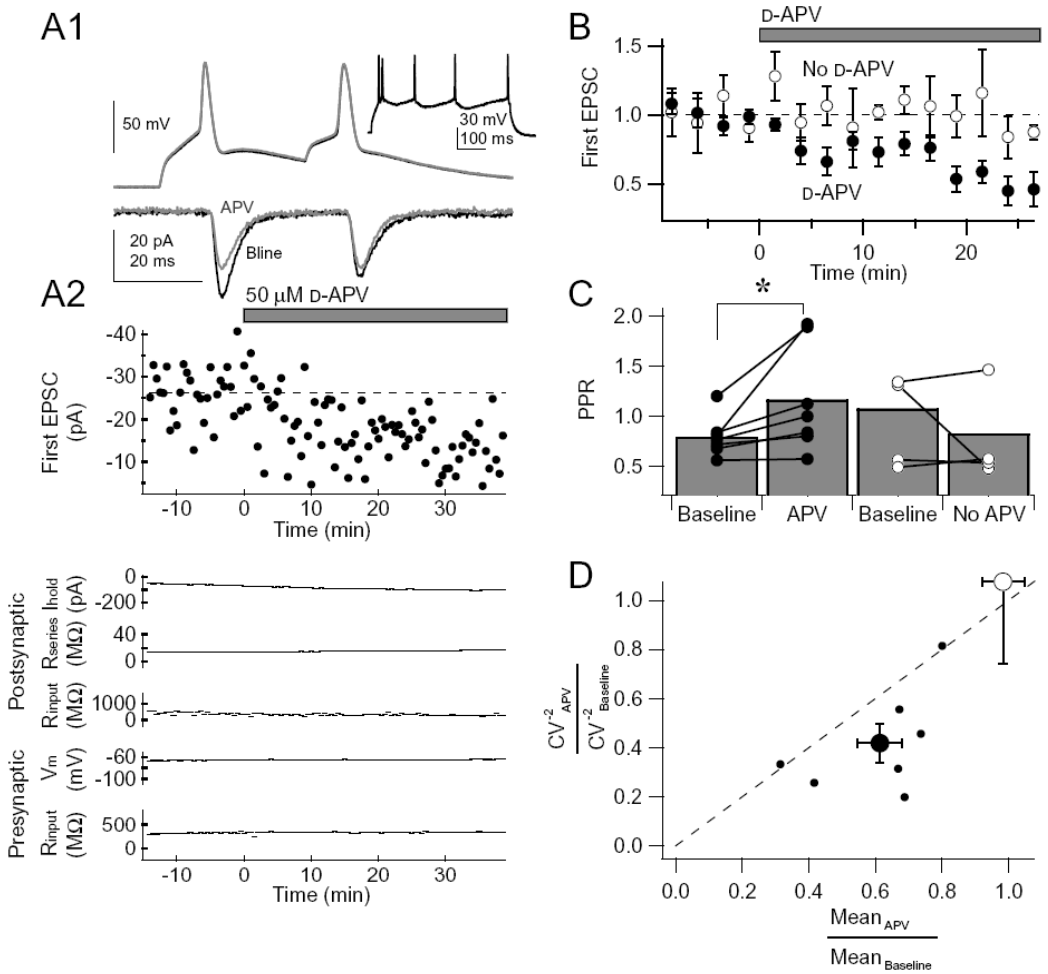



Fig. 4.8: PreNMDARs regulate transmission at synaptically-coupled L4-2/3 pairs. A1, Average traces from example presynaptic L4 and postsynaptic L2/3 cells during baseline (solid black) and 50 μM D-APV application (grey). Inset: regular-spiking pattern for presynaptic L4 cell. A2, Top: Amplitude of the first AMPA-uEPSC during D-APV application. Bottom: postsynaptic holding current, postsynaptic series resistance, postsynaptic input resistance, presynaptic membrane potential, and presynaptic input resistance for this pair. B, Normalized timecourse of the first EPSC amplitude during D-APV application (n=7, filled circles) and for control experiments without D-APV (n=4, open circles). E, PPR for D-APV application (filled circles) and control (open circles), bars represent population means (* = $p < 0.05$). F, CV analysis indicates a presynaptic locus for depression of the amplitude of the first EPSC. $CV^{-2}$ vs. mean EPSC amplitude for individual pairs in which 50 μM D-APV was applied (small filled circles), and population averages and standard error for D-APV (large filled circle) and control (large open circle, upward error bar omitted for clarity); all values are normalized to the baseline period.

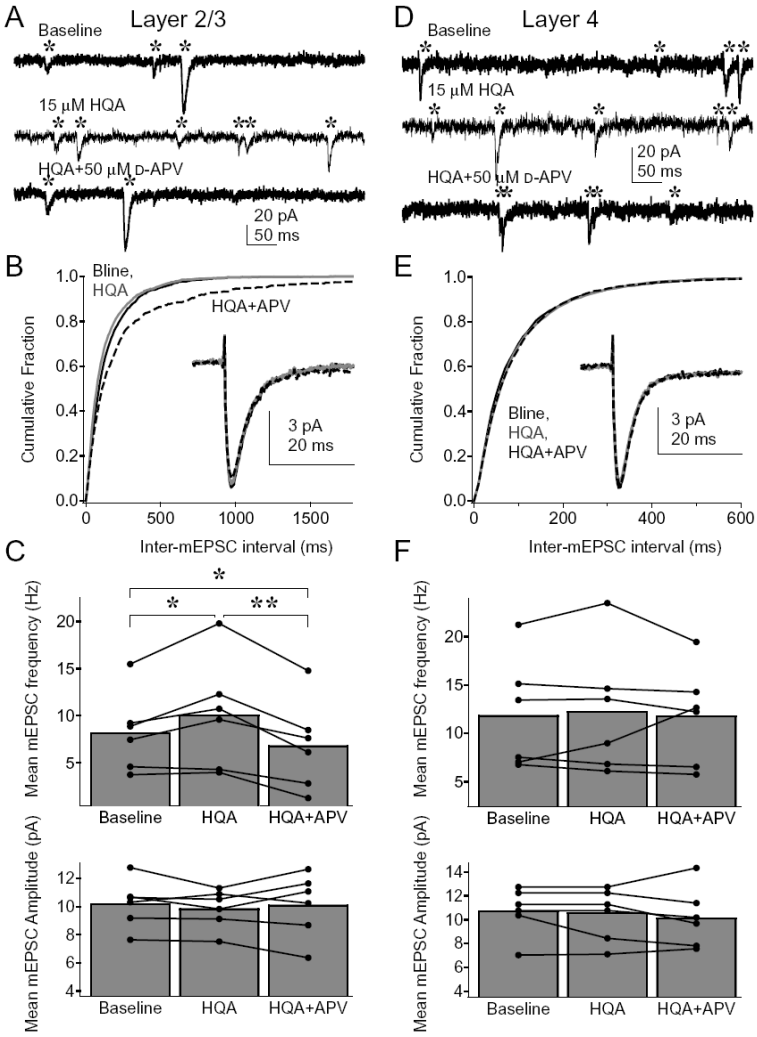



Fig. 4.9: PreNMDARs are tonically active at physiological temperatures. All recordings in 500 nM TTX, 100 μM picrotoxin, and iMK-801 at 30-32°C. A, Representative mEPSC from a single L2/3 pyramidal neuron during baseline (top), 15 μM HQA application (middle), and 15 μM HQA + 50 μM D-APV application (bottom). B, Mean cumulative probability histogram for inter-mEPSC interval during baseline (solid black), HQA (grey), and HQA+APV (dashed black); ($p < 0.001$ for baseline vs. HQA, $p < 0.0001$ for baseline vs. HQA+APV and for HQA vs. HQA+APV, Kolmogorov-Smirnov test). Inset: Average mEPSC waveform across the population (black: baseline, grey: HQA, dashed: HQA+APV). C, Upper: Mean frequency for each cell during each condition, bars represent population mean (* = $p < 0.05$, ** = $p < 0.01$). Lower: Mean amplitude for each cell during each condition, bars represent population mean. D-F, Conventions as for A-C, but for L4 excitatory cells. E, $p < 0.001$ for baseline vs. HQA and for baseline vs. HQA+APV, $p < 0.05$ for HQA vs. HQA+APV.

## V. Concluding remarks on functional heterogeneity and presynaptic NMDA receptor function

A great deal has been learned about excitatory (glutamatergic) synapses in the brain. However, despite all that is known, the problem of understanding how our synapses function is far from complete. The work presented here sheds light on the mechanisms underlying functional diversity at central synapses and demonstrates one way in which presynaptic release is modulated. The fundamental contribution of this body of work is to explore non-classical roles of NMDA receptors (NMDARs) at different synapses in S1. Taken together as well as in the context of other findings, our observations show that there is a great deal of functional heterogeneity of pre- and postsynaptic functions of NMDARs in central synapses. A key player in this heterogeneity appears to be the presynaptic NMDAR (PreNMDAR); understanding how PreNMDARs regulate release will become important for future models of functional heterogeneity in cortex.

### Heterogeneity between cortical areas

While striking similarities in functional processing and plasticity have been observed between visual cortex (V1), somatosensory cortex (S1), and other primary sensory cortices such as auditory cortex (A1), notable differences do exist. For example, under normal development, cells in V1 make long distance, diffuse lateral projections compared to the dense, local projections made by cells in A1 (Sharma et al., 2000; Linden and Schreiner, 2003). Even more notable is the different degrees to

which bilateral information is processed in the different cortical regions: auditory information is integrated binaurally at the subcortical level (Linden and Schreiner, 2003); visual information is integrated binocularly in V1 itself (Hubel and Weisel, 1962); somatosensory information is only weakly bilateral (Armstrong-James and George, 1988; Glazewski et al., 2007). In addition to the differences in processing mechanisms, differences in plasticity between cortical areas have been observed (Fox and Wong, 2005). Most notably, experience-dependent plasticity causes substantial rearrangement of axonal arbors in V1 (Antonini and Stryker, 1993; 1996; Antonini et al., 1999), but it has been observed that such a reorganization is lacking in S1 (Bender et al., 2006a) although some evidence for anatomical reorganization of S1 has been observed (Kossut and Juliano, 1999).

The recent observation that synaptic contacts onto the apical dendrites of layer (L) 2/3 pyramidal cells in V1 detect timing-dependent long-term depression via calcium-dependent desensitization of postsynaptic NMDARs (Froemke et al., 2005) appears, in the context of the work presented here, not to be a mechanism of coincidence detection shared with L2/3 pyramidal cells in S1 (Chapter 3). In addition, robust spike-timing dependent plasticity (STDP) has been observed *in vivo* in V1 (Meliza and Dan, 2006). By contrast, the work we presented here and we published indicates that, while present in S1, *in vivo* STDP is markedly less robust in S1 than what has been observed *in vitro* (Chapter 2; Feldman, 2000; Jacob et al., 2007). Thus, there appear to be differences in mechanisms of processing, plasticity, and coincidence detection between cortical areas. However, as many of the observed differences are because of experiments done with different protocols in different laboratories, it

remains to be seen if some of the differences are experimental, rather than biological. A full, systematic study of these differences within a single lab has yet to be done.

**Synaptic heterogeneity within a cortical area**

Heterogeneity of synaptic properties seems to be the rule for central synapses. Different classes of excitatory neurons in cortex that converge on a common postsynaptic target can have very different release properties. Although this has been seen outside of the cortex (e.g. inputs onto Purkinje cells in the cerebellum), a systematic study of this input-selectivity (Fig. 1.2A) is lacking. We have now identified PreNMDARs and mediating one instantiation of input-selectivity for different excitatory afferents onto L2/3 pyramidal cells in S1 (Chapter 4).

Several studies in cortex, hippocampus, and other brain areas have identified target-selectivity (Fig. 1.2B) of synaptic properties. An emerging theme is that heterogeneous expression of presynaptic neurotransmitter receptors underlies at least some of this heterogeneity. This has been seen in hippocampus for presynaptic kainate receptors (PreKARs) at synapses onto different types of interneurons (Sun and Dobrunz, 2006). It has also been seen in cortex for presynaptic metabotropic glutamate receptors at synapses onto excitatory vs. inhibitory cells (Scanziani et al., 1998). We have now shown it to be true for PreNMDARs at L4 synaptic projections onto two classes of excitatory neurons in S1 (Chapter 4). Taken together, these observations in different brain areas may indicate that differential expression of presynaptic neurotransmitter receptors is a common mechanism by which cells achieve input-selectivity and target-selectivity of synaptic properties.

Although target-selective synaptic properties have been identified in a number of systems, aside from the differential expression of presynaptic metabotropic glutamate receptors, KARs, and NMDARs (see above; Scanziani et al., 1998; Sun and Dobrunz, 2006; this thesis, Chapter 4), no mechanism for target-selective differences in synaptic properties has been identified. Although no other mechanism for target-selective release properties has been found, there are a few candidate mechanisms. First, it has been shown that expression of vesicular glutamate transporters (VGLUTs) predicts differences in release probability with low release probability synapses expressing VGLUT1 and high release probability synapses expressing VGLUT2 (Fremeau et al., 2001; 2004a; 2004b). Second, it expression of synaptotagmin isoforms can alter release probability; synaptotagmin IV knockout animals exhibit increased paired-pulse ratio, indicating a decrease in release probability (Ullrich et al., 1994; Ferguson et al., 2004). Third, neuronal calcium channels respond differently to voltage (Nowycky et al., 1985; Llinas et al., 1992) and are expressed differentially across brain areas (Evans and Zamponi, 2006). It has been observed that N-type and P/Q-type channels have different paired-pulse ratios, suggesting that their expression affects release probability (Inchauspe et al., 2004). However, despite the evidence that these three mechanisms can alter release probability, which, if any, of them do so in a target-selective manner remains to be seen.

**Speculative model of PreNMDAR function**

Our data indicate the PreNMDARs are active only under conditions where glutamate concentration is enhanced. PreKARs are activated phasically by release

from the excitatory terminal itself (Sun and Dobrunz, 2006); the absence of tonic activation of PreKARs likely owes to their low affinity for glutamate (Pinheiro et al. 2007). PreNMDARs, by contrast, do not appear to be activated by release from the terminal itself, but appear to have tonic activation in S1 and V1, given that effects of NMDAR blockade are visible in miniature excitatory postsynaptic current frequency and on the first pulse in a pair or train of pulses (Chapter 4; Sjöström et al., 2003; Corlew et al., *in press*); which probably owes to their high affinity for glutamate (Sah et al., 1989; Le Meur et al., 2007). Tonic activation of PreNMDARs at room temperature is only observed under conditions of elevated extracellular glutamate, but at higher temperatures, baseline concentration of glutamate is sufficient (Fig. 4.9).

Given that they appear not to be activated by release from the terminal itself, what is the source of glutamate? A recent paper has found PreNMDARs located along the side of the presynaptic terminal in hippocampal terminals, closely apposed to astrocytes (Jourdain et al., 2007). Additionally, the same group has found evidence that astrocytes contain glutamate vesicles and that these vesicles are very close to the extrasynaptic NMDARs on the presynaptic terminal (Bezzi et al., 2004, Jourdain et al., 2007). It is possible that glia are the source of glutamate for PreNMDARs, in which case they either tonically release it or it is released under some as-yet-unidentified regulation. Alternatively, ambient glutamate levels in the slice may be high enough to activate PreNMDARs without the need for release from glutamate, as has been observed for postsynaptic NMDARs in some preparations (Sah et al., 1989; Le Meur et al., 2007).

Although we cannot yet distinguish between these two possibilities, we have determined that PreNMDARs are unlikely to be near the site of synaptic release and thus excitatory amino acid transporters (EAATs) scavenge glutamate before it can reach them when it is released from the terminal itself (Fig. 5.1; O'Shea, 2002). Thus, we predict that PreNMDARs are not located close to the release machinery and are therefore not well positioned to contribute calcium to directly affect release (Kim and Catterall, 1997; Catterall, 1998; Zhang et al., 2000). Instead, we propose a few possible mechanisms by which they may act. First, they may depolarize the terminal which can increase release probability (Turecek and Trussell 2001, 2002; Trussell 2002). Second, and more speculative, they may provide calcium which activates a presynaptic protein kinase and produces a longer-lasting enhancement of release. Third, calcium influx through PreNMDARs, while not positioned to induce release per se, may serve to partially saturate some cytosolic calcium buffers in the presynaptic terminal and thus enhance subsequent release probability (Felmy et al., 2003).

**References**

Antonini A, Stryker MP (1993) Rapid remodeling of axonal arbors in the visual cortex. Science 260:1819-1821.

Antonini A, Stryker MP (1996) Plasticity of geniculocortical afferents following brief or prolonged monocular occlusion in the cat. J Comp Neurol 369:64-82.

Antonini A, Fagiolini M, Stryker MP (1999) Anatomical correlates of functional plasticity in mouse visual cortex. J Neurosci 19:4388-4406.

Armstrong-James M, George MJ (1988) Bilateral receptive fields of cells in rat Sm1 cortex. Exp Brain Res 70:155-165.

Bender KJ, Allen CB, Bender VA, Feldman DE (2006a) Synaptic basis for whisker deprivation-induced synaptic depression in rat somatosensory cortex. J Neurosci 26:4155-4165.

Bender VA, Bender KJ, Brasier DJ, Feldman DE (2006b) Two coincidence detectors for spike timing-dependent plasticity in somatosensory cortex. J Neurosci 26:4166-4177.

Bezzi P, Gundersen V, Galbete JL, Seifert G, Steinhauser C, Pilati E, Volterra A (2004) Astrocytes contain a vesicular compartment that is competent for regulated exocytosis of glutamate. Nat Neurosci 7:613-620.

Catterall WA (1998) Structure and function of neuronal Ca2+ channels and their role in neurotransmitter release. Cell Calcium 24:307-323.

Corlew R, Wang Y, Ghermazien H, Erisir A, Philpot BD (2007) Developmental switch in the contribution of presynaptic and postsynaptic NMDA receptors to long-term depression. J Neurosci, *in press*.

Evans RM, Zamponi GW (2006) Presynaptic Ca2+ channels--integration centers for neuronal signaling pathways. Trends Neurosci 29:617-624.

Felmy F, Neher E, Schneggenburger R (2003) Probing the intracellular calcium sensitivity of transmitter release during synaptic facilitation. Neuron 37:801-811.

Ferguson GD, Wang H, Herschman HR, Storm DR (2004) Altered hippocampal short-term plasticity and associative memory in synaptotagmin IV (-/-) mice. Hippocampus 14:964-974.

Fox K, Wong RO (2005) A comparison of experience-dependent plasticity in the visual and somatosensory systems. Neuron 48:465-477.

Fremeau RT Jr, Troyer MD, Pahner I, Nygaard GO, Tran CH, Reimer RJ, Bellocchio EE, Fortin D, Storm-Mathisen J, Edwards RH (2001) The expression of vesicular glutamate transporters defines two classes of excitatory synapse. Neuron 31:247-260.

Fremeau RT Jr, Kam K, Qureshi T, Johnson J, Copenhagen DR, Storm-Mathisen J, Chaudhry FA, Nicoll RA, Edwards RH (2004a) Vesicular glutamate transporters 1 and 2 target to functionally distinct synaptic release sites. Science 304:1815-1819.

Fremeau RT Jr, Voglmaier S, Seal RP, Edwards RH (2004b) VGLUTs define subsets of excitatory neurons and suggest novel roles for glutamate. Trends Neurosci 27:98-103

Froemke RC, Poo MM, Dan Y (2005) Spike-timing-dependent synaptic plasticity depends on dendritic location. Nature 434:221-225.

Glazewski S, Benedetti BL, Barth AL (2007) Ipsilateral whiskers suppress experience-dependent plasticity in the barrel cortex. J Neurosci 27:3910-39120.

Hubel DH, Wiesel TN (1962) Receptive fields, binocular interaction and functional architecture in the cat's visual cortex. J Physiol 160:106-154.

Inchauspe CG, Martini FJ, Forsythe ID, Uchitel OD (2004) Functional compensation of P/Q by N-type channels blocks short-term plasticity at the calyx of held presynaptic terminal. J Neurosci 24:10379-10383.

Jourdain P, Bergersen LH, Bhaukaurally K, Bezzi P, Santello M, Domercq M, Matute C, Tonello F, Gundersen V, Volterra A (2007) Glutamate exocytosis from astrocytes controls synaptic strength. Nat Neurosci 10:331-339.

Kim DK, Catterall WA (1997) Ca2+-dependent and -independent interactions of the isoforms of the alpha1A subunit of brain Ca2+ channels with presynaptic SNARE proteins. Proc Natl Acad Sci U S A 94:14782-14786.

Kossut M, Juliano SL (1999) Anatomical correlates of representational map reorganization induced by partial vibrissectomy in the barrel cortex of adult mice. Neuroscience 92:807-817.

Le Meur K, Galante M, Angulo MC, Audinat E (2007) Tonic activation of NMDA receptors by ambient glutamate of non-synaptic origin in the rat hippocampus. J Physiol 580:373-383.

Linden JF, Schreiner CE (2003) Columnar transformations in auditory cortex? A comparison to visual and somatosensory cortices. Cereb Cortex 13:83-89.

Llinas R, Sugimori M, Hillman DE, Cherksey B (1992) Distribution and functional significance of the P-type, voltage-dependent Ca2+ channels in the mammalian central nervous system. Trends Neurosci 15:351-335.

Meliza CD, Dan Y (2006) Receptive-Field Modification in Rat Visual Cortex Induced by Paired Visual Stimulation and Single-Cell Spiking. Neuron 49, 183–189.

Nowycky MC, Fox AP, Tsien RW (1985) Three types of neuronal calcium channel with different calcium agonist sensitivity. Nature 316:440-443.

O'Shea RD (2002) Roles and regulation of glutamate transporters in the central nervous system. Clin Exp Pharmacol Physiol 29:1018-1023.

Pinheiro PS, Perrais D, Coussen F, Barhanin J, Bettler B, Mann JR, Malva JO, Heinemann SF, Mulle C (2007) GluR7 is an essential subunit of presynaptic kainate autoreceptors at hippocampal mossy fiber synapses. PNAS. in press.

Sah P, Hestrin S, Nicoll RA (1989) Tonic activation of NMDA receptors by ambient glutamate enhances excitability of neurons. Science 246:815-818.

Scanziani M, Gahwiler BH, Charpak S (1998) Target cell-specific modulation of transmitter release at terminals from a single axon. Proc Natl Acad Sci U S A 95:12004-12009.

Sharma J, Angelucci A, Sur M (2000) Induction of visual orientation modules in auditory cortex. Nature 404:841-847.

Sjöström PJ, Turrigiano GG, Nelson SB (2003) Neocortical LTD via coincident activation of presynaptic NMDA and cannabinoid receptors. Neuron 39:641-654.

Sun HY, Dobrunz LE (2006) Presynaptic kainate receptor activation is a novel mechanism for target cell-specific short-term facilitation at Schaffer collateral synapses. J Neurosci 26:10796-10807.

Trussell LO (2002) Modulation of transmitter release at giant synapses of the auditory system. Curr Opin Neurobiol 12:400-404.

Turecek R, Trussell LO (2001) Presynaptic glycine receptors enhance transmitter release at a mammalian central synapse. Nature 411:587-590.

Turecek R, Trussell LO (2002) Reciprocal developmental regulation of presynaptic ionotropic receptors. Proc Natl Acad Sci U S A 99:13884-13889.

Ullrich B, Li C, Zhang JZ, McMahon H, Anderson RG, Geppert M, Sudhof TC (1994) Functional properties of multiple synaptotagmins in brain. Neuron 13:1281-1291.

Zhang L, Volknandt W, Gundelfinger ED, Zimmermann H (2000) A comparison of synaptic protein localization in hippocampal mossy fiber terminals and neurosecretory endings of the neurohypophysis using the cryo-immunogold technique. J Neurocytol 29:19-30.

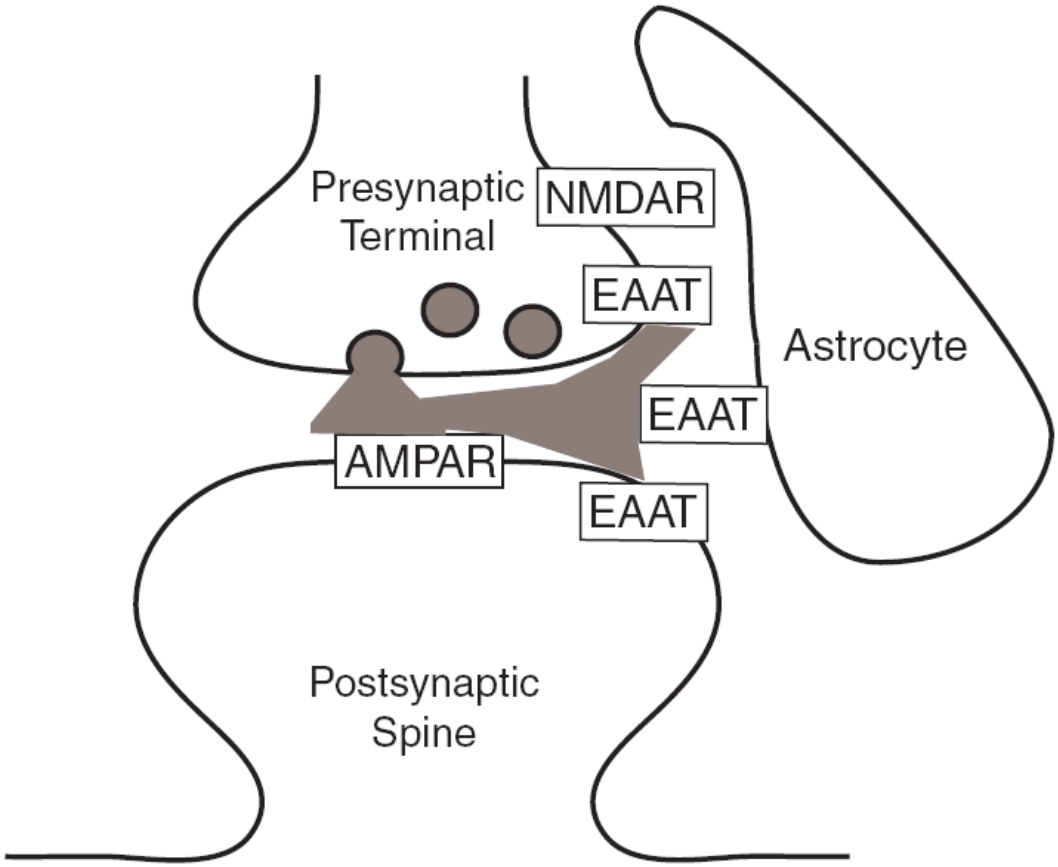



Fig. 5.1: Putative localization of PreNMDARs within the synaptic terminal. The absence of phasic activation of PreNMDARs during synaptic release indicates that they are not located in the synaptic cleft, but up along the sides of the terminal: glutamate released from the terminal (grey) most likely is scavenged by excitatory amino acid transporters (EAAT) before it reaches the PreNMDAR. Thus, PreNMDARs are unlikely to be positioned to contribute calcium to directly influence release, but probably influence release by some other mechanism (e.g. depolarization of the terminal). The physiological source of glutamate has not been fully determined, but may be ambient glutamate in the slice or glutamate released by a third cell (e.g. the astrocyte shown apposed to the PreNMDAR.